

Università degli Studi di Bologna

FACOLTÀ DI INGEGNERIA

**DOTTORATO DI RICERCA IN INGEGNERIA ELETTRONICA,
INFORMATICA E DELLE TELECOMUNICAZIONI**

Ciclo XIX

**ELECTRONIC BIOSENSOR ARRAYS
FOR LABEL-FREE DNA AND
PROTEIN ANALYSIS**

Tesi di Dottorato di:

CLAUDIO STAGNI DEGLI ESPOSTI

Relatori :

Chiar. mo Prof. Ing. **BRUNO RICCÒ**

Chiar. mo Prof. Ing. **LUCA BENINI**

Coordinatore:

Chiar. mo Prof. Ing. **PAOLO BASSI**

Settore Scientifico Disciplinare: ING/INF01 Elettronica
Anno Accademico 2006/2007

Keywords:

Biosensors
label free
capacitance measurements
array
low cost

”L’universo risponde
il vero
se interrogato onestamente”
C.S. Lewis

”— *Don Camillo, perché ce l’hai tanto con i numeri?*
— Perché , secondo me, gli uomini
non funzionano piú proprio a causa dei numeri.
Essi hanno scoperto il numero
e ne hanno fatto il supremo regolatore dell’universo. [...]
— Gesù le idee sono dunque finite?
Gli uomini hanno pensato tutto il pensabile?
— *Don Camillo cosa intendi tu per idea?*
— Idea, per me, povere prete di campagna, é una lampada
che si accende nella notte profonda dell’ignoranza umana
e mette in luce un nuovo aspetto della grandezza del creatore.
Il Cristo sorrise...”
G. Guareschi

Contents

1	THE GENOMIC AND POST-GENOMIC ERA	1
1.1	Life and the Genome	1
1.2	Genetic Analysis	3
1.2.1	Tracing the genome: achieving the genomic era	4
1.2.2	Application of DNA-sequences detection	6
1.3	Figures	10
2	MICROFABRICATED ELECTRONIC SENSORS FOR GENETIC ANALYSIS	17
2.1	Role of technology and electronics	17
2.2	Technology, microfabrication and micromachining of silicon and other materials	18
2.2.1	Pattern definition of high-density spots of different probes molecules on a substrate. DNA Microarray technology	18
2.2.2	Microfluidics on chip	20
2.3	Electronics and microelectronics	21
2.3.1	Electrical-addressing of conductive sites	21
2.3.2	Electronic Circuits for signal detection and processing in biosensors application	22
2.3.3	Semiconductor sensors	23
2.4	Figures	24
3	BASIC THEORY OF ELECTROCHEMISTRY	29
3.1	Physics and Chemistry of the sensing principle	29
3.2	Sensing layer formation on electrodes	31
3.2.1	Organosilicon derivatives	31
3.2.2	Thiol Layers	31
3.3	Previous work on Interface capacitance sensing	32
3.4	Impedance measurement technique	34
3.4.1	Standard Methods. Impedance Spectroscopy	34

3.5	Figures	36
4	ELECTRICAL TECHNIQUE FOR DNA DETECTION ON PASSIVE GOLD MICROELECTRODES ON SILICON	39
4.1	Passive Microarrays vs Active Matrices	39
4.1.1	Label-free techniques	40
4.2	Bio-functionalization of micro-fabricated electrodes . . .	41
4.2.1	Microfabricated electrodes	41
4.2.2	Basic process	41
4.2.3	Compatibility	42
4.3	Experimental Results	43
4.3.1	Complex impedance measurements	43
4.3.2	Integrable circuitry	46
4.4	Tables	47
4.5	Figures	48
5	Smart sensor on PCB based on μ-controller for genetic analysis	55
5.1	State-of-the-art and detection principle	56
5.2	Hardware and Software Design	58
5.3	Experimental results	61
5.3.1	Tuning	61
5.3.2	Electrical characterization	61
5.3.3	DNA Detection Measurement	62
5.4	Figures	64
6	On Chip DNA detection based on CBCM capacitance measurement	67
6.1	Related Work	68
6.2	Capacitance-based DNA Detection Principle	69
6.3	Chip	71
6.3.1	Chip architecture	71
6.3.2	Sensing site circuitry	71
6.3.3	Physical layout	72
6.4	Measurement set-up	73
6.5	Experimental results	74
6.5.1	Electrical Characterization of gold electrodes . . .	74
6.5.2	Electrode bio-modification	75
6.5.3	DNA detection	76
6.6	Tables	79

6.7	Figures	80
7	Capacitance measurement for DNA detection with on chip A/D conversion	85
7.1	Introduction	85
7.2	Related Work	86
7.3	Capacitance-based DNA Detection Principle	88
7.4	Label-free DNA chip	90
7.4.1	Chip architecture	90
7.4.2	Sensing site circuitry	90
7.4.3	Physical layout	91
7.5	Experimental results	92
7.5.1	Measurement set-up	92
7.5.2	Electrical Characterization	92
7.5.3	DNA detection	93
7.6	Figures	95
8	Application on tumor marker and future steps on DNA	105
8.1	Tumor marker analysis	105
8.2	Immunosensors	106
8.3	Device and methods	106
8.4	Experimental results	107
8.5	Figures	108
9	EEPROM memory as DNA sensor	113
9.1	Introduction	113
9.2	Devices and method	114
9.3	Measurement setup	116
9.4	Experimental results	117
9.5	Discussion	118
9.6	Figures	120
10	Conclusions and perspectives	123
11	Publications	125
11.1	Conferences	125
11.2	Journals	126
11.3	Patents	126

Chapter 1

THE GENOMIC AND POST-GENOMIC ERA

1.1 Life and the Genome

The feature of life is its ability to reproduce itself, but this ability alone is not enough. Crystals influence the matter around them to create structures similar to themselves but they are not alive. Life can be defined by recognizing its fundamental interrelatedness which means that all living things are related to each other: they all have a common ancestor in the distant past [1]. Organisms came to differ from each other through evolution, which can be described as a cumulative process of the following three components: inheritance, variation and selection. Evolution not only helps us to define what life is, but also to understand how living system function. All of an organism inherited characteristics are contained in a single messenger molecule, the deoxyribonucleic acid, or DNA. The characteristics are defined in a simple, linear, four element code. The genetic encoding for an organism is called genotype, the resulting physical characteristics of an organism is called phenotype. Evolutionary variation (mutation, sexual recombination and genetic rearrangements) allows modification of a genotype, that can have large consequences in phenotype. On the other side, selection acts only on phenotypes. Diversity generated by evolution is enormous and very evident, but, although our understanding of the molecular level of life is less detailed, this diversity is encoded there. In fact, protein with very similar shapes and function can have very different chemical composition. Organism that look quite similar be very different from their genetic code. Despite this incredible diversity, nearly all of the same basic mechanisms are present in all or-

ganism. All living things are made of cells. The thousands of substances that make up the basic reactions inside the cell are remarkably similar across all living things. The genetic material that codes for all of these substances is written more or less in the same molecular language in every organism. The genetic material is organized in the genome which is characterized by a defined and very variable size and it is contained identical in the nucleus of every cell of an organism. The smallest known genome is the one of the bacterium which contains about 600,000 DNA base pairs. Human and mouse genomes have some 3 billion base pairs. Except for mature red blood cells, all human cells contain a complete genome. DNA in the human genome is arranged into 24 distinct chromosomes-physically separate molecules that range from about 50 million to 250 million base pairs. Each chromosome contains many genes, the basic physical and functional units of heredity. Genes are specific sequences of bases that encode instructions on how to make proteins. Genes comprise only about 2% of the human genome; the remainder consists of non-coding regions, whose functions may include providing chromosomal structural integrity and regulating where, when, and in what quantity proteins are made. The human genome, at present, is estimated to contain 30,000 genes. Proteins, expressed by genes by means of RNA sequence, first, and subsequently amino acids, perform most life functions and even make up the majority of cellular structures. Proteins are large, complex molecules made up of smaller subunits called amino acids. Chemical properties that distinguish the 20 different amino acids cause the protein chains to fold up into specific three-dimensional structures that define their particular functions in the cell. The constellation of all proteins in a cell is called its proteome. Unlike the relatively unchanging genome, the dynamic proteome changes from minute to minute in response to tens of thousands of intra- and extracellular environmental signals. A protein's chemistry and behaviour are specified by the gene sequence and by the number and identities of other proteins made in the same cell at the same time and with which it associates and reacts. The DNA sequence is the particular side-by-side double-helix arrangement of bases along the DNA strand (see Fig. 1.1). This order defines the exact instructions required to create a particular organism with its unique traits. Bases are parts of nucleic acid molecules which forms the DNA. They are of four kinds: adenine, thymine, cytosine, guanine. All of the adenines on one side of the DNA (one single strand) recognize the thymines on the other side, in the sense that they bind together specifically by means of two hydrogen bonds. In fact, the guanines recognize cytosines binding themselves by means of three hydrogen bonds. This reaction is known as

base pairing and it is the basis of two molecular mechanisms: replication and recognition (see Fig. 1.2). Replication: related to base pairing for the first time by Watson and Crick: April, 25. 1953 Nature".It has not escaped our notice that specific base pairing we have postulated immediately suggests a possible copying mechanism for the genetic material." Recognition: A DNA sequence is defined and described by each of the complementary single-strands which form the double-helix. Moreover, if they are separated, they can recognize specifically each other. This affinity reaction is known as hybridization. Together with the number of complementary bases which composes two single strands, many parameters influence their binding: temperature, ionic force, the number of C-G couples (which implies a stronger bond). In the literature there exist at least two nomenclature systems for referring to molecular elements involved in hybridization. Both use common terms "probes" and "targets". According to [2, 3] probe is the tethered nucleic acid with known sequence, while target is the free nucleic acid sample whose sequence or quantity is to discover. The DNA is expressed during the cell life by transcription of selected parts copied into the RNA molecule and then by translation of the RNA into proteins. Recognition of DNA (or RNA) sequence by hybridization is the key molecular reaction and analysis principle for genetic research and gene-bases tests. This dissertation concerns electronic-microfabricated solutions for automated, low-cost, easy-to-use tools to improve speed, efficiency, reliability and diffusion of DNA-based research and tests.

1.2 Genetic Analysis

Genetics and proteomic may lead to the development of extremely powerful tools. Benefits of genetic research in several scientific matters are enunciated as follows, according to the HGP: In Molecular Medicine to: improve diagnosis of disease, detect genetic predispositions to disease, create drugs based on molecular information, use gene therapy and control systems as drugs, design "custom drugs" based on individual genetic profiles. In Microbial Genomics to: rapidly detect and treat pathogens (disease-causing microbes) in clinical practice, develop new energy sources (biofuels), monitor environments to detect pollutants, protect citizenry from biological and chemical warfare, clean up toxic waste safely and efficiently.

1.2.1 Tracing the genome: achieving the genomic era

Human Genome Project

In June 2000, scientists announced the completion of the first working draft of the entire human genome. Lately, in April 2003 - the 50th anniversary of Watson and Crick's publication of DNA structure - the high-quality reference sequence was completed, marking the end of the Human Genome Project. The two-step analysis procedures which are at the basis of genome description are i) *mapping* and ii) *sequencing*:

Mapping means to make descriptive diagrams maps of each human chromosome. Mapping involves (1) dividing the chromosomes into smaller fragments that can be propagated and characterized and (2) ordering (mapping) them to correspond to their respective locations on the chromosomes. A genome map describes the order of genes or other markers and the spacing between them on each chromosome. Human genome maps are constructed on several different scales or levels of resolution. At the coarsest resolution are genetic linkage maps, which depict the relative chromosomal locations of DNA markers (genes and other identifiable DNA sequences) by their patterns of inheritance. Geneticists have already charted the approximate positions of over 2300 genes, and a start has been made in establishing high-resolution maps of the genome.

Sequencing: After mapping is completed, the next step is to determine the base sequence of each of the ordered DNA fragments. The completed map will provide biologists with a Rosetta stone for studying human biology and enable medical researchers to begin to unravel the mechanisms of inherited diseases. Much effort continues to be spent locating genes; if the full sequence were known, emphasis could shift to determining gene function. Technological advances are leading to the automation of standard DNA purification, separation, and detection steps. Sequencing procedures currently involve first Constructing Clones (Fig. 1.3). The next step is amplification, which can be performed in vivo, through a suitable host cell or in vitro by means of the Polymerase Chain Reaction (Fig. 1.4). PCR amplify a desired DNA sequence of any origin (virus, bacteria, plant, or human) hundreds of millions of times in a matter of hours. The reaction is highly specific, easily automated, and capable of amplifying minute amounts of sample. PCR has also had a major impact on clinical medicine, genetic disease diagnostics, forensic science, and evolutionary biology. The next step is to make the sub-cloned fragments into sets of nested fragments differing in length by one

nucleotide, so that the specific base at the end of each successive fragment is detectable after the fragments have been separated by gel electrophoresis (Fig. 1.5). This detection step can be performed by means of other techniques which may involve sequence recognition by hybridization [4].

Single Nucleotide Polymorphisms and the Hap-Map Project

When the HGP began officially in 1990 a heated debate started concerning which Genome had to be sequenced. Fortunately, geneticists were not forced to make this choice. During the accomplishment of the project, scientists have described not only a single human genome sequence, composed of little bits from many humans, but also some 3 million sites of variation mapped along that reference sequence (2001). The effort in localizing and determining these variations or 'polymorphisms', is related to the fact that genetics simply cannot exist without understanding their function. Genomes most often differs in terms of Single nucleotide polymorphisms (SNPs, snips) [5]. The 3 million known SNPs are found at a density of one SNP per 1.91 kilobases. This means that more than 90% of any sequence 20 kilobases long will contain one or more SNPs. Therefore, 93% of genes contain a SNP which implies that, at present, nearly every human gene and genomic region is marked by a sequence variation. In 2002 the International HapMap project started. Its goal is to compare the genetic sequences of different individuals to identify chromosomal regions where genetic variants are shared. The Project will help biomedical researchers find genes involved in diseases and responses to therapeutic drugs. Being able to "type" individual genomes and make comparisons will be essential to understand

- how variation shapes biochemical and cellular functions
- in illuminating past human evolution;
- dissecting the contributions of individual genes to diseases that have a complex, multigene basis;
- know how to implement patient care in relation to genetic variation (tissue and organ incompatibility, affecting the success of transplants);

The research of disease-related SNPs is carried on comparing the haplotypes in individuals with a disease to the haplotypes of a comparable group of individuals without a disease. If a particular haplotype occurs more frequently in affected individuals compared with controls, a gene

influencing the disease may be located within or near that haplotype. Common diseases such as cancer, stroke, heart disease, diabetes, depression, and asthma usually result from the combined effects of a number of genetic variants and environmental factors. According to an idea known as the common disease-common variant hypothesis, the risk of contracting common diseases is influenced by genetic variants that are relatively common in populations. More and more widely distributed genetic variants associated with common diseases are being discovered, including variants that contribute to autoimmune diseases, schizophrenia, diabetes, asthma, stroke, and heart attacks. Variation in genome sequences underlie differences in our susceptibility to, or protection from, all kinds of diseases; in the age of onset and severity of illness; and in the way our bodies respond to treatment.

1.2.2 Application of DNA-sequences detection

Gene tests (DNA-based tests)

Gene testing exams an organism's DNA, taken from cells in a sample of blood or, occasionally, from other body fluids or tissues. The most widespread applications are the search for DNA change that flags a disease or disorder, or for DNA sequences that could describe a reaction to drugs. A few types of major chromosomal abnormalities, including missing or extra copies or gross breaks and rejoinings (translocations), can be detected by microscopic examination. Most changes in DNA, however, are more subtle and require a closer analysis of the DNA molecule to find perhaps single-base differences. Genetic tests are used for several reasons, including: (i) carrier screening, which involves identifying unaffected individuals who carry one copy of a gene for a disease that requires two copies for the disease to be expressed; (ii) pre-implantation genetic diagnosis; (iii) prenatal diagnostic testing; (iv) newborn screening; (v) pre-symptomatic testing and confirmational diagnosis of a symptomatic individual; (vi) forensic/identity testing. For some types of gene tests, researchers design short pieces of DNA called probes, whose sequences are complementary to the mutated sequences (see Fig. 1.6). These probes will seek their complement among the three billion base pairs of an individual's genome. If the mutated sequence is present in the patient's genome, the probe will bind to it and flag the mutation. Another type of DNA testing involves comparing the sequence of DNA bases in a patient's gene to a normal version of the gene. Cost of testing can range from hundreds to thousands of dollars, depending on the sizes of the genes and

the numbers of mutations tested. Gene testing already has dramatically improved lives. Some tests are used to clarify a diagnosis and direct a physician toward appropriate treatments, while others allow families to avoid having children with devastating diseases or identify people at high risk for conditions that may be preventable. On the horizon is a gene test that will provide doctors with a simple diagnostic test for a common iron-storage disease, transforming it from a usually fatal condition to a treatable one. Limitations and ELSI (Ethical, Legal and Social Issues) The tests give only a probability for developing the disorder. One of the most serious limitations of these susceptibility tests is the difficulty in interpreting a positive result because some people who carry a disease-associated mutation never develop the disease. Scientists believe that these mutations may work together with other, unknown mutations or with environmental factors to cause disease. A limitation of all medical testing is the possibility for laboratory errors. These might be due to sample misidentification, contamination of the chemicals used for testing, or other factors. Few treatments or preventive strategies exist for patients testing positive for most gene tests. Unfortunately, knowledge of a gene mutation alone is insufficient information for researchers trying to devise intervention strategies. Researchers must first understand the normal function of the disease-associated gene(s) and determine how the mutation disrupts that function. Therefore, many in the medical establishment feel that uncertainties surrounding test interpretation, the current lack of available medical options for these diseases, the tests' potential for provoking anxiety, and risks for discrimination (by employers, insurers, commercial institutions, schools, army) and social stigmatization could outweigh the benefits of testing. Other important ethical issues are also very controversial, such as privacy and confidentiality, fairness in use of information, reproductive rights.

Expression analysis

When proteins are needed, the corresponding genes are transcribed into RNA (transcription). RNA polymerase II, together with the necessary transcription elongation factors, travels along the DNA template and polymerizes ribonucleotides into an RNA copy of the gene. The polymerase moves at a regular speed (approximately 30 nucleotides per second) and holds on to the DNA template efficiently, even if the gene is very long. At the end of the gene, the RNA polymerase falls off the DNA template and transcription terminates. The RNA is first processed so that non-coding parts are removed (processing) and is then trans-

ported out of the nucleus (transport). Outside the nucleus, the proteins are built based upon the code in the RNA (translation). The information contained in the nucleotide sequence of the mRNA is read as three letter words (triplets), called codons. Each word stands for one amino acid. During translation amino acids are linked together to form a polypeptide chain which will later be folded into a protein. The translation is dependent on many components, of which two are extra important. First of all; the ribosome which is the cellular factory responsible for the protein synthesis. It consists of two different subunits, one small and one large and is built up from rRNA and proteins. Inside the ribosome the amino acids are linked together into a chain through multiple biochemical reactions. The second component is the tRNA, a specialised RNA molecule that carries an amino acid at one end and has a triplet of nucleotides, an anticodon, at the other end. The anticodon of a tRNA molecule can basepair, i.e. form chemical bonds, with the mRNA's three letter codon. Thus the tRNA acts as the translator between mRNA and protein by bringing the specific amino acid coded for by the mRNA codon (see Fig. 1.7).

The study of gene expression on a genomic scale is the most obvious opportunity made possible by complete genome sequences of the model organisms, and experimentally the most straightforward. Four characteristics of the regulation of gene expression at the level of transcript (RNA) abundance account for the great value and appeal of genome-wide surveys of transcript levels. First, it is eminently feasible - DNA microarrays (see Chapter 2) make it easy to measure the transcripts for every gene at once. The second reason is the tight connection between the function of a gene product and its expression pattern. As a rule, each gene is expressed in the specific cells and under the specific conditions in which its product makes a contribution to fitness. Just as natural selection has precisely tuned the biochemical properties of the gene product, so it has tuned the regulatory properties that govern when and where the product is made and in what quantity. The logic of natural selection, as well as experimental evidence, partially provides that there is a sensible link between the expression pattern and the function of its gene product. Thirty years of molecular biology have provided numerous examples of genes that function under specific conditions and whose expression is tightly restricted to those conditions. Historically, transcript abundance is assayed by immobilizing mRNA or total RNA (electrophoretically separated or in bulk) on membranes and then incubating with a radioactively labelled, gene-specific target. If multiple RNA samples are immobilized on the same matrix, one obtains information about the quantity of a particular message present in each RNA pool. In the last ten years cDNA

arrays have altered this strategy in several ways. In an array experiment, many gene-specific polynucleotides derived from the 3' end of RNA transcripts are individually arrayed on a single matrix. This matrix is then simultaneously probed with fluorescently tagged cDNA representations of total RNA pools from test and reference cells, allowing one to determine the relative amount of transcript present in the pool by the type of fluorescent signal generated. Relative message abundance is inherently based on a direct comparison between a 'test' cell state and a 'reference' cell state; an internal control is thus provided for each measurement.

1.3 Figures

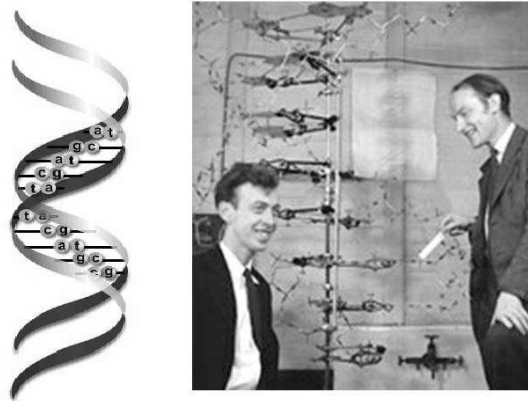


Figure 1.1: "The specific base pairing immediately suggests a possible copying mechanism for the genetic material" (Watson and Crick, 1953).

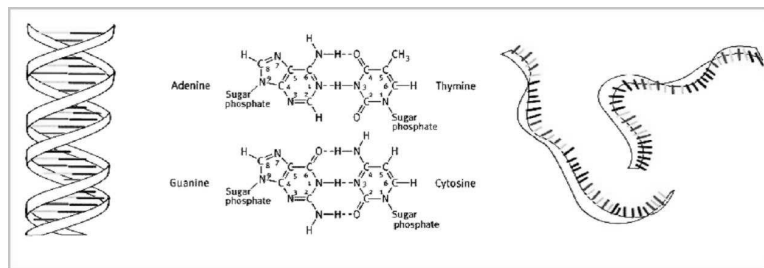


Figure 1.2: *Base Pairing* is the basis of two molecular mechanisms: replication and recognition.

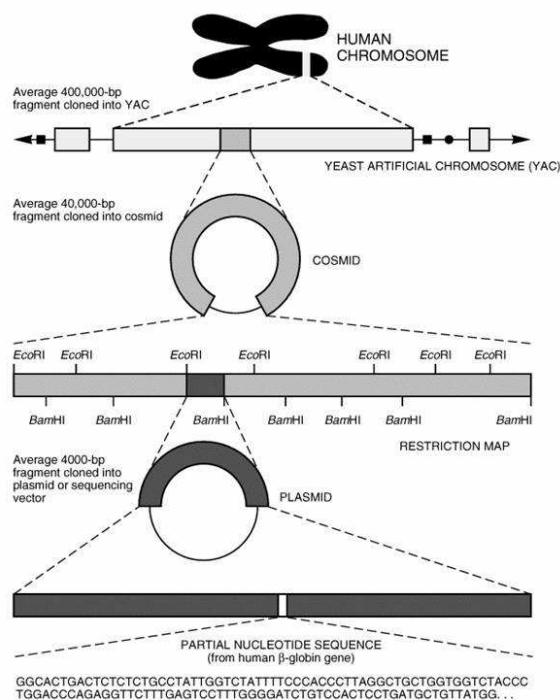


Figure 1.3: Cloning for Sequencing. Cloned DNA molecules must be made progressively smaller and the fragments subcloned into new vectors to obtain fragments small enough for use with current sequencing technology. Sequencing results are compiled to provide longer stretches of sequence across a chromosome.

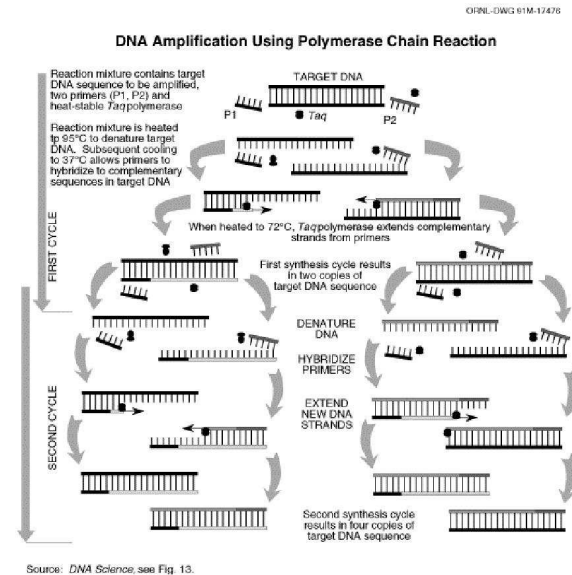


Figure 1.4: Amplification. Polymerase Chain Reaction. PCR is a process based on a specialized polymerase enzyme, which can synthesize a complementary strand to a given DNA strand in a mixture containing the 4 DNA bases and 2 DNA fragments (primers, each about 20 bases long) flanking the target sequence. The mixture is heated to separate the strands of double-stranded DNA containing the target sequence and then cooled to allow (1) the primers to find and bind to their complementary sequences on the separated strands and (2) the polymerase to extend the primers into new complementary strands. Repeated heating and cooling cycles multiply the target DNA exponentially, since each new double strand separates to become two templates for further synthesis. In about 1 hour, 20 PCR cycles can amplify the target by a millionfold.

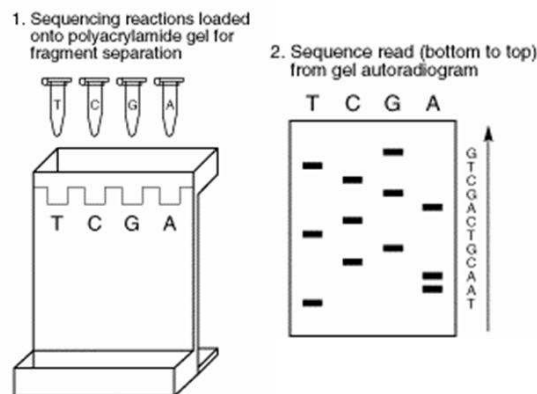


Figure 1.5: Standard Sequencing (Sanger Method): Dideoxy sequencing uses an enzymatic procedure to synthesize DNA chains of varying lengths, stopping DNA replication at one of the four bases and then determining the resulting fragment lengths. Each sequencing reaction tube (T, C, G, and A) in the diagram (1) contains (i) a DNA template, a primer sequence, and a DNA polymerase to initiate synthesis of a new strand of DNA at the point where the primer is hybridized to the template; (ii) the four deoxynucleotide triphosphates (dATP, dTTP, dCTP, and dGTP) to extend the DNA strand; (iii) one labeled deoxynucleotide triphosphate (using a radioactive element or dye); (iv) and one dideoxynucleotide triphosphate, which terminates the growing chain wherever it is incorporated. Tube A has didATP, tube C has didCTP, etc. For example, in the A reaction tube the ratio of the dATP to didATP is adjusted so that each tube will have a collection of DNA fragments with a didATP incorporated for each adenine position on the template DNA fragments. The fragments of varying length are then separated by electrophoresis (1) and the positions of the nucleotides analyzed to determine sequence. The fragments are separated on the basis of size, with the shorter fragments moving faster and appearing at the bottom of the gel. Sequence is read from bottom to top (2).

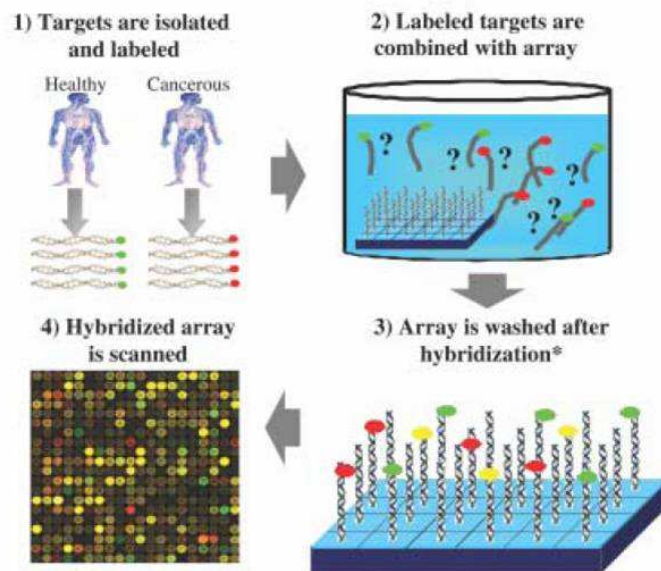


Figure 1.6: Gene test with microarray technology.

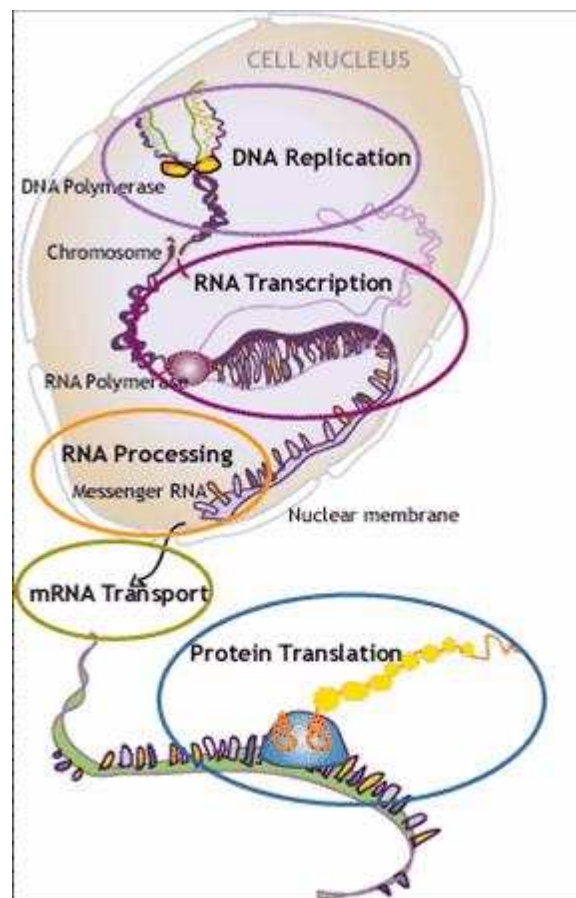


Figure 1.7: Gene Expression: from DNA to protein.

Chapter 2

MICROFABRICATED ELECTRONIC SENSORS FOR GENETIC ANALYSIS

2.1 Role of technology and electronics

In 1 we described the promising and in some cases already achieved accomplishment of genetic research based on the detection of a specific nucleotide sequence in solution. This can be a DNA strand extracted from a cell of interest or a DNA copied from an RNA which have been expressed by the cell in particular conditions (cDNA). The desire of the author is to give a feeling of the crucial role of electronics and technology in developing efficient, innovative and mass produced devices for nucleic-acids sequence detection. The scientific and technological areas which are involved in designing and implementing genetic assay may be listed as follows: (i) *element 1*: Technology, microfabrication and micro-machining of silicon and other materials; (ii) *element 2*: electronics and micro(nano)electronics; (iii) *element 3*: semiconductor sensors.

These elements would lead to

- miniaturization of reaction sites and cell (less sample and reagent) (Element 1)
- miniaturization of measurement system (less noise and portability) (Elements 1-2-3)
- high-parallelism (order of magnitude improvement in speed of analysis until the extreme achievements of a genome-wide screening (elements 1-2-3))

- integration of mechanical and fluidic functions for sample handling, delivery, mixing, purification, separation, amplification. (multi-functionality and stand-alone devices, easy-to-use devices) (element 1)- miniaturization. The small dimensions also reduce the amounts of carriers (reagents) necessary to conduct a chemical process: for miniaturized handling volumes are often in the nanoliter to picoliter range rather than the microliter range or larger in conventional experiments.
- batch production (low-cost mass-produced assays) (Elements 1-2-3)
- generation of electrical read-out from the sensor (a multitude of microelectronic circuits are available for electric signal conditioning and modification as amplification, filtering, modulation) (Elements 2-3) the electrical signal is very well suited for signal transmission (Elements 2-3)
- high performance sensors through the employment of ultra-sensitive electron devices (Element 3)

All of the listed characteristics, or a selection of them, may describe the so called Lab-on-a-chip technology, which aims at implementing miniaturized, stand-alone, low-sample and fast analysis tools. At present, only part of these issues have been considered and traduced in sensors or systems. Some general references on the issues related are [6, 7, 8].

2.2 Technology, microfabrication and micromachining of silicon and other materials

2.2.1 Pattern definition of high-density spots of different probes molecules on a substrate. DNA Microarray technology

The possibility of to attach and localize (and or address) receptors onto a substrate in a very precise and dense way has been a fundamental innovation achieved in early 90s. This technology lead to high parallelism of analysis with the possibility to test an eventually huge number of probes sequence at the same time and on the same substrate. In addition, probes

sites (or features) are very little and dense. At present, 1.2 cm^2 substrate may contain more than 500000 different probe sequences [Lipshutz, 1999]. Several techniques, with very different density results, are employed. The list that follows is in growing order of spot *density/cm*²

- Mechanical Micro-spotting 3000 *spot/cm*² probe cDNA (500-5,000 bases long) are immobilized to a solid surface such as glass using high-speed robot spotting and exposed to a set of targets either separately or in a mixture. This method, traditionally called DNA microarray, is widely considered as developed at Stanford University [9].
- Electric-Filed assisted immobilization (Nanogen, San Diego, California) (5000 *sites/cm*²) (see chapter 1) [10]
- Electro-immobilization by copolymerization (10000 *sites/cm*²) (Leti, Grenoble, France) [11]
- Inkjet technology (IBM) (10000 *sites/cm*²) [Bietsch, 2004] In this approach, a DNA sample is loaded into a miniature nozzle equipped with a piezoelectric fitting (or other form of propulsion) which is used to expel a precise amount of liquid from the jet onto the substrate. After the first jetting step, the jet is washed and a second sample is loaded and deposited to an adjacent address. A repeat series of cycles with multiple jets enables rapid microarray production. Bubble Jet Technology (Canon) (20000/cm²) [Okamoto, 2000] Photolithography (390000 features/cm²) (Affymetrix, Santa Clara, California) [Lipshutz, 1999]. The probe is synthesized either in situ : an array of oligonucleotide (20 80-mer oligonucleotides) or peptide nucleic acid (PNA) (labelled sample DNA, hybridized, and on-chip) or by conventional synthesis followed by on-chip immobilization. The array is exposed to the identity/abundance of complementary sequences are determined. The method, "historically" called DNA chips, was developed by Affymetrix, Inc, which sells its photolithographically manufactured wafers under the GeneChip trademark. Probe synthesis occurs in parallel, resulting in the addition of an A, C, T, or G nucleotide to multiple growing chains simultaneously. To define which oligonucleotide chains will receive a nucleotide in each step, photolithographic masks, carrying 18 to 20 square micron windows that correspond to the dimensions of individual features, are placed over the coated wafer. The windows are distributed over the mask based on the desired sequence of each probe (see Fig. 2.1).

The techniques listed above are employed in the so-called microarrays devices. Microarrays are defined here as monolithic, flat surfaces that bear multiple probe sites and each bear a reagent whose molecular recognition of a complementary molecule can lead to a signal that is detected by an imaging technology, most often fluorescence. Literature references to microarrays before 1995 concerned arrays of electrodes rather than arrays of different molecules. The first molecular microarray, reported in 1991, was composed of peptides, not DNA, and was not even identified as a microarray [12].

2.2.2 Microfluidics on chip

A number of basic fluidic components have been assembled in different ways to perform various chemical measurements. Many of these are based on electrokinetic transport principles, and include valves, mixing structures, chemical reactors, and chemical separation channels. In addition, chemical separation mechanisms have been miniaturized, including free-solution and gel electrophoresis, solvent programmed chromatography, isoelectric focusing, isotachopheresis, and two-dimensional separations based on liquid chromatography and free-solution electrophoresis. Surface interactions have been exploited for solid-phase extraction to process samples and for hybridization of target DNAs, and nanoliter-scale reactors have been demonstrated for continuous flow, stopped flow, and thermal cycling reactions [13]. Chips integration microfluidics may be made from plastic, glass, quartz, or silicon. Bulk and surface micromachining performed with sophisticated etching, patterning and deposition techniques are at the basis of channel implementation. One of the most interesting microfabricated implementation in chip is the PCR molecular amplification. This approach has been widely investigated exploiting the good properties of thermal conductivity of silicon and the possibility to easily integrate thermal resistances [14, 15] (see Figure 2.2).

- Cantilever-array production for mass and stress molecular detection techniques. Recent works have reported the observation that when specific biomolecular interactions occur on one surface of a microcantilever beam, the cantilever bends. The recent discovery of the origin of nanomechanical motion generated by DNA hybridization and protein-ligand binding provided some insight into the specificity of the technique. In addition, its use for DNA-DNA hybridization detection, including accurate positive/negative detection of one-base pair mismatches, was also reported [16]. This tech-

nology readily lends itself to formation of microarrays using well-known microfabrication techniques, thereby offering the promising prospect of high-throughput protein analysis (see Fig. 2.3).

- Porous material for sensing based on high surface/volume ratio. High surface/area materials technology is directed primarily towards the creation of inexpensive low bulk volume/area media for applications that involves chemical reaction on surfaces. High surface areas provide a mechanism to achieve detection sensitivities that are in the range of parts per billion on a short time scale [17].

2.3 Electronics and microelectronics

2.3.1 Electrical-addressing of conductive sites

Some examples of use of electrical addressing of probe-sites are here described:

- Functional probes immobilization: CEA-LETI and Cisbio International developed a CMOS platform able to address and polarize 128 test sites to perform electrochemical immobilization of probes by means of a pyrrole bearing an oligonucleotide. A local electrocopolymerization allows oligonucleotide probes to attach permanently on the electrode. Biocompatibility issue requires specific insulation layer and surface metal materials to form the electrodes. The design of the cells has been modified to be compatible with the pyrrole electro copolymerization step. It means that the voltage applied during this step has to be fully withstood by the CMOS structure.
- Enhanced immobilization and hybridization by electrical polarization: Nanogen's technology utilizes the natural positive or negative charge of most biological molecules. Applying an electric current to individual test sites on the NanoChip microarray enables rapid movement and concentration of the molecules. Through electronics, molecular binding onto the NanoChip-microarray is accelerated up to 1000 times faster than traditional passive methods. Nanogen's technology involves electronically addressing biotinylated probe samples for immobilization, hybridizing complementary DNA and applying stringency to remove unbound and non-specifically bound DNA after hybridization [18, 10] (see Fig. 2.4)

2.3.2 Electronic Circuits for signal detection and processing in biosensors application

Infineon developed a fully electronic 16×8 sensor array. The chip is based on a standard $0.5 \mu m$ CMOS process extended with additional process steps to form sensor electrodes made of gold. A single sensing site within these array consists of interdigitated gold electrodes (width = spacing = $1 \mu m$) arranged within a circular compartment (diameter = $250 \mu m$). Using a microspotter, single-stranded DNA probe molecules are spotted and immobilized at the Au surface. After immobilization, an analyte containing target molecules to be detected is applied to the whole chip and hybridization occurs in case of matching DNA strands. For read-out, a redoxcycling based electrochemical sensor principle is used: After a washing step, a suitable chemical substance (p-aminophenyl-phosphate) is applied and electrochemically redox-active compounds are created by an enzyme label (alkaline phosphatase) bound to the target DNA strands. Applying simultaneously an oxidation and a reduction potential to the interdigitated gold electrodes, a redox current between these electrodes occurs whose magnitude depends on the amount of double-stranded DNA at this sensor position. The circuits within each position allow operation over five decades, sensor currents between 10^{-12} A and 10^{-7} A are detectable [19] (see Fig. 2.5).

Motorola (Clinical Microsensors Division) developed a novel electronic detection format for nucleic acids that utilizes electronic instrumentation including a disposable DNA chip (see Fig. 2.6). Printed circuit board technology is used to manufacture chips with 14 exposed gold electrodes, each of which is wired to a connector at the chip edge. A solder mask defines the electrode diameter (250 or $500 \mu m$) and covers the lead to the connector. DNA capture probes are deposited as a mixed solution with the other components of the self-assembled monolayer (SAM). After deposition, chips are rinsed, dried, and sealed in a housing for hybridization. Signalling probes containing ferrocene moieties, redox active metal centres that facilitate the detection of nucleic acid targets in homogeneous assays that eliminate the need for separate labelling and washing steps, form the basis of this electronic detection platform. Hybridization is measured by alternating current voltammetry (ACV) [20].

2.3.3 Semiconductor sensors

The most relevant applications of semiconductor sensors in biomolecular detection can be summarized as follows:

Electrolyte/Insulator/Semiconductor structures

These include (i) one-dimensional vertical capacitor similar to MOS structures where metal has been substituted with an electrolyte conductive solution; (ii) Field effect transistors where the gate has been substituted as well. Such devices have been widely employed in the last twenty years in electrochemistry and analytical chemistry for ion and pH sensing. More recently great efforts have been done to detect DNA hybridization occurring at the interface between the electrolyte and the insulator. The detection is based on field-effect of DNA negative charge on the gate oxide [21, 22, 16, 23].

Other sensing devices

Several semiconductor sensing techniques have been tested for molecular detection. Some of them are here listed:

- Surface and Bulk Acoustic Wave Sensors [24]
- Fiber Optics [25]
- Nanowires [26]

2.4 Figures

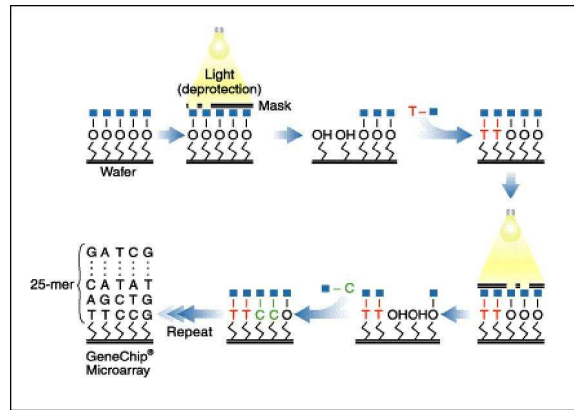


Figure 2.1: Photolithographic technique for in situ probe synthesis (Affymetrix, Santa Clara, California).

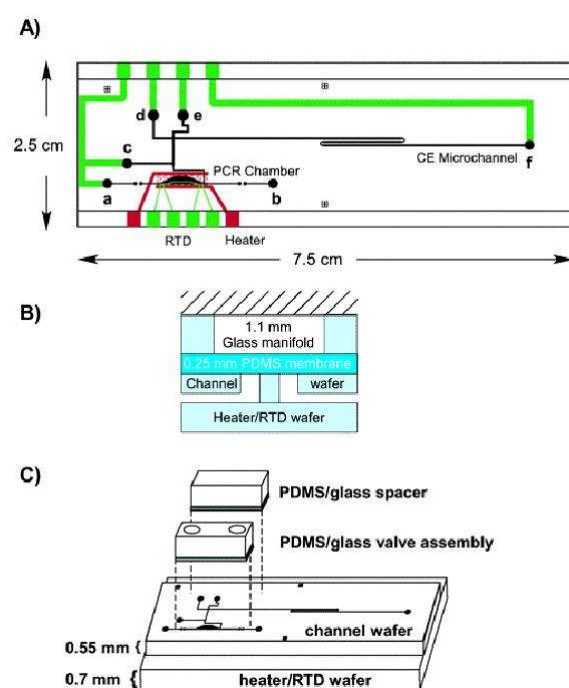


Figure 2.2: (A) Mask design for the portable PCR-CE microchip. The glass microchannels are indicated in black, the RTD and microfabricated electrodes are in green, and the heater (located on the backside of the device) is shown in red. The PCR chamber is loaded through reservoirs a and b. Reservoir c is the co-inject reservoir, d is the cathode, e is the waste, and f is the anode. (B) Schematic side view of a PDMS microvalve. (C) Exploded view of the assembly of the PCR-CE microchip, showing PDMS microvalve construction and PDMS gaskets [15].

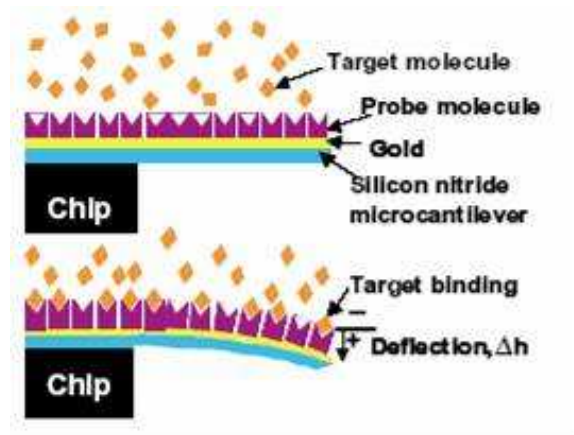


Figure 2.3: Bending of a cantilever due to the change in surface stress after target specific binding.



Figure 2.4: Motorola e-sensor.

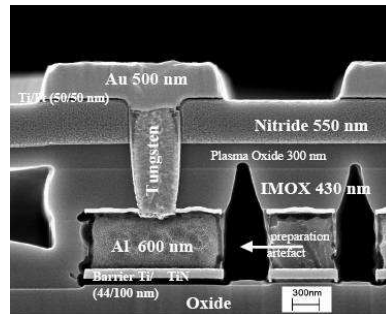


Figure 2.5: Integrated gold electrodes on silicon chips for DNA detection. Infineon Technologies.

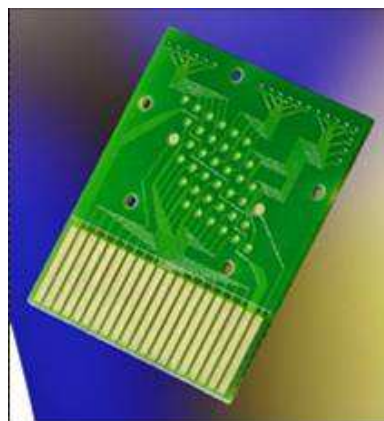


Figure 2.6: Nanogen Nanochip.

Chapter 3

BASIC THEORY OF ELECTROCHEMISTRY

3.1 Physics and Chemistry of the sensing principle

A capacitor is formed when two conducting plates are separated by a non-conducting medium. The capacitance depends on the size of the plates, the distance between the plates and the properties of the dielectrical layer, according to following equation:

$$C = \frac{S_0 \epsilon \epsilon_0}{d} \quad (3.1)$$

With S_0 = surface of the electrode, d = thickness of the dielectrical layer, ϵ_0 = dielectric constant and ϵ = relative dielectric constant. The dielectric constant is a physical parameter, while the relative dielectric constant depends on the material. It should be noticed that there is a large difference between the dielectric constant of water (about 78) and that of an organic coating (4-8). The formation of ultrathin organic films, e.g. alkanethiols, on bare metal electrodes leads to changes of the electrode capacitance. To preserve electrical neutrality, an opposite charge in the bulk solution has to compensate for the electrode charge and an electric double-layer is formed. The capacitance of the double layer depends on many variables including electrode potential, temperature, ionic concentrations, types of ions, oxide layers, electrode roughness, impurity adsorption. Further, this double layer can ideally be considered as a plate-capacitor. For description of this effect the Gouy-Chapman or Stern model is often used [27]. When the self-assembly of

the thiol molecules on the metal surface is complete, the double layer is shifted because of the new dielectrical layer. A further capacitor c_{thiol} is added to the electrical circuit. The total capacitance can be described by two capacitors c_{thiol} and c_{dl} in a serial arrangement, where c_{thiol} represents the capacitance of the alkanethiol and c_{dl} the capacitance of the ionic double layer (Gouy-Chapman layer) of the bulk phase. While the capacitance of the ionic double layer depends on the electrolyte concentration the capacitance of the thiol layer is nearly independent on the electrolyte concentration. By measuring the electrode capacitance of a bare metal electrode, the capacitance of the electric double-layer is obtained which according to the Gouy-Chapman theory is proportional to $c^{1/2}$. A simplified circuit diagram is shown in Fig. 3.1. Values for the electrode capacitance of bare gold electrodes are in the range of 1 to 100 $\mu F/cm^2$. This is related to the influence by Faradaiyic currents, which simulate a pseudo-capacitance [28] and in some cases can be much higher than the electrode capacitance. Self-assembled alkanethiols monolayers form an insulating coating. That additional capacitor requires a new circuit diagram. The major part of the potential drop will be in this case inside of the dielectric layer. Therefore, the capacitance of the Gouy-Chapman layer can be neglected. Also in the experiment the influence of the electrolyte concentration on the capacitance of alkanethiol layers was found to be very small. Because of the high ohmic resistance of the alkanethiol layer (about $500k\Omega$ [29]), the electric current after application of an AC voltage is almost purely capacitive, therefore the circuit diagram can be simplified. The advantage of the alkanethiol covered electrodes for capacitive biosensors is that electron transfer is strongly limited or even totally blocked, which allows an undisturbed capacitance measurement. Also, ion adsorption, electrolyte activity of redox active substances is minimized. After formation of the dielectric self-assembled alkanethiol monolayer, further molecules can be immobilized or adsorbed on this basis. Adsorption of molecules leads to an increase of the dielectrical thickness of the organic layer, and therefore decreases the electrical capacitance. If the specific capacitance of the uncovered receptor (no analyte is present) layer is C_0 , follows for the capacitance of this layer covered partly with analyte (specific capacitance C_{ads})

$$\frac{\Delta C}{C_0} = \frac{S_{ads}}{S_0} \frac{c_0}{c_0 + C_{ads}} \quad (3.2)$$

With S_{ads} = surface covered with analyte.

3.2 Sensing layer formation on electrodes

The modification of a transducer surface with an organic interface is one of the critical steps in biosensor preparation. It can be achieved by polymer-coating, by electrochemical polymerisation (e. g. polypyrrole), or of self-assembled monolayers. SAMs are molecular assemblies that are formed spontaneously by the immersion of an appropriate substrate into a solution. A series of SAMs are known in literature, including organosilicone on hydroxylated surfaces as SiO_2 on Si , Al_2O_3 on Al or glass [30], sulphur containing compounds (R-SH, RS-SR, R-S-R) on metal surfaces, amines on platinum [31].

3.2.1 Organosilicon derivatives

The reaction of alkanesilanes of the general structure $RSiX_3$, R_2SiX_2 or R_3SiX , where R is a carbon chain that can be functionalised with, e. g., amino, carboxy or pyridyl groups, and X is chloride or hydroxy with hydroxylated surfaces as SiO_2 , SnO_2 or TiO_2 , is well established. A schematic view of this structure is shown in Fig. 3.2. The formation of the self-assembled monolayer is an in situ formation of polysiloxane, which is connected to surface silanol groups via Si-O-Si bonds. The typical preparation is very easy: immersion of a hydroxylated surface into an organic solution of the organosilicon derivatives for a few hours. Even multilayers, i.e. three-dimensional polymer networks, can be built by introduction of further hydroxy groups (e. g. tetrahydroxysilane) into the structure. In consideration of these qualities, a large variety of sensors and biosensors are nowadays described in the literature [32].

3.2.2 Thiol Layers

The first paper on the formation of self-assembled monolayers of dialkanesulfides (RS-SR) on gold surfaces was published in 1983 by [33]. In the following years, numerous publications on this topic displayed its interesting properties for a variety of applications. In this chapter a short overview is presented. Chemisorption of sulfur-containing compounds, especially thiols (R-SH), on gold [34], silver [35], have been investigated. Also, alkanethiols on copper and silver are described to form well ordered and closely packed systems, the main scientific interest was focused on gold surfaces. The fact that gold does not have a stable oxide, and thus can be handled in ambient conditions, is a major reason. Further advantages of this noble metal are high oxidation stability, easy cleaning

procedures, well-defined surfaces, i.e. Au (111) or Au (100), and nearly defect-free SAMs. Bain et al. in 1989 reported on the effect of the formation of ultrathin layers on gold by comparison of different organic compounds, for example disulfides, sulfides, isonitriles or trialkane phosphines. They found the thiol group to undergo the strongest interaction with the gold surface, which are even 150 kJ/mol or higher [36]. This is in the range of covalent bonds as known in organic chemistry (e. g. $S-S$ 226 kJ/mol). The structure of long-chain chemisorbed alkanethiols with more than nine methylene groups is significantly different from the structure of short-chain alkanethiols. Long-chain compounds are postulated to exist at room temperature in crystal-like periodicity, while for short-chain compounds a liquid state is claimed. The symmetry of sulfur atoms in a monolayer of alkanethiols on mono-crystallised (111) gold is hexagonal, with a S-S spacing of about 5 \AA , and a calculated area of 21.4 \AA^2 (Fig. 3.3) [37]. The chains are in all-trans conformation and have an angle of inclination in the range of 25 to 30° (Fig. 3.3) [38]. Also, the preparation of thiol monolayers on a metal surface is simple. Clean surfaces (wafers or wires) are dipped into dilute thiol solutions (typically 10^{-3} mol/l). The choice of the organic solvent, ethanol or chloroform are mostly used, and the incubation time depends on the solubility and the chain length of the thiol. Alkanethiols show no further changes after 6 to 8 hours. Some working groups connect a formation of good layers already after one hour. In case of disulfides the adsorption time is about two times longer. This close-packed layer has excellent insulator properties, which can be proved, i.e. by cyclic voltametry [34], ellipsometry, contact angle or impedance measurements. SAMs are nearly defect-free and produce an ideally polarizable ultrathin basis. Alkanethiols with carboxy-, amino- or other head groups can be used as coupling positions for the immobilization of receptor molecules by a variety of methods. Therefore, self-assembled monolayers of alkanethiols seem to be an optimal system for the preparation of capacitive (affinity) sensors.

3.3 Previous work on Interface capacitance sensing

Capacitive interface detection of DNA hybridization is a label-free, fully electrical technique, thus it represents in principle the simplest, most direct, hence also best solution. In this field, bio-functionalized gold electrodes have been used in connection with electrochemical impedance

spectroscopy performed with a standard three-electrode system. A significant example of this approach [29] exploits single crystal gold surface modified with a self-assembled mono-layer of alkanethiols, used as linker molecules for DNA probes to form a compact, stable and dense layer, that featured an area of 8.56 mm^2 and a capacitance of about $2 \mu\text{F}/\text{cm}^2$. However, three-terminal techniques are too complex for cost-effective fully integrated solutions. Therefore, two-electrodes alternative, such as that of interest for this work, have also attracted significant interest. For example a two-electrode set-up using 2.4 mm^2 gold- and an Ag/AgCl counter- electrode has been studied. In this case, gold was covered with a 24-base oligonucleotides layer, realized by means of alkanethiols, and the interface exhibited ideal capacitive behaviour in the $10 - 100 \text{ Hz}$ frequency range [39]. As for the effects of DNA hybridization, a capacitance decrease before and after insertion of 179-base long target molecule has been observed [Berggren, 1999] in a flow cell containing a gold surface of 7.065 mm^2 covered with 26-base complementary oligonucleotides. Furthermore, interface capacitance has been measured in a three-electrode set-up by applying a 50 mV potentiostatic step and measuring the current in the circuit. The interface capacitance, as well as the series resistance of the system, have been extracted observing the transient response. Comparisons between surface capacitance values reported in the literature can be misleading as they are strongly affected by the electrolyte parameters, by the alkanethiol chain length and most of all by the effective surface which depends on the electrode surface roughness. Nevertheless, capacitance of bio-modified gold-electrodes is expected to vary between 1 and $5 \mu\text{F}/\text{cm}^2$. As far as integrable capacitance methods are concerned, recently an advance in the state of the art has been made [40] demonstrating that DNA hybridization can be detected by measuring interface capacitance with a two-gold-electrode system (without the use of a reference electrode). In any case, all the works mentioned above have been based on measurements performed on gold electrodes larger than 2 mm^2 . In contrast, several attempts to perform DNA detection on micro-fabricated devices has been based on Electrolyte-Insulator-Semiconductor structures [21, 22, 16, 41, 23]. In these cases a reference electrode acting as control gate has been placed in the solution to allow electrical polarization. Probe molecules have been attached covalently or by absorption on the insulator surface (or on a thin metallic layer deposited on it) to form a sensing molecular layer affecting the interface potential. The binding event can be detected by impedance measurements of the this structure with a two- or three-electrode setup. Ideal capacitive behaviour has been observed [21] between 10^2 and 10^4 Hz .

Alternatively, the field-effect has been used on transistor-like devices by polarizing the semiconductor and by measuring the current change flowing between drain and source. The EIS approach is very attractive, because the transduction device integrates the sensing element and can be easily reduced in dimensions. However, it presents problems related to the counterions screening while detecting intrinsic molecular charge at the insulator/solution interface.

3.4 Impedance measurement technique

3.4.1 Standard Methods. Impedance Spectroscopy

Part of the experiments shown in this work were performed by measuring the changes of electrode capacitance or even the whole impedance spectra. It offered the possibility to monitor the immobilization of DNA probes as well as the DNA target hybridization on the electrodes. Electrochemical impedance is a general parameter for the measurement of circuit elements with a complex behaviour, which do not follow the basic concept of the ideal resistor ($R = V/I$). It is usually measured by applying an AC potential to an electrochemical cell and measuring the current through the cell. When a sinusoidal potential excitation is applied, the response to this potential is an AC current signal, containing the excitation frequency and its harmonics. This current signal can be analyzed as a sum of sinusoidal functions (Fourier series). Usually, electrochemical impedance is measured by using a small excitation signal. Therefore lock-in amplifiers or frequency response analyzers can be used. In a linear or pseudo-linear system, the current response to a sinusoidal potential will be a sinusoid at the same frequency but shifted in phase (see Fig. 3.4). The excitation signal, expressed as a function of time, has the form:

$$E(t) = E_0 \cos(\omega t) \quad (3.3)$$

where $E(t)$ is the potential at time t , E_0 is the amplitude of the signal and ω is the radial frequency ($\omega = 2\pi f$). The response signal $I(t)$ is shifted in phase and has a different amplitude I_0 .

$$I(t) = I_0 \cos(\omega t + \phi) \quad (3.4)$$

According to previous equations a generalized Ohms law for the impedance of the system was formulated.

$$Z = \frac{E(t)}{I(t)} = \frac{E_0 \cos(\omega t)}{I_0 \cos(\omega t + \phi)} = Z_0 \frac{\cos(\omega t)}{\cos(\omega t + \phi)} \quad (3.5)$$

where the impedance Z is expressed in terms of a magnitude Z_0 and a phase shift ϕ . Using Eulers relationship:

$$\exp(i\phi) = \cos(\phi) + i\sin(\phi) \quad (3.6)$$

the impedance can be expressed as a complex function. Therefore, the potential (E), current response (I) and impedance (Z) are described as

$$E(t) = E_0 \exp(i\phi t) \quad (3.7)$$

$$I(t) = I_0 \exp(i\phi t) \quad (3.8)$$

$$Z = \frac{E(t)}{I(t)} = Z_0 \exp(i\phi t) = Z_0(\cos(\phi) + i\sin(\phi)) \quad (3.9)$$

Three major plotting graphs are used in impedance analysis: the Nyquist plot (real part of impedance vs. imaginary part), and the Bode plot (impedance with log frequency vs. both absolute value of impedance and phase-shift). Electrical circuit theory differentiates between linear and non-linear systems. Electrochemical cells in general have a non-linear behaviour. For such systems a doubling the voltage (input) will not be followed by double the current (output). If the system is non-linear, the current response will contain harmonics of the excitation frequency. However, electrochemical systems can be considered in first approximation as pseudo-linear, if only a small AC signal is applied to the electrochemical cell; a pseudo-linear segment of the cells current vs. voltage curve. Electrochemical impedance spectroscopy can be used for capacitance and conductivity measurements. While changes in solution resistance of the electrochemical cell causes changes in conductance, capacitance changes only occur because of modification of the electrodes surface. An exhaustive compendium of Impedance Spectroscopy can be found in [42].

3.5 Figures

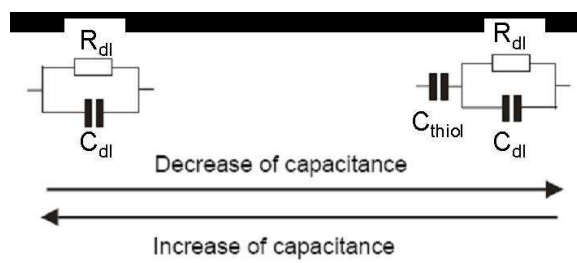


Figure 3.1: Adsorption and desorption of alkanethiols on an electrode. The self-assembly results in a dielectrical layer with insulating properties, which leads to a decrease of capacitance. C_{thiol} represents the capacitance of the alkanethiol and C_{dl} the capacitance of the ionic double layer of the bulk phase. If the thiols desorb from the electrode opposite direction molecules desorb from the structure, the capacitance increases. This could be achieved for example by applying a very negative potential, see electrically addressable immobilization.

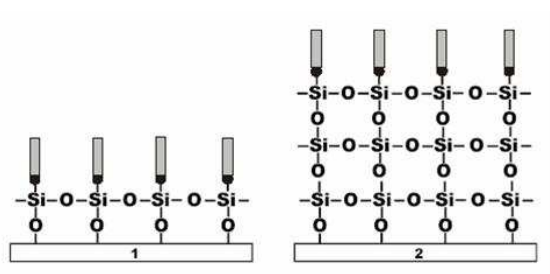


Figure 3.2: Self-assembled monolayer (1) and multilayer (2) of alkanetrihydroxysilane on a hydroxylated surface. The molecules in the layers are connected both to each other and to the surface by chemical bonds.

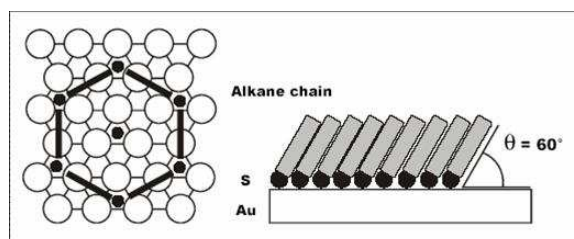


Figure 3.3: Proposed coverage scheme and orientation of alkanethiols on a gold (111) surface.

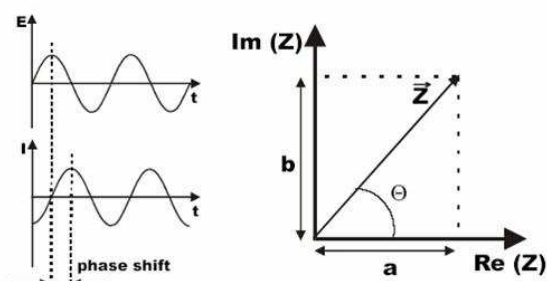


Figure 3.4: (left) Sinusoidal current response in a linear system. (top) Vector diagram of the phase-sensitive current analysis. The AC current can be presented as a sum of two vectors: conductive current (a) and capacitance current (b). A phase angle θ can be calculated as $\arctan(b/a)$. If the conductive component is zero, $\theta = 90^\circ$, it corresponds to ideal capacitance behaviour.

Chapter 4

ELECTRICAL TECHNIQUE FOR DNA DETECTION ON PASSIVE GOLD MICROELECTRODES ON SILICON

This Chapter presents the experimental characterization of two-terminal micro-fabricated capacitors for microarrays with electrical sensing of label-free DNA. So far [40], such a concept has been demonstrated only in experimental set-ups featuring dimensions much larger than those typical of micro-fabrication. Therefore, this work investigates: a) the compatibility of the silicon microelectronic processes with biological functionalization procedures; b) the effects of parasitics when electrodes have realistic dimensions; c) measurement stability and reproducibility; d) the possibility of a fully integrated, stand-alone device. The obtained results clearly indicate that two-terminal capacitive sensing with fully integrated electronics represents a realistic prospective for DNA label-free detection/recognition.

4.1 Passive Microarrays vs Active Matrices

Passive DNA chips based on optical detection of the hybridization of labelled DNA [43] and capable of testing hundreds of thousands dif-

ferent probes in parallel are technologically mature devices already on the market. The targets are labelled with chromophores molecules and spread on the array surface. Successively, all this material is removed and only the (labelled) targets that have hybridized with complementary probes remain immobilized on their specific sensing sites. Finally, the device is observed optically to localize the chromophores, revealing where hybridization has taken place, i.e. the "optical" signature of the analyzed DNA. Often, the resulting optical image is not immediately recognizable, because hybridization can involve many adjacent sites resulting in a complex optical pattern to be resolved by means of adequate image processing. This technology presents two main drawbacks: cost of the instrument to detect and resolve the optical signal; necessity of a labelling step, with the need of additional reagents and the possibility of sample pollution. To eliminate the former problem, methods based on the generation of electrical signals upon hybridization have been developed. However, some of these techniques are not label-free, as they use mediator elements to generate the electrical signals [44, 45].

4.1.1 Label-free techniques

Our interest is for label-free devices with fully integrated electrical reading, a subject largely still at the research and development level. Within this category, another distinction can be made between devices exploiting active elements as sensor and transducer (producing electrical signals) and those featuring passive sensing elements, in practice capacitors made sensitive to DNA hybridization. The former case is scientifically very interesting, but has significant disadvantages in terms of noise, sensitivity and repeatability. Therefore, we are currently pursuing a solution based on electrical measurements of DNA sensitive capacitances, already shown to be viable at the level of discrete lab prototypes. However, current research on label-free, fully electrical devices has not yet satisfactorily investigated the main problems posed by micro-fabrication, namely: a) compatibility of bio-functionalization procedures with silicon microelectronic processes; b) effects of the large parasitics, inevitably present in the structures; c) stability and repeatability of the measurements; d) possibility to integrate reading circuits together with the sensors (so as to achieve fully integrated, stand-alone devices).

4.2 Bio-functionalization of micro-fabricated electrodes

This Section investigates the compatibility of bio-functionalization procedures with silicon micro-electronic processes. To this aim, first the basic principles of the functionalization techniques are briefly illustrated, then the key problems are analyzed.

4.2.1 Microfabricated electrodes

The experiments here presented have been performed on micro-fabricated test-chips featuring 1800 μm^2 gold electrodes deposited by sputtering and contacted with buried aluminum wires. Two different chip types have been tested. The first-one (STM CH268A) hosted an array of twenty identical gold electrodes of 1800 μm^2 and a unique counter electrode surrounding the others. The second one (STM CH402A) instead presented forty-eight electrodes and the counter. The surface structure of electrodes have been observed with Atomic Force Microscopy (Fig. 4.1)

4.2.2 Basic process

The basic processes involved in gold bio-functionalization for DNA detection are illustrated in Fig. 4.2. First, a careful pre-cleaning must be performed (*step 1*) to allow efficient attachment of tethered probes by means of Au-S bonds. Gold is extremely reactive and has to be freed from organic and inorganic molecules. Cleaning can be attained by oxygen plasma [Berggren, 1999], chemical etching with hot piranha solution bathes (1 : 3 H_2O_2/H_2SO_4) [39, 46], ultrasonic bathes [Peterlinz, 1996], electrochemical stripping techniques [29]. Mechanical polishing with alumina [47] or silicon carbide powders [29] has sometimes been employed to improve surface cleaning and to provide better electrode flatness. In fact, Losicet al. have found that surface roughness can cause an increase of defects in the molecular layer. Immediately after cleaning, the surface must be bio-functionalized with the sensing layer of probe-molecules (*step 2*). Several biochemical procedures have been proposed and tested to bind covalently short oligonucleotide chains on gold surfaces and create dense and homogeneous bio-molecular layers. The most efficient techniques employ an anchoring alkanethiol chain attached to an extreme of the sequence of nucleic acid. The thiol group provides a covalent bond with gold atoms and the small alkanic chain acts (depending on its length)

to form a compact layer. Molecules can be spotted by micro-spotting, inkjet printing [Bietsch, 2004] or deposited on the surface by immersion (dipping) in a micro-molar concentration solution [46]. The solvent where molecules are dissolved should contain salts to avoid electrostatic repulsion between charged molecules during layer formation. Then, the surface must be rinsed with ultra pure water or buffers to remove non-covalently attached probe molecules and to obtain a layer of ordered and well-oriented receptors (*step 3*). Then, gold can be dried and briefly stored. DNA bio-affinity recognition reaction (*step 4*) is performed by immersing the electrodes modified with different probes sequence in a buffer solution with suitable physical and chemical parameters (temperature, ionic strength, pH). The solution conditions are extremely important to ensure efficient and specific sensing. The formation of the double helix is a reversible reaction, thus the target can be eventually desorbed from the surface by a heat treatment which consists of rinsing the electrode with hot solution of low ionic strength to observe an increase in capacitance (opposite signal) (*step 5*). At this stage, hybridization specific binding can be repeated. Beside bio-chemical procedures, electrical characterization also involves immersion of gold electrodes in a conductive (ionic) solution and polarization with low-voltage levels. Electrical measurements are usually performed before and after complementary sequences recognition.

4.2.3 Compatibility

Some of the procedures illustrated in Fig. 4.2 may permanently damage the silicon chip hosting the electrodes as well as the devices and the interconnects. For example, concerning step 1, polishing and strong acid surface cleaning should be avoided. In fact, electric tests of wires conductivity performed after 30 sec of piranha surface cleaning indicated extensive damages (see Fig. 4.3). Thus low-impact bio-functionalization procedures must be developed to limit damages. To this purpose, the cleaning procedures have been restricted to ethanol bathes, ultrasonic bathes and oxygen plasma cleaning, which are standard processes for silicon chips. Immobilization of single-stranded probe sequences has been achieved by exposing the electrode surfaces for 72 h to a 3 μM molecule concentration in a phosphate saline buffer solution (10 mM phosphate buffer and 0.3 M NaCl). However, a much shorter immersion time can be sufficient, provided a proper optimization of the chemical conditions; in particular a 90% layer formation [Gergiadis, 2000] can be obtained with a 5 h functionalization process in a 1 M NaCl buffer.

Nevertheless, an ideal immobilization process would be driven by microspotting or inkjet printing techniques to limit the wet chip surface. Probe molecules have been synthesized as 30-base thiol-modified oligonucleotides (5'gatcatctacgccggaccggcatcgtgg-3') with $(CH_2)_6 - SH$ at the 5' position. After exposure the electrodes have been rinsed thoroughly with Milli-Q deionized water and immersed in the annealing buffer (0.01 M EDTA, phosphate 0.01 M and 0.5 M NaCl) for electrical measurement. Hybridization has been performed at room temperature by spreading overnight on the chips a 3 μM sample molecule concentration in the annealing buffer. Molecules have been expected to bind to probes on the surface thanks to their strand of complementary sequences (target sequence: 5'-ccacgatgcccgggtccggcgtaga-3'). The chips have been rinsed with the same buffer and measured again. The processing steps outlined above can be used as the basis for building a front-end biofunctionalization process, which is fully compatible with standard CMOS-type silicon technology.

4.3 Experimental Results

The results have been described by means of an equivalent circuit to investigate the role of parasitic capacitances, interface charge-transfer resistances and series resistances; the stability and reproducibility of the capacitive elements involved in detection. In addition, we have also investigated another measurement approach, comparing the result obtained with the impedance analyzer to those obtained by means of the charge-based capacitive technique described in [48, 40], that is suitable for integration on the same chip as the capacitive sensors (although in the present work no attempt has been made to integrate sensors and reading circuitry).

4.3.1 Complex impedance measurements

The bio-functionalization process introduces insulating layers between electrode and solution and the value of the capacitive component of the surface impedance is strongly affected by their chemical-physical characteristics. When DNA hybridization occurs, target molecules are blocked near the surface and change the structure of the interface. In particular they increase the distance between electrode and solution, thus modifying surface impedance. The aim of the proposed DNA sensing technique is to measure two-electrode cells and to analyze the capacitive behaviour

of the interfaces before and after hybridization to observe the change that are lead by hybridization.

A high precision impedance analyzer (Agilent 4294A) has been employed to characterize electrochemical cells formed by two micro-gold electrodes integrated on the same chip and immersed in a conductive solution. The cells have been electrically characterized. In the frequency range from 100 Hz to 1 MHz (400 measurement points distributed in logarithmic scale) a 20 mV sinusoidal signal amplitude has been applied between the two electrode. For each frequency, data describing complex admittance $Y(\omega)$ have been obtained.

$$Y(\omega) = \frac{1}{Z(\omega)} = G(\omega) + jC_P(\omega) \quad (4.1)$$

Where ω is $2\pi f$. The Nyquist plot ($-Im(Z(\omega))$ vs $Re(Z(\omega))$) corresponding to a system of two identical gold electrodes is traced in Fig. 4.3 starting from 1 MHz down to 100 Hz . The experimental points in the frequency range from 1 MHz to 10 kHz have been traced in Fig. 4.4 a describing an almost complete semicircle. For lower frequencies a second capacitive element dominates and the resistance in parallel to such capacitance is very high, since the second semicircle is left incomplete for frequency higher then 100 Hz . The behaviour of the two-electrode system can be interpreted with a simple four-element equivalent circuit (see Fig. 4.5) [42], that has been used to fit the experimental points as shown in in the same figure (Bode plot). A small capacitive element (CG) is originated by the geometrical capacitor made of the two electrodes and by other parasitics as wire capacitances. This value depends on the configuration of the two electrodes and by the permittivity of the solution. Moreover, the solution is conductive and it gives a resistive parameter dependent on salts concentration. This contribute can be added to the other parasitic series resistance of the system (wires) and counted in a general parameter R_S . When the interface is not exchanging charge with the solution, the two gold/solution interfaces are characterized by a high resistance parameter (R_{INT}) and a capacitive parameter (C_{INT}). R_{INT} is expected to be very high for microelectrodes and C_{INT} , which depends strongly on the bio-layer characteristics, is expected to have a surface density between 0.1 and 1 $pF/\mu m^2$. The capacitive elements of the interface C_{INT} is frequency dependent. Nevertheless, they can be modelled and extracted as Constant-Phase Elements (CPEs), which can be described by a couple of parameters Q and α as [MacDonald, 1987]:

$$CPE = \frac{1}{(j\omega Q)^\alpha} \quad (4.2)$$

The $Z(\omega)$ is described by two main RC contributes: a higher one related to C_{INT} and RINT and a smaller one that comes from CG and RS. According to the complex impedance theory [MacDonald, 1987], the R_{INT} - C_{INT} couple will be measured at low frequencies, where RC of higher value dominates. These parameters are defined by the contributes of both interfaces in solution. In particular, if the electrodes were identical, C_{INT} would be the half of each single interface capacitance, while R_{INT} would be the double of each interface resistance. Results have been obtained on chip STM CH268A with an electrode configuration employing one of the electrodes of the array (see Fig. 4.1) and the surrounding counter one. The CPE originated by the gold/solution interfaces can be extracted by fitting the Bode plot of $-Im(Z(\omega))$ at low frequency. Fig. 4.6 shows the Bode plot of the imaginary part related to a chip with non-modified gold electrodes and a chip modified with single-stranded receptors chains. A decreasing value of (Q) after bio-modifications has been found, as already reported [40]. This difference can be observed at low frequency where the interface parameters plays a dominant role. Experimental curves related to bio-modified gold electrodes before and after complementary DNA recognition have been plotted (Fig. 4.7). From the extracted values reported in Tab 4.1 (extraction frequency range: 40 Hz-2000 Hz) a further decrease of (Q) can be deduced after target molecules surface adsorption. The stability of bio-modified gold surfaces has been tested over time. The imaginary part of the impedance is plotted in Fig. 4.8 for three measurements taken every fifteen minutes. For chip STM CH268A, impedance plots of gold electrodes before immersion in solution have been traced to define the role of resistance and capacitance parasitics. Geometric capacitance can reach 80 pF when measuring connecting an electrode and his counter electrode. Moreover, 10 pF have been measured for geometric capacitance of two near gold array electrodes. Parasitic capacitances are not negligible compared to interface constant phase elements. However, Impedance Spectroscopy can easily separate in frequency these capacitance contributes thanks to the large difference between the two resistances. On the contrary, a total capacitance measurement technique could not. In this case, issues related to the parasitics variability between different chips should be taken into account as well as their stability during time.

4.3.2 Integrable circuitry

This section investigate the possibility to measure the variation of capacitance induced by DNA hybridization by means of a simple circuits, suitable for easy integration in standard CMOS technology, in the prospective of a fully integrated, stand- alone DNA micro-arrays.

The results of the previous section suggest that interface capacitance components in microfabricated devices should be significantly affected by DNA hybridization. Therefore, we have applied the Charge-Based Capacitance Measurement (CBCM) technique [40] to the microfabricated devices of this work to verify that it is not invalidated by the presence of large parasitics and unexpected phenomena at chip level. The capacitance value obtained with this technique accounts for the total capacitance of the two-electrode system [40], which is a composition of all capacitive contribution of the chip. Moreover, the interface capacitances C_{INT} has a non-ideal capacitive behavior and they are correctly described by a Constant Phase Element (CPE) which takes into account the frequency dependent behaviour. Consequently the measured result of capacitance values represents an average effect. Consequently, no attempt has been made to compare absolute capacitance value obtained with the two employed measurements set-up. Nevertheless, consistent variation after DNA detection of the Q parameter extracted from impedance measurements and the total capacitance obtained with the CBCM setup have been found. The CBCM technique has been employed to detect the decrease of the interface capacitive component after hybridization. Two couples of identical array-electrodes of chip STM CH402A have been contacted and immersed in solution to form the electrochemical cell. The results obtained are reported in Tab. 4.2 showing a capacitance decrease between 18% and 37% when complementary sequences hybridize with probes on the surfaces after an overnight complementary-sequence solution exposure. When non-complementary sequences are used or when no DNA at all is present in the sample, no decrease of interface capacitance can be detected but only a slight increase.

4.4 Tables

Table 4.1: Extracted values of interface CPE before and after hybridization. A decrease of the Q parameter is observed, while an increase of the parameter is observed.

	Before Hyb.		After Hyb.	
	Q (pF)	α	Q (pF)	α
Chip1	997	0.905	736	0.926
Chip2	667	0.955	649	0.948

Table 4.2: Percentage decrease of two-electrode interface capacitances after specific binding between probes on electrodes and complementary target sequences. In case of no complementary sequence or of DNA-free sample no decrease can be detected. Instead a slight increase can be observed. The last row shows the negligible decrease of capacitance due to non specific adsorption of DNA target on bare gold electrodes (no probes were previously attached on the surface).

Tested sample	Decrease of Capacitance (%)
Complementary sequence	37.7
Complementary sequence	29.5
Complementary sequence	18.3
Non-Complementary Sequence	-5.2
DNA-free sample	-6.2
DNA-free sample	-3.7
DNA target on bare electrodes	1.8

4.5 Figures

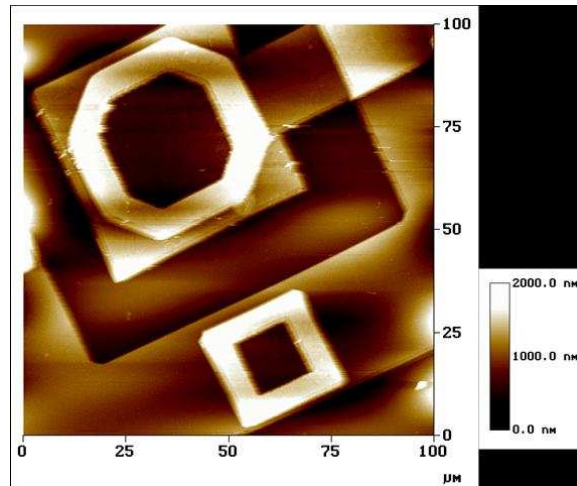


Figure 4.1: Atomic Force Microscopy Measurement of the surface of the chip in correspondence of gold exposed electrodes.

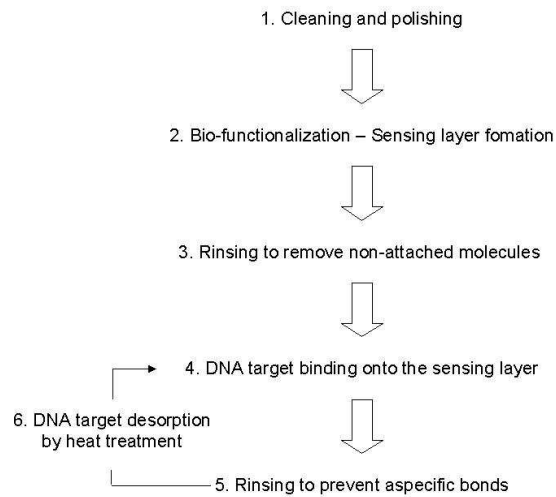


Figure 4.2: Basic Process of bio-modification of gold microfabricated electrodes from probe deposition, target detection and successive desorption.

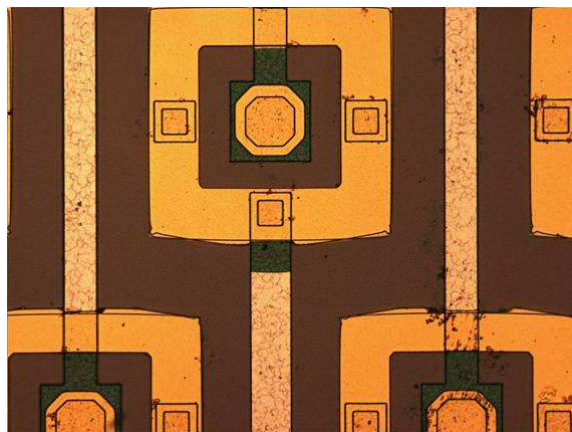


Figure 4.3: Evidence of extensive damages caused by piranha cleaning of the chip surface.

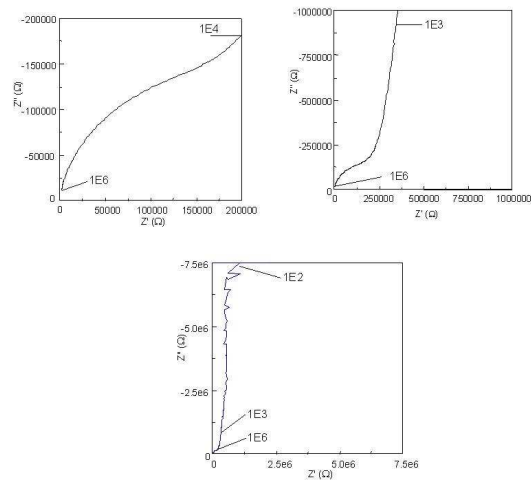


Figure 4.4: Nyquist plots ($-Im(Z(\omega))$ vs $Re(Z(\omega))$) of a system composed by two identical gold electrodes for frequency range 1 MHz -100 Hz . The experimental points in the frequency range from 1 MHz to 10 kHz have been traced in part (a) describing an almost complete semicircle. For lower frequencies a second capacitive element dominates and (b) the resistance in parallel to such capacitance is very high, since the second semicircle is left incomplete for frequency higher than 100 Hz (see c).

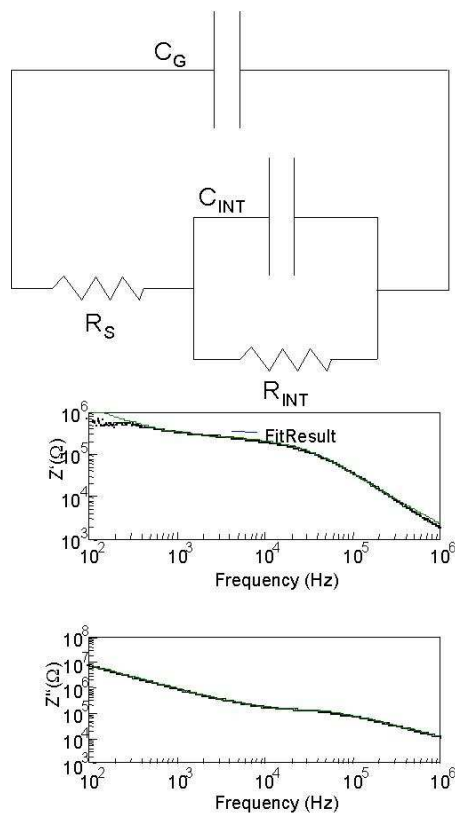


Figure 4.5: 5 Fit of complex impedance measurements (b) performed with the simple four-element circuit of (a). Extracted electrical parameters to fit the experimental points in the whole frequency range are: $R_S = 309020\Omega$; $R_P = 2.37510^{11}\Omega$; $Q_{INT} = 2.88710^{-10}F$; $\alpha_{INT} = 0.91873$; $Q_G = 6.62610^{-11}F$; $\alpha_G = 0.89826$.

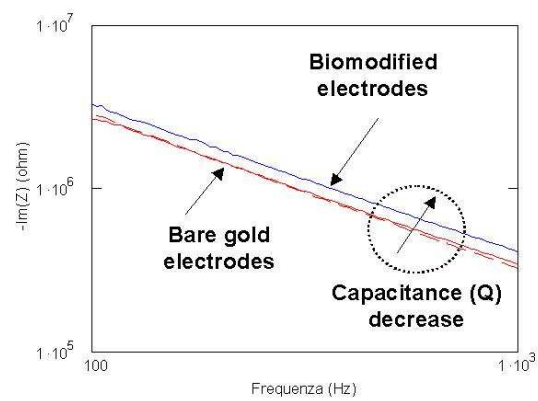


Figure 4.6: Bode plot of the imaginary part related to a chip with non-modified gold electrodes and a chip modified with single-stranded receptors chains. A decreasing value of (Q_{INT}) after bio-modifications has been found.

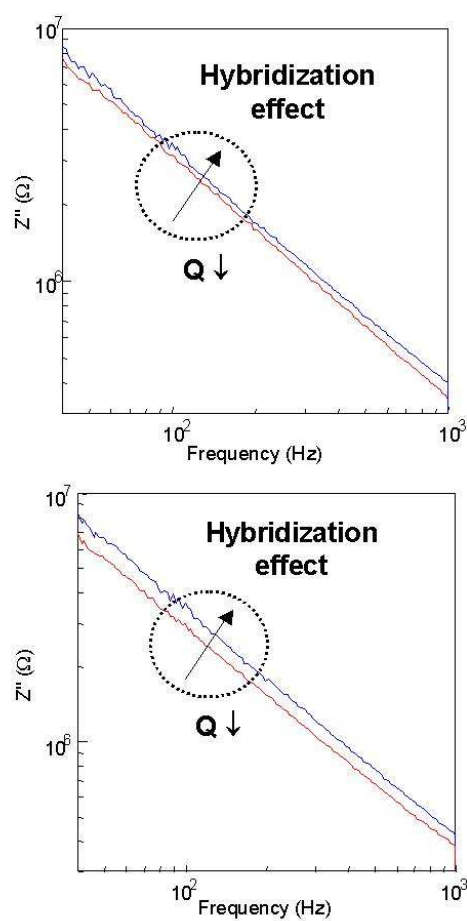


Figure 4.7: Two couples of bio-modified gold electrodes have been tested before and after complementary DNA recognition. A decrease of electrode interface CPE due to the change in chemical and physical characteristics of the sensing bilayer.

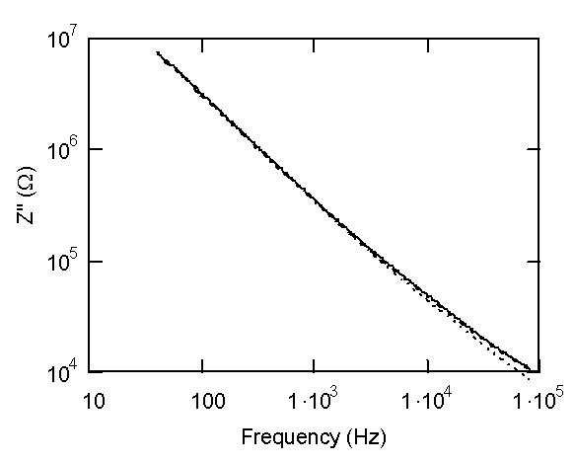


Figure 4.8: Imaginary part of the impedance plotted for three measurements taken every fifteen minutes.

Chapter 5

Smart sensor on PCB based on μ -controller for genetic analysis

Smart sensor, i.e. embedded systems integrating transducers, signal conditioning and processing, represent the end point of an evolutionary path that starts from the discovery and understanding of the sensing principle, followed by the development of laboratory set-ups based on high-cost measurement equipment. This paper describes the design and implementation of a smart sensor for DNA hybridization detection. In particular, as far as the sensing principle is concerned, this work is based on two-electrode measurements of interface capacitance variations induced by hybridization of target DNA with suitable probes immobilized on the capacitors' electrode [40]. So far, this sensing and transduction principle has been studied using laboratory instrumentation for impedance measurement and the generation of input waveforms. All the required signal generation, conversion and processing circuitry has been designed and integrated on a single board (PCB) by means of standard components (COTS). The result is a low-cost, low-power and compact system, with significant advantages compared to the complex and expensive optical scanning devices used today to read state-of-the-art DNA micro-arrays. Thus, the smart sensor presented here represents a significant step forward toward the long-awaited new generation of low-cost point-of-care systems for genetic screening and diagnosis [49]. As for performance, the system described in this chapter has been compared against a measurement setup based on laboratory instrumentation both for the cases of test capacitances, as well as for the detection of DNA in real operating conditions. Results have been satisfactory in both cases. In particular,

the smart sensor is as accurate as the laboratory setup for measuring test capacitances, and it has been shown to reliably detect DNA hybridization in a number of experiments with real biosamples.

5.1 State-of-the-art and detection principle

Biosensors, i.e., sensors incorporating biological elements, are finding increasing use in clinical diagnosis and biomedicine, food production and analysis, bacterial and viral analysis, and many others. Within this broad field, DNA sensors aim at the detection of the highly-specific binding reaction between two molecules of DNA (hybridization). A detailed treatment of the biochemical basis of hybridization is beyond the scope of this paper (the interested reader is referred [50] for an excellent introductory treatment). For our purpose, it is sufficient to understand that DNA molecules can be described as linear sequences of four different basic components (called nucleotides). As known, DNA can be found in two states: single-stranded (i.e., a single linear sequence) and double-stranded. During hybridization, two single-stranded molecules bind to become a double-stranded molecule. This chemical reaction takes place (with high probability) only if the nucleotide sequences of the two single-stranded molecules match on a nucleotide-by-nucleotide basis. DNA biosensors use custom-designed single-stranded DNA molecules as recognizing elements (probes) for sub-sequences in the DNA of test samples. If hybridization between the probe and the sample DNA can be reliably detected, then the genetic signature of the organism can be determined by virtue of the one-to-one affinity relationship. State-of-the-art of DNA (gene) sensors for high throughput analysis are microfabricated matrices (microarrays) requiring labeling of the DNA targets in order to generate optical or electrochemical signals [4]. However, the fluorescent molecules commonly used for this purpose require expensive external instruments. Furthermore, the need of sample pre-treatment as well as increased background noise represent further drawbacks [6]. Several label-free approaches have been intensively studied in recent years, such as, for instance, micro-gravimetric and the electrochemical approaches, measuring the molecular-layer mass difference of the molecules before and after hybridization [51, 52], and the changes of electrical properties (impedance) of the substrate/electrolyte interface, respectively. The latter approach has been implemented starting

from standard methodologies for electrochemical interface analysis, such as chronoamperometry [53], impedance spectroscopy [29], or exploiting field effect devices [23]. The main disadvantage of these techniques is the use of three electrodes (two for the measurements and one as potential reference) that increases the complexity of the system. Two-electrode alternatives, such as that of interest for this work, have also attracted significant interest. For example, a two-electrode setup using 2.4mm^2 gold- and a Ag/AgCl counter-electrode has been studied and found to exhibit ideal capacitive behavior in the $0 - 100\text{Hz}$ frequency range [39]. From this point of view, an important advance in the state-of-the-art has recently been made [40] demonstrating that DNA hybridization can be detected by measuring interface capacitance with a two-electrode system (avoiding the use of a reference electrode). Our work builds upon these findings.

As anticipated, our system is based on an electrochemical approach featuring the immobilization of single-stranded DNA molecules (probes) of known sequence on metal electrodes. This process is normally called surface bio-modification or electrode functionalization. The sensing process is performed by dipping the electrodes in a physiologic solution containing target DNA molecules to be captured by the probes in case of sequence matching (hybridization). The binding event changes the impedance of the electrode-solution interface [40], and in particular its capacitive component, which is strongly affected by the type of molecules attached to the surface (single or double-stranded). The interface can be modeled with capacitance and resistance as shown in Fig. 5.1. The presence of DNA molecules at the electrode surface strongly affects the chemical-physical characteristics of the electrode-solution interface. We are interested in the capacitance variation that takes place when target DNA molecules in a liquid sample are captured by known DNA probes on the electrode surface. Measuring the capacitance changes induced by hybridization implies recognizing the occurrence of hybridization, hence the nucleotide sequence of the target DNA.

Capacitance variations can be measured in many ways [54, 29]. In this work we have used a Charge-Based Capacitance Measuring (CBCM) technique, which has been shown to provide high accuracy even the case of small on-chip parasitic capacitance [55]. The principle of this technique is to charge and discharge the impedance under test, using a voltage pulse of known amplitude ΔV at an appropriate frequency f (period $T = 1/f$), and to measure its equivalent capacitance from the average current in a half-period (Fig. 5.2).

In fact, if interfaces can be modeled as simple capacitors, the average

current can be expressed as:

$$I_{AVG} = \frac{Q}{T/2} = \frac{C\Delta V}{T/2} = 2C\Delta Vf, \quad (5.1)$$

where I_{AVG} is the the measured average current, and C is the only unknown quantity. In our case, in order to increase precision and reduce noise capacitance extraction is performed by measuring I_{AVG} for different frequencies and calculating the slope of the linear interpolated curve I_{AVG} vs f . To this purpose, the current signal is converted into a digital voltage signal and processed by a μ -controller to implement averaging operations and determine the capacitance value. The main advantage of CBCM technique compared to standard complex impedance measurements based on analog sinusoidal signals is that it lends itself to a simple implementation using digital input signals. In fact, the analog part can be reduced to an I/V converter followed by an A/D converter. A laboratory setup implementing the CBCM technique requires a signal generator, to control the switches, and a current meter.

5.2 Hardware and Software Design

The purpose of our design is to develop a low cost system to replace all the laboratory instruments that are connected to the cell, as well as the data-processing software running on the PC. The output of the system is in digital form, and can be either directly visualized on a LCD or forwarded to other subsystems through standard digital links (e.g. RS232, USB, etc.). Our implementation is based on μ -controller directly processing the signals produced by the measurement cell. The μ -controller also controls pulse generation (frequency and amplitude) by mean of a DAC converter, processes data sampled by the ADC converter and calculates I_{AVG} in charge and discharge cycles. In the next sub-section we describe in details both the hardware and software design of our smart sensor. The system is based the Atmega128 μ -controller [56], controlling a DAC device, Max536 [57], and an ADC device, MAX186 [57], (Fig. 5.3). The I/V conversion is performed with a precision resistor and before digital conversion the output signal is amplified by means of an OpAmp (TL081) [58].

At the end of the measurement, the capacitance value is available in digital form on a serial interface. More in details, the Atmega128 is an 8-bit μ -controller, with low power consumption and very low cost.

It is based on RISC architecture with 32 8-bit general-purpose registers, 6 I/O configurable ports, one SPI interface and two serial ports (USART protocol). It also provides useful devices for embedded usage, like counters and a timer, associated with interrupt generation. The μ -controller is the core of the system, since it controls time and synchronization among all components. The possibility to program this device is essential to guarantee the flexibility of our smart sensor. The DAC features four out-channels and 16 bits program word. The output signal is a 12 bits data which represents a voltage within the range $2.048V$ and $-1.2V$ as inputs of the cell. The upper value ($2.048V$) is generated by an ADR290 [59] and the lower value ($-1.2V$) by means of a zener diode LT1034 [60]. The control word is sent every time it is necessary to change the output signal, exploiting a standard SPI protocol. The TL081 component, used to amplify the output signal, is a low noise OPAMP and it is connected with a variable feed-back resistance to regulate gain. The ADC is a 12 bits and 8 channels converter. In case of both positive and negative values (as in our case), a 2's complement integer between $-V_{REFADC}/2$ to $+V_{REFADC}/2$ is generated. The resolution of the ADC is $1mV$ with $V_{REFADC} = 4.096V$. At every sampling instant, the μ -controller sends 8 control bits and receives 16 data bits of which only 12 are significant. Flexibility and portability of the sensor are guaranteed by the programmability of the system (programmed in C and Assembler). The μ -controller determines frequency and amplitude of the input signal, generated by the DAC, calculates the average current for each frequency, hence the capacitance according with Eq. 5.1. As anticipated, the CBCM technique assumes that charge and discharge transients are completed in each half-period of the input signal: hence, the maximum frequency that can be used depends on the capacitance value of the cell. For this reason, a preliminary step is necessary to determine the maximum frequency (f_{MAX}) of the input waveform (the typical range is from $5Hz$ to $100Hz$ and the system does not perform measurements out of this range). In standard lab set-up, this step is usually performed manually or semi-automatically. In our system, instead, a fully-automated self-tuning procedure has been implemented that, starting from a given upper frequency, verifies if the transient are completed by comparing partial areas of the output signal in the proximity of the end of the half period. If the difference between these areas exceeds pre-defined thresholds, the frequency is decreased and the procedure is repeated (Fig. 5.4). When the system finds the maximum frequency, the test is stopped and a variable is set. This self-tuning procedure, lasting about $1s$, ends with the generation of a vector of suitable input frequencies.

After self-tuning, capacitances can be correctly measured. To do that, it is necessary to calculate average currents for different frequencies and then calculate capacitance from equation 5.1. In order to measure the I_{AVG} parameter, the system measures an average voltage by mean of trapezoidal integration,

$$V_{AVG} = \frac{1}{T} \int V dt = \frac{1}{T} \sum_{i=1}^{N-1} c_{i+1} + c_i \cdot \frac{h}{2} \quad (5.2)$$

where V is the voltage output of the cell, c_i is the i -sample, N is the number of samples for every half-period, and h is the distance between two samples (the voltage output signal is sampled at a maximum rate of $40kHz$ and converted to a digital value). The V_{AVG} parameter is proportional to average current thanks to the resistor (R_L) between the output cell and ground (Fig. 5.3):

$$I_{AVG} = \frac{V_{AVG}}{R_L}, \quad (5.3)$$

Moreover, the I_{AVG} can be written taking into account the gain due to the OP-AMP (A_v) and the same resistor R_L as:

$$I_{AVG} = \frac{Q}{T/2} = \frac{C\Delta V}{T/2} = 2C\Delta V f R_L A_v = mf, \quad (5.4)$$

where m can be evaluated by the slope of the I_{AVG} vs f plot by mean of regression linear method. Finally, the capacitance can be calculated as:

$$C = \frac{m}{2\Delta V A_v R_L}, \quad (5.5)$$

where R_L is the current-to-voltage resistance as previously indicated.

Capacitance is calculated sampling 10 half-period voltage transients. Each transient is sampled up to $250\mu s$ before the end of the half-period to enable the μ -controller interrupts, disabled during ADC sampling. In fact, an internal counter generates an interrupt twice in a period to warn the μ -controller to change the DAC output voltage. Nevertheless, if the frequency has been defined according to the previous tuning process, the transient is expected to end at least $625\mu s$ before the end of the half-period.

5.3 Experimental results

Since cheap and off-the-shelf components can be satisfactorily used, the cost of the system is approximately 100 times smaller than that of a standard laboratory set-up. The power consumption is $520mW$ in both idle state and operating state without important variations during measurements. The system has been tested on a wide range of discrete capacitances (from $10pF$ to $4.7\mu F$) and it has also been employed to determine the equivalent capacitance of an electrochemical two-electrode cell to detect DNA hybridization. Fig. 5.5 shows a photo of the system set-up. The tuning procedure has been tested with $2.2\mu F$ and $4.7\mu F$ discrete capacitances to verify the correct estimate of maximum frequency.

5.3.1 Tuning

The tuning procedure determines the maximum frequency allowing the RC circuit (load resistor-cell capacitance) to be completely charged and discharged. This is the highest frequency for which (5.4) is verified. Hence, the linear relationship between f and ΔV predicted by Equation 5.4 is observed for all frequencies lower than f_{MAX} . The value of f_{MAX} can be observed on the $I_{AVG} - f$ plot (Fig. 5.6) clearly showing the deviation from the linear behavior at high frequencies due to incomplete charging and discharging of the capacitance. In order to confirm the robustness and accuracy of the self-tuning procedure, we have evaluated the deviation from the linear behavior at the frequency determined by the system which results always below 1%.

5.3.2 Electrical characterization

Our system has been tested and compared to National Instrument PXI [61] measuring discrete capacitances of $10pF$ - $4,7\mu F$, that corresponds to the expected electrode area ranging from $2*10^3\mu m^2$ to $1cm^2$ that are characteristic of macro and micro electrodes, respectively. The *macro-electrode* range was chosen from $350nF$ to $4.7\mu F$ while the *micro-electrodes* range was chosen from $10pF$ to $700pF$, according to available data [53] which associates $20\mu F$ capacitance for $1cm^2$ to an electrode/solution interface. The current to voltage conversion resistor was 750Ω for larger capacitances and $2.3M\Omega$ for smaller ones, respectively. For large capacitances the accuracy of our smart sensor and of PXI are comparable, corresponding to a relative percentage error below 3,5%. For lower capacitances the smart sensors achieves better accuracy than PXI. In particular, for

a $150pF$ capacitance value, relative error is 0.5% and 1.5%, respectively. For low capacitances a calibration curve is necessary for both set-ups to compensate parasitic which can be estimated $50pF$ for the PXI and $2 - 3pF$ for the smart sensor. Therefore, the calibration is necessary in particular for the implementation based on the PXI ($50pF$ compared to $2 - 3pF$). The reduction of parasitic is a consequence of the more compact on-board implementation. Nevertheless, exploiting the calibration curves it is possible to eliminate the systematic error.

5.3.3 DNA Detection Measurement

The system of this work has also been employed to detect when the hybridization reaction occurs. The system has been connected to a cell of two $0.8cm^2$ gold electrodes immersed in an electrolyte solution. The equivalent capacitance measured with our setup of in case of bare gold electrodes is $19.04\mu F/cm^2$ (as expected from literature [53, 29]). Bio-modification of the gold surface leads to an interface capacitance decrease. The entity of the variation is related to the biochemical nature of the molecular layer formed on the surface and to its conformation. In fact, a lower capacitance value has indeed been measured for the cells that hosted bio-modified electrodes.

The cell used for this experiments was composed by electrodes modified overnight with single-stranded DNA probe molecules ($3\mu M$ in saline solution). Successively, experiments were performed through the following steps. 1) The capacitance of the cell has been measured. 2) The cell has been immersed in a $70^\circ C$ solution containing target molecules and cooling down the cell to room temperature. 3) Capacitance has been measured at the end of the binding reaction after extensive rinsing with saline solution to remove unbound molecules. 4) The sample molecules can be removed by heat-treatment (electrode regeneration). 5) The equivalent capacitance of the regenerated electrodes has also been measured and compared with measurements at steps 1 and 3.

As shown in Fig. 5.7, four repeated measurements have been performed in 6 minutes on the same electrodes couple for each step and the average values are compared. As expected, measurements at steps 1 and 5 both correspond to electrode interfaces modified with a layer of probe molecules: in fact their capacitances differ by less than 1.31% (3.10 and $3.06\mu F$ respectively). In contrast, the presence of target molecules captured by probes on the interface (measurements at Step 3) leads to a capacitance decrease of 16, 5% ($2, 59\mu F$).

Therefore, the described smart sensor has several advantages with re-

spect to commercial systems based on optical scanners. First, it avoids the use of high-cost detectors and the pre-treatment of the sample to introduce marker molecules. Moreover, the programmability of the system μ -controller guarantees the flexibility and self-tuning capability of the smart sensor. In particular, the system could host and manage additional components, such as a wireless interface or other sensors. The system has been tested and compared in terms of accuracy with a high-cost laboratory implementation of the same charge-based capacitance measurement technique, showing competitive performance. Finally, capacitance measurements performed on typical set-up, show the capability of our system to detect DNA hybridization reaction occurring in on the surface of gold electrodes.

5.4 Figures

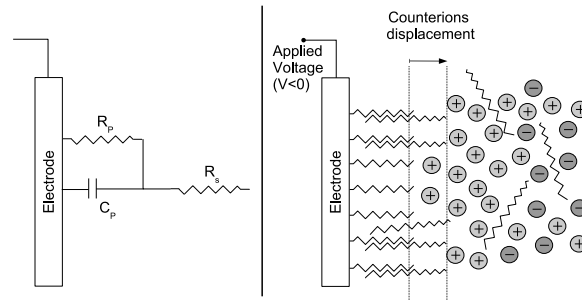


Figure 5.1: Electrical model of Electrode/Solution interface.

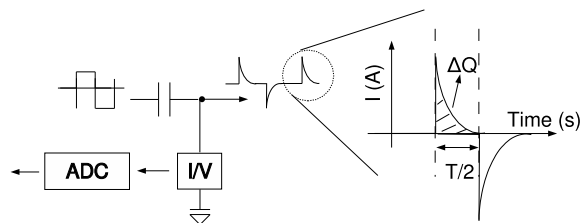


Figure 5.2: Schematic description of Capacitance-Based Capacitance Measuring technique.

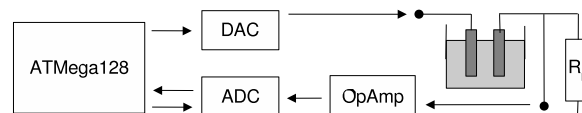


Figure 5.3: Sensor block diagram where are indicated connection between the core of the system, μ -controller, and the devices controlled by it, ADC and DAC.

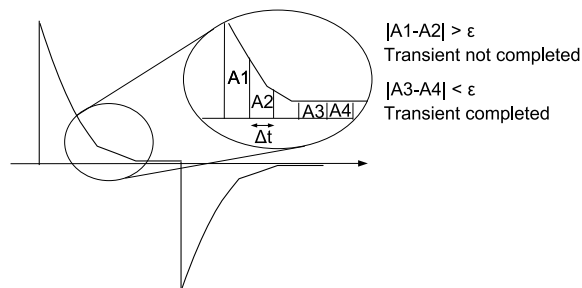


Figure 5.4: Tuning principle.

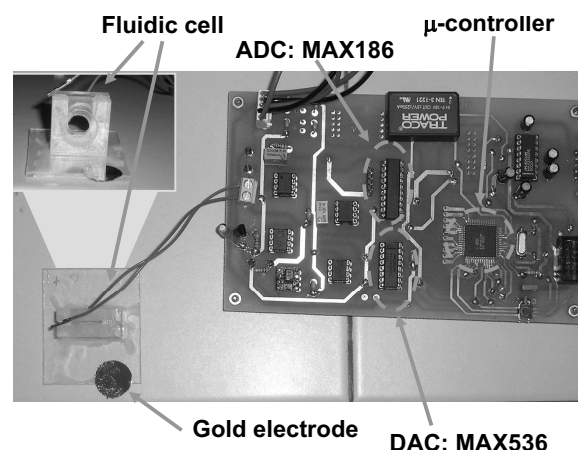
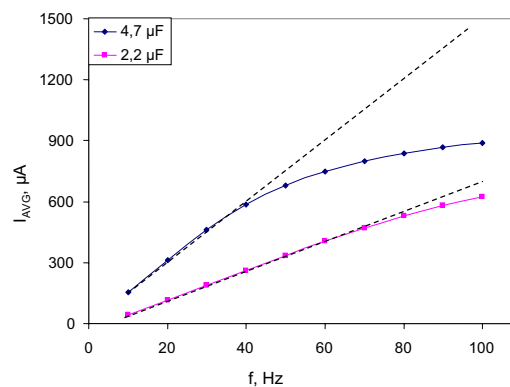


Figure 5.5: The photo shows the PCB implementation of the system and the fluidic cell used for the experiments.

Figure 5.6: Graphical evaluation of f_{MAX} . A deviation from the linear behavior is observed around $40 Hz$ and $70 Hz$ for $4.7 \mu F$ and $2.2 \mu F$ respectively, which indicate that for highest frequencies capacitance measurements cannot be correctly performed.

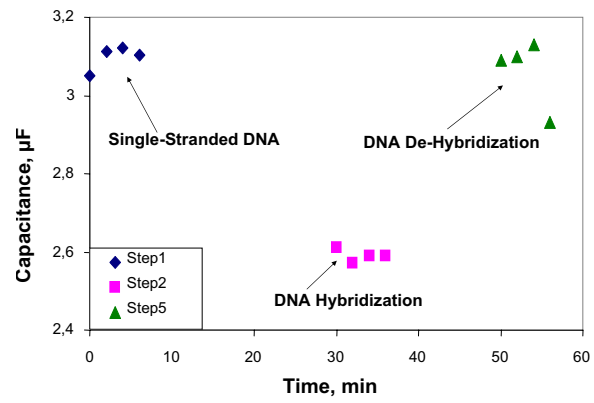


Figure 5.7: Experimental results of hybridization and de-hybridization capacitance measurements.

Chapter 6

On Chip DNA detection based on CBCM capacitance measurement

In the last decade, miniaturized arrays for gene-based tests (known as DNA microarrays) have been introduced in genetic research. These are fabricated on glass or quartz slides where different DNA probe molecules are immobilized in a two-dimensional array of small sites. Some of these devices, implemented with photolithographic techniques, are able to test a whole genome, with densities of a million sites per square centimeter [4]. The DNA strands of the organism under test are preliminary marked with fluorescent molecules. Their presence at specific sites of the array is measured by an optical scanner or a fluorescence microscope, after binding to matching probe molecules. These devices have also been employed for population genotyping [62] and research on cancer predisposition [63]. Nevertheless, the high-cost of the scanner and the processing steps required to tag the samples with markers (also called labels), pose critical limits to the use of these tools in point-of-care analysis. For these reasons, a large effort is devoted to the development of devices suitable for low-cost mass production and ease to be used not only in highly specialized laboratories. A single-chip solution, implementing a detection technique with direct electrical read-out and avoiding labeling of the DNA target molecules, would significantly enhance portability, as well as high-parallelism, on-site sensing and data processing.

The chip features a number of sensing sites, each containing two gold electrodes [64] that can be independently selected by means of on-chip addressing circuitry, while the read-out electronics has been realized essentially by means of external standard components in order to exploit the

advantages of large experimental flexibility. The surface of the electrodes is bio-modified (functionalized) by covalent binding of single-stranded DNA probes. During in-field operation, the capture of complementary DNA strands from the liquid samples is signaled by a variation of the capacitance between electrode pairs, which can be measured by connecting them (through on-chip addressing logic) to an external capacitance-measurement circuit.

The chip is bonded on a PCB (Printed Circuit Board) and is connected to external processing and storage devices, resulting in a complete analysis system that has been characterized and tested for DNA recognition. To this end, the capacitor electrodes have been functionalized and their capacitance variation has been measured after exposition to both complementary and non-matching target molecules (to test specificity). Reversibility has also been tested by measuring sensor capacitance before and after sensing molecule regeneration, obtained by temperature treatment. The results demonstrate that a DNA sensor based on the electronic detection technique described in this paper can be fabricated as a single chip with standard CMOS technology augmented with gold deposition for the capacitor electrodes.

6.1 Related Work

DNA microarrays allow highly parallel and low-cost analysis. In fact, they exploit the capability to fabricate a large number of miniaturized detection sites on a substrate and to extract information after exposition to the target DNA to be detected/recognized. In general, such devices work as described in Fig. 6.1. Each site is specifically bio-functionalized by means of DNA probe molecules of known sequence immobilized on its surface. Target molecules in the sample solution bind only to probes with complementary sequences (hybridization): thus, their presence at specific sites reveals their composition.

Most of current microarrays require optically active labels attached to the target DNA and fluorescence sensing. Some innovative microarrays employ electrochemical labels (redox-active molecules or enzymes) that produce an electrical current through conductive electrodes in case of hybridization ([65, 66, 19]).

Label-free techniques are intensively investigated, since they avoid expensive reagents and pre-treatment steps. To this end, recently, several approaches have been proposed, based on piezoelectric materials ([24, 67]), microfabricated cantilevers ([68, 69]). Other techniques detect the

variations of electrical properties of electrode/solution interfaces induced by DNA recognition. Within this category, a distinction can be made between devices where sites exploit passive components or semiconductor sensors ([21, 22, 16, 41, 23, 70]).

The approach of interest in this work is based on interface capacitance measurements, whose conventional implementation exploits a three-electrodes setup allowing bio-functionalized gold electrodes to be investigated with impedance spectroscopy ([29] [47]).

Much simpler two-electrodes configurations, such as that used in this work, have also attracted significant interest. For example, a two-electrode set-up using 2.4 mm^2 gold- and a Ag/AgCl counter- electrode has been found to work properly in capacitive detection at 20 Hz [39]. As far as integrable capacitance methods are concerned, it has already been shown that DNA hybridization can be detected by measuring interface capacitance with a system making use of two (gold) electrodes only (i.e. without the use of a reference terminal) [40]. Furthermore, more recently it has been shown that reliable measurements can be done exploiting passive microfabricated electrodes [71]. Arrays made of passive electrodes are pad-limited, as each electrode pair requires two pads for connecting to external measurement circuits.

In such a context, this work represents an advance in the state of the art in that it presents a silicon chip featuring micrometric capacitors and on-chip logic for selecting and multiplexing the on a limited number of I/O pins. The chip has been implemented with standard CMOS technology (with the addition of gold deposition for capacitor electrodes). Capacitance measurements are performed by means of the Charge-Based Capacitance Measurement (*CBCM*) technique [72], which is suitable for low-complexity, small-area on-chip implementation.

The chip includes addressing circuitry, while the read-out electronics has been realized externally by means of standard components in order to exploit the advantages of large experimental flexibility (although it could eventually be easily integrated with the rest of the system).

6.2 Capacitance-based DNA Detection Principle

Under suitable electrochemical conditions, bio-modified metal interfaces in saline solution exhibit a capacitive behavior. This is the case if gold electrodes are modified with short DNA strands immobilized with alka-

nethiol linkers on the surface ([39, 29]). In this case, capacitance values of electrode/solution interface have been estimated between 1 and $20\mu F/cm^2$ (although this value strongly depends on electrode surface treatment). A first-approximation model of the electrode/solution interface is the equivalent circuit depicted in Fig. 6.2 (left) ([42, 73]), where: R_S depends on the interface and solution characteristics; R_P is related to the insulating properties of the interface (for well-formed layers it can be considered infinite); C_P is mainly affected by the physical and chemical characteristics of the insulating bio-layer immobilized on the surface. In this model, the geometrical capacitance formed by the electrodes would be in parallel to C_P but, since it is several orders of magnitude smaller than the interface-capacitance, its contribution is negligible: thus it is not considered here.

This simple model provides an intuitive explanation of the basic sensing principle exploited in our work. Considering a capacitor formed by two neighboring electrodes of our chip, when a complementary DNA strand binds with the surface probes and the DNA duplex is formed, the solution counterions present in the liquid solution are pushed further away from the polarized metal surface: this increases the distance between the charge inside the electrodes and the ions in the electrolyte: thus C_P decreases ([47, 39, 40]) (Fig. 6.2, right).

When measuring a capacitance with CBCM technique, an input square wave is applied to one electrode, while the current required to completely charge (or discharge) the capacitance is measured at the second electrode. The measured capacitance value equals the product of the average value of: the output current, the applied voltage step, the frequency of applied clock signal. With this technique, the measurement of the capacitive component of an impedance is independent from the resistive components provided that: (a) the charging and discharging current transients have the time to settle during the period of the square wave (i.e. all the charge stored in the reactive component is transferred); (b) the static current flowing through the R_P and R_S resistive path is negligible compared with the average output current (i.e. most of the charge transfer is due to the reactive component). Previous work on *CBCM* has demonstrated that both these requirements can be met in a practical experimental setting [40].

It is important to stress however that the model of Fig. 6.2 is a highly idealized view of more complex physical phenomena, namely charge transfer at the electrode-solution interface in presence of biological molecules immobilized on the electrode surface. Thus, we cannot assume, for instance, that capacitances and resistances in Fig. 6.2 are constant over a

wide frequency range. Sensing of impedance variations requires therefore careful selection of the frequencies used for CBCM excitation waveforms.

6.3 Chip

This section describes the architecture and the operation of the test chip designed, fabricated and characterized in this work. The chip contains a number of sensing sites and the addressing circuitry, while read-out is realized by means of by external components in order to systematically explore different measurement configurations and parameters. The chip is packaged on a PCB to form a system suitable for test measurements and characterization.

6.3.1 Chip architecture

Essentials of chip architecture and signal flow are shown in Fig. 6.3. Both analog and digital input signals are required. The former ones determine the voltage range used for the measurements, while the latter ones include a seven bit address to select the sensing sites. An external clock is used to provide the measurement frequency, which is the same as the external signal, as well as to synchronize the different blocks. Each sensing site features a block that, controlled by external clock, generates a four square-wave signal with high timing precision.

The on-chip address signals are generated by means of two decoders. If one sensing site is selected, the input signals coming from the pulse generator are enabled and measurement is performed. Only the output signal of the selected site is connected to the shared output pad (Fig. 6.3).

At the output pad, the transient current is converted by means of an external circuit into a voltage signal, that is sampled and processed by a PC to calculate the capacitance value. With respect to an on-chip implementation of the I/V conversion, this external solution allows larger flexibility in experimenting different measurement parameters.

6.3.2 Sensing site circuitry

The circuit implemented for each sensing sites, illustrated in the dotted box in Fig. 6.4, includes a pulse generator and four switches which selectively connect the electrodes of the sensing capacitances to one of three different reference voltages: $V+$, $V-$ and V_{REF} . Between the pulse generator and the switches a multiplexer is inserted which allows the clock

pulses to drive the electrodes of the sensing element only if it is selected. The switches are implemented with both n- and p-channel transistors in order to exploit full voltage range.

Exploiting its proximity with the switches, the (local) pulse generators provide very precise signals controlled by the external clock. A critical timing issue has to be considered at this regard in that $Ck1$, $Ck1_$ and $Ck2$, $Ck2_$ must not close the switches at the same time in order to avoid shorting $V+$ and $V-$. For this reason, a suitable delay is inserted and non-overlapping clock signals are used (as shown in the inset of Fig. 6.5) in order to avoid that two transistors at the same time see a gate voltage larger than their threshold. The delay used for this purpose is 1 ns and is obtained by means of the pulse generator block reported in Fig. 6.6, also showing the output buffer following the multiplexer.

The switches allow to connect the electrodes of the sensing capacitors either to $V-$ and to V_{REF} , or to $V+$ and the voltage about V_{REF} at the negative input of the opamp shown in Fig. 6.6 (see also Table 6.1). When switching between these two bias conditions, a voltage step is applied at the sensing electrodes and a transient current is generated. With the circuits shown in Fig. 6.4, the charging and discharging currents are driven to two different output pads, $OUT1$ and $OUT2$, thus allowing measurement of the average value using only one of them.

6.3.3 Physical layout

The chip is fabricated in 6" n-well 0.5 μm CMOS process with two metal layers. The gold electrodes are deposited after standard CMOS processing on silicon nitride (Si_3N_4) as described in [64]. Annealing steps are introduced to guarantee good CMOS performance after gold deposition [64]. The area of the three sensing capacitors used in this work is 1 mm \times 1 mm and the distance between them is 500 μm , while that of total chip, featuring 44 electrode couples of different size, is 6.5 mm \times 4.6 mm (Fig. 6.7). The parasitic capacitance between gold electrodes and substrate has been estimated to be 6 aF/ μm^2 therefore it is several order of magnitude smaller than electrode/solution interface capacitance (about 35 nF as shown in section 6.5).

The pin-out includes analog as well as digital signals, power supply and ground. Table 6.1 provides all I/O signals, with indications of the label and the value of the voltage applied during the measurements.

The main analog signals are $V+$, $V-$, determining the voltage step ($V+$) - ($V-$) = ΔV) applied to the electrodes. Digital inputs include the seven bit address signals and one external clock to set the measurement

frequency. The power supply voltage V_{DD} is the same for the whole chip.

In order to reduce interferences and noise, analog ground is $V_{REF} = V_{DD}/2$. Our choice of V_{DD} and V_{REF} allows to generate only positive signals (e.g. $V+$, $V-$), while the digital ground can be made negative respect to V_{REF} . In fact, the signal voltage levels $V_{S1} = V+ = V_{REF} + 0.1V$, and $V_{S2} = V- = V_{REF} - 0.1V$ are generated by external voltage sources related to digital ground.

6.4 Measurement set-up

The chip described in the previous section is glued to a PCB featuring large contacts on one side to be connected to standard instrument and small ones on the other side connected to the chip by means of gold bonding wires (Fig. 6.8). A passivation process protects both wires and chip from the saline solutions used in the experiments. To this purpose, epoxy glue is placed on the critical electrical parts. Since to bind the DNA probes to the gold electrodes, these must be accurately cleaned with plasma oxygen and epoxy glue is damaged by this process a further SU-8 layer is added to protect the glue from treatment.

In our electrical measurements, the transient discharging current is driven to an external I/V converter (Fig. 6.9) implemented off-chip by means of the operational amplifier *OPA103AM* [61] and precision resistors. The voltage signal at the op-amp output is sampled by means of a National Instruments DAQ board (PCI-6032E [61]). Finally, the average value of the output voltage (V_{avg}) is calculated by means of a trapezoidal integration and the average discharge current (I_{avg}) is then obtained as:

$$I_{avg} = V_{avg}/R_C. \quad (6.1)$$

I_{avg} can be expressed as:

$$I_{avg} = 2C\Delta Vf + I_{offset}. \quad (6.2)$$

Here, ΔV , $((V+) - (V-))$, and f are controlled parameters, while C is the capacitance to be extracted from experimental data.

For higher precision, the value of I_{avg} is measured at 9 different frequencies (from 60 *Hz* to 100 *Hz* and step of 5 *Hz* for each measurement) as the average of 10 charging transient.

Finally, C is computed by least squares fitting on equation 6.2 providing the slope m :

$$C = \frac{m}{2\Delta V} \quad (6.3)$$

6.5 Experimental results

6.5.1 Electrical Characterization of gold electrodes

Our chips have been tested in wet conditions at room temperature. After cleaning, a saline solution, TE (Tris 10 *mM*, EDTA 1 *mM*) 0,3 *M NaCl pH* 7, is spread on the electrode surface and CBCM measurements are performed to characterize differences between electrode couples. In a first phase, test measurements are performed to set two important parameters, namely R_C , which determines the I/V conversion factor, and the frequency range to be used in the measurements.

From section 6.2, we recall that CBCM frequency should be low enough to reach steady state in cell current, and that the DC current flowing through the R_P and R_S resistive path should be negligible compared with the average output current. By analyzing current transients in response to voltage steps, we determined that steady state was reached in a few tenths of *ms*. We therefore set the period of the excitation waveform 1 order of magnitude larger than transient time. Moreover, R_P and R_S have been estimated with a standard impedance spectroscopy measurement and found to be about 10 *MΩ* and 10 Ω , respectively. R_P is large enough to ensure that the DC current flowing between the electrodes falls below the noise level of the experimental set-up. Thus, both requirements for applicability of *CBCM* are met¹.

However, the experimental measurements of C_P , in contrast with the first-approximation model of Fig 6.2, (left), have shown a large frequency dependence (Fig. 6.10). The behavior can be attributed to electrochemical effects taking place at the electrode-solution interface of the sensing device. These effects can, in fact, be accounted by modeling C_P with a Constant Phase Element [74]. Indeed, Fig. 6.10 reports a good fit of our experimental data obtained with the described model.

It is worth pointing out that detection does not require determining a single value of the sensing capacitance, but to distinguish between the device behavior in the presence rather than in the absence of DNA hybridization and, as shown later, this is indeed the case.

The I/V converter is implemented with the operational amplifier *OPA103AM* [61] featuring a gain-bandwidth product of 10^6 , a value

¹To further strengthen this point, PSPICE simulations have been done considering the circuit represented in Fig. 6.2, (left), with a constant value of C_P . With this model, the capacitance is then extracted from the (average) transient discharge current as done in the experiments (described in Section 6.4) and the results indicate a dependence on f smaller than 7% in the frequency range from 10 Hz to 1 kHz).

of interest in the perspective of fully integrated electronics. This characteristic plays a crucial role in the choice of the frequency range. The optimal value of f for the CBCM voltage excitation frequency to be used in the measurements is chosen taking into account the frequency dependence shown in Fig. 6.10 and also the characteristics of the I/V converter. Lower frequencies (hence longer periods) lead to long measurements, with lots of noise. On the other hand, when frequency is too high, small gains of the I/V converter lead to small signals, again critically affected by noise.

In practice, if f is 1 kHz , the gain-bandwidth product of our amplifier would require $R_C = 1\text{ k}\Omega$. Unfortunately, in this case, gain would be rather low, and the Signal to Noise ratio (S/N) would be too low (about 5 dB). On the other hand, if $f < 10\text{ Hz}$, then $R_C > 10^5\text{ k}\Omega$ and gain would be high enough, but the measurements would be too noisy, as shown in by the error bars of Fig. 6.10.

Therefore, the optimal condition of the I/V converter circuit is $R_C = 10^4\text{ k}\Omega$ (leading to $S/N = 34\text{ dB}$ and total measurement time around 20 s for each site), and f in the range $10\text{--}100\text{ Hz}$. The frequency dependence of C_P suggests to work at a measurement frequency as high as possible. Therefore, we have used frequencies in the range $60\text{--}100\text{ Hz}$.

Typical experimental results, obtained with equation 6.3, are shown in Fig. 6.11 and in Table 6.2. "Couple 1" refers to the electrode plates on the left of the chip while "Couple 2" refers to those on the right. The standard deviation reported in Fig. 6.11 come from several measurements for each sensing site. Relative differences between capacitance measurements for two different couples on the same chip are evaluated to be less than 4.2% . Moreover, statistics on data shows that the capacitance values measured on the same chip but on two different couples are almost the same. Differences among several chip are due mainly to differences in the level of cleanliness of the electrodes after the cleaning step.

6.5.2 Electrode bio-modification

First, the gold electrodes have been cleaned by exposure for 20 minutes to plasma oxygen at 200 W . After this step, single stranded DNA molecules modified with alkanethiol groups are immobilized on the gold electrodes by covalent S-Au bonds (a $3\text{ }\mu\text{M}$ DNA $1\text{ M Na}_2\text{HPO}_4$ solution is spread on the electrode surface for 18 hours). Two different probe molecules of the same length (25-mer) and thiol modified with a chain of 6 carbon atoms as a spacer are bound to different electrodes on the same chip (electrode couple on the left and on the right). To this end, two separate

droplets are placed by mean of microliter pipettes to obtain sites which will and will not experience hybridization reaction. Before measurements, the gold surfaces are extensively rinsed with ultra pure water to remove molecules that are not covalently bound to the gold electrodes or to the passivation layer of the chip.

Target DNA solution ($3 \mu M$ DNA 30-mer and TE 0,3 M NaCl pH 7) is heated up to $80^\circ C$, spread on the electrodes and cooled down to room temperature (for about 30 minutes). Finally the sample is rinsed in the same saline solution (TE 0,3 M NaCl pH 7) in order to remove the unbound DNA target (Fig. 6.12).

In order to verify the biological steps previously described, we have performed an independent standard optical detection test based on fluorescence molecules bound to DNA molecules. Probe molecules are labeled with fluorescein and target molecules with tetrametil-rhodamine. In order to perform quantitative analysis after electrical measurements the DNA molecules, both probes and targets have been removed from the surface by mean of β -mercaptoethanol 12 mM solution for 10 hours. Then, to increase the optical signal, the pH of the sample solution has been brought to 10 adding a solution NaOH 10 M (the pH has been checked with the HI-9023 pH meter). Before DNA experiment a calibration curve has been done with the LSB-50 fluorescence spectrometer (Perkin Elmer, Boston, USA) using DNA sample solutions, (12 mM β -mercaptoethanol and pH 10 adding NaOH 10 M solution as previously described) of different known concentrations. Results of optical detection of our unknown samples compared with the calibration curve show that the density of our probes layer is about $10^{13} \text{ molecules/cm}^2$, a value close to that reported in the literature [75]. Moreover, we have tested the efficiency of the hybridization reaction in the case of complementary and a-specific target molecules: the first one indicates that the 80% of the probes react with target forming the double helix while the second one indicates that less than 10% of probe react with target, demonstrating the good quality of our process.

6.5.3 DNA detection

DNA detection is demonstrated comparing measurements on electrode couples subjected to the same reaction but with different DNA strands bound on the surface, complementary and non complementary to target molecules, respectively (the latter for negative control). All measurements are performed in the same saline solution of the hybridization step (TE 1X 0,3 M NaCl pH 7). Since capacitances exhibit significant mis-

matches, a measurement after functionalization is performed and these values are used as a reference to be compared with the results obtained after (tentative) hybridization. The capacitance absolute values after functionalization show a decrease around 25% respect to clean gold for each couple. Results of 3 experiments over all the chip previously measured after cleaning are summarized in Fig. 6.13, where positive variations correspond to capacitance decreases.

Fig. 6.13 clearly indicates that significant capacitance decreases are found as a result of hybridization, while smaller or even opposite variations occur in the other case, thus demonstrating the capability of our approach to distinguish between hybridization and non-hybridization events.

After measurements, the sensing layers have been regenerated removing all target molecules. For this purpose, a rinsing step with hot ultra-pure water is performed to break hydrogen bonds between the two DNA strands, leaving only the probe oligonucleotide chains covalently bound on the surface. After this step, new capacitive measurements are performed and Fig. 6.14 illustrates the measured capacitance variations.

As expected, an increase of interface capacitance is observed where hybridization had previously occurred, while electrodes with non-complementary probes show only negligible variations. Moreover, it is worthwhile to note that the absolute variations of capacitance in de-hybridized chips are of the same amount occurring in hybridized ones.

Since the applications envisaged in this work, normally make use of DNA amplification by means of PCR-Polymerase Chain Reaction, tests of the device sensitivity to DNA concentration, thus no attempt has been made in this direction.

In view of a simple and effective DNA analysis, a significant effort is currently dedicated to the development of single-chip, fully-electronic devices and this paper illustrates a step forward in this direction since it demonstrates the viability of a simple approach suitable for stand alone and portable diagnosis equipments based on two-electrode capacitive measurements implemented with micro-fabricated capacitors.

In particular, this work presents a test chip, fabricated with standard CMOS technology with the addition of gold deposition for the sensing capacitors. The chip includes the addressing circuitry, while standard external components are used to realize the read-out electronics, in order to improve measurement flexibility and help the search for optimum conditions.

The chip has been fully characterized and measurements have been performed exposing the device to target DNA solutions. The results

clearly indicate that DNA hybridization produces a significant decrease in the capacitance of the sensing capacitors, that can be safely recognized by the on-chip read-out circuitry.

The paper then suggests that a chip, potentially containing thousands of sensing sites, with fully integrated circuitry for DNA recognition can be fabricated exploiting the approach described in this work.

6.6 Tables

Table 6.1: Description of the chip pinout.

N. Pin	Label	Value	Type
1-6	A0-A5	$0, V_{DD}$	Digital
7	Clock	$0, V_{DD}$	Digital
8	C1	0	Digital
9	C2	V_{DD}	Digital
10	V_{DD}	5V	Power Supply
11	V_{SS}	0V	Ground
12	Vs1	$V_+ = 2.6V$	Analog
13	Vs2	$OUT1 = V_{DD}/2$	Analog
14	Vs3	$V_- = 2.4V$	Analog
15	Vs4	$OUT2 = V_{DD}/2$	Analog
16	Vs5	$V_{REF} = V_{DD}/2$	Analog
17	Ref-Pot	$V_{REF} = V_{DD}/2$	Analog

Table 6.2: Capacitance measurement on 6 different chip

Couples	1	2
Chip 1 \Rightarrow CAP (nF)	50.4	48.1
Chip 2 \Rightarrow CAP (nF)	31.7	33.1
Chip 3 \Rightarrow CAP (nF)	32.2	36.3
Chip 4 \Rightarrow CAP (nF)	25.4	24.4
Chip 5 \Rightarrow CAP (nF)	32.6	34.6
Chip 6 \Rightarrow CAP (nF)	34.9	34.7
Standard Deviation (nF)	8,3	7,5

6.7 Figures

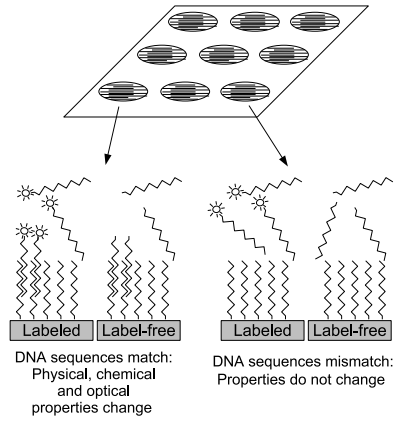


Figure 6.1: Schematic representation of microarray principle.

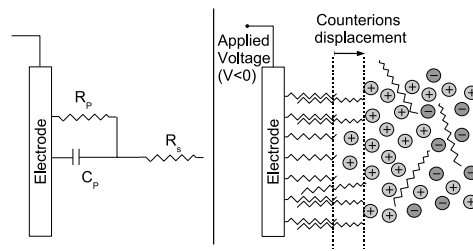


Figure 6.2: Left: Schematic representation of the lumped-element electrical model of the metal/solution interface of the capacitors used in this work. Right: Schematic illustration of the DNA hybridization process and the induced (further) displacement of counterions within the liquid solution.

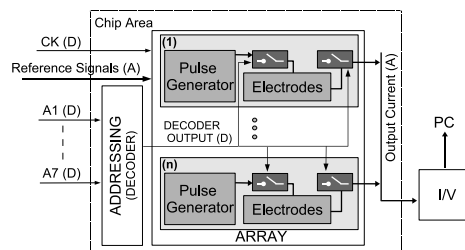


Figure 6.3: Schematic representation of the system and signal flow. A and D indicate analog and digital signals, respectively.

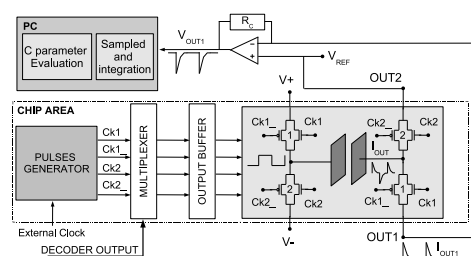


Figure 6.4: Schematic of the circuit associated to each sensing element.

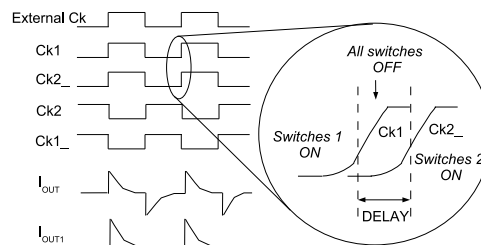


Figure 6.5: Schematic representation of the signals flow used in the experiments.

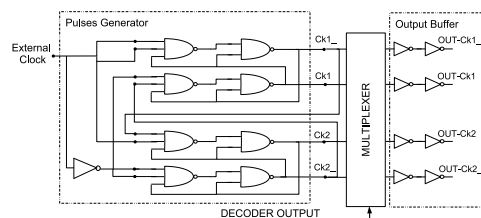


Figure 6.6: Schematic plot of the block used to generate not overlapping clock signals.

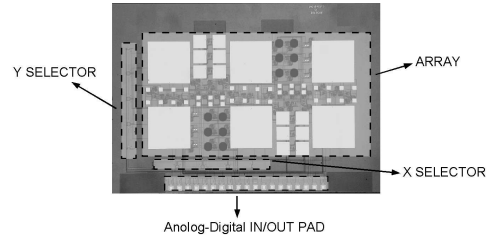


Figure 6.7: Chip photograph.

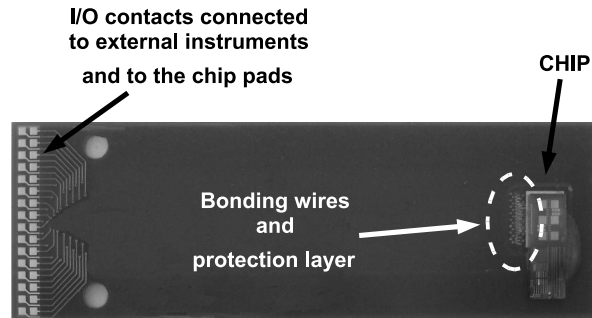


Figure 6.8: Photo of the PCB used for measurements. The chip is highlighted in the box on the right.

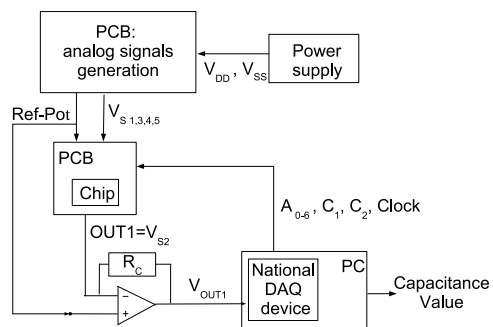


Figure 6.9: Schematic representation of the measurement set-up.

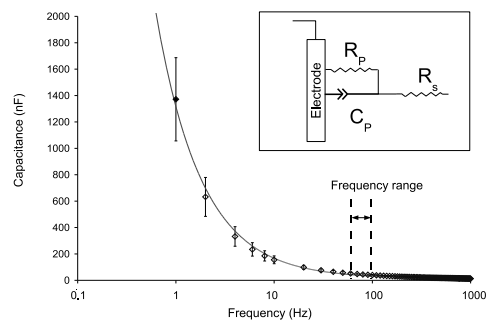


Figure 6.10: Measured capacitance vs charge/discharge frequency on clean gold electrodes. The continuous line shows the fitting.

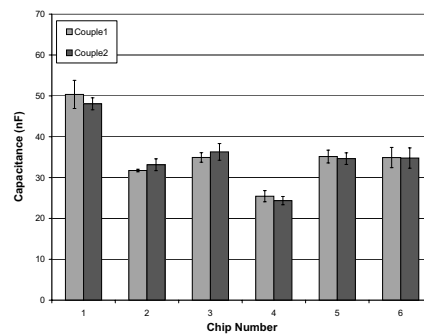


Figure 6.11: Capacitance measurements of electrode couples on different chips.

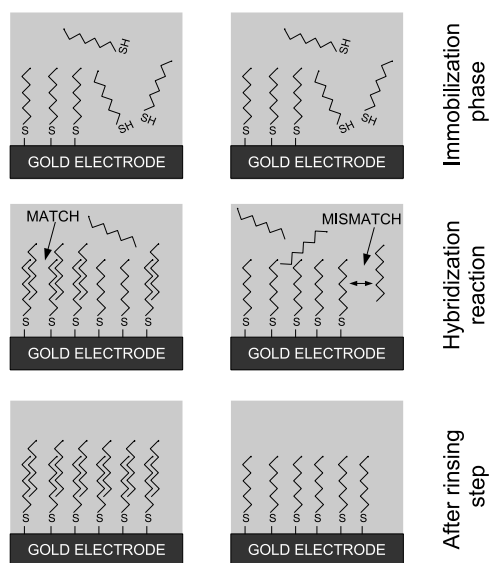


Figure 6.12: Schematic representation of the functionalization and hybridization steps.

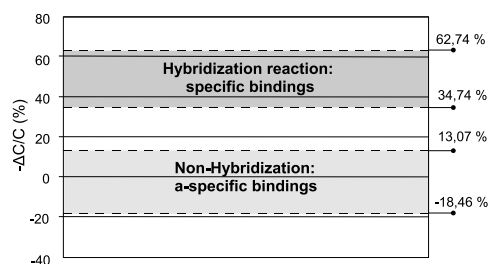


Figure 6.13: Capacitance variations due to specific and a-specific bindings (upper and lower bands of measured capacitances, respectively). Positive values indicate capacitance decrease.

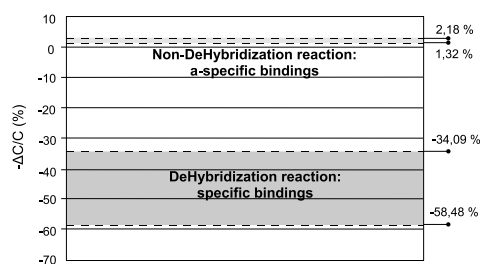


Figure 6.14: Capacitance variations due to de-hybridization process in the case of complementary (lower) and non-complementary (higher) probes previously subjected to hybridization reaction. Negative values indicate capacitance increase.

Chapter 7

Capacitance measurement for DNA detection with on chip A/D conversion

7.1 Introduction

Miniaturized arrays for gene-based tests, known as DNA microarrays, have drastically changed the way genetic analysis and research are performed, by enabling the user to perform a huge number of analysis in parallel. These devices are typically based on glass slides where different DNA probe molecules with known sequences are located on the surface within a two-dimensional array. The DNA strands within a sample to be analyzed are marked with fluorescent label molecules during preparation of the sample liquid. A label is an extra molecule added to a DNA segment that reveals the presence of target DNA bound on a site of the array. After binding to matching probe molecules during incubation of the sensor array, the label's presence within a specific site of the array is detected by an optical scanner or a fluorescence microscope. State-of-the-art optical DNA microarrays can test a whole genome, as they achieve densities of a million sites per square centimeter [4]. Moreover, they have also been employed for population genotyping [62] and research on cancer predisposition [63]. Nevertheless, the high cost of the scanner, the sensibility of optical systems and the processing steps needed to label the samples pose critical limits to widespread diffusion and point-of-care usage. For these reasons, significant effort is being devoted to develop devices suitable for low-cost mass production and use outside highly specialized laboratories. A solution implementing direct electrical read-out

and avoiding labeling of the DNA target molecules would significantly enhance portability while maintaining high-parallelism, as well as on-site sensing and data processing. In fact, the miniaturization of sensor chip and readout unit opens the way for completely new applications and markets in the field of bio-molecular diagnostics. Due to the ease of use of these highly integrated microsystems, point of care diagnostics, e.g. in the doctor's office, comes into reach.

The main technical advantage of monolithically integrated, fully electronic DNA sensor devices is the capability of signal processing in the direct proximity of the sensor. This results in the highest sensitivity with respect to the transducer signal. Furthermore, CMOS allows to integrate large number of sensors on a single die requiring only few electrical connections to the outside world, which significantly eases the packaging of the devices.

The focus of this paper is to present a CMOS DNA-chip featuring 128 sensing sites which implement a label-free fully-electronic capacitance measurement technique. Each sensor site in the 8×16 array consists of two interdigitated gold electrodes [64] and an integrated measurement circuit. The single sensor can be independently selected by means of on-chip addressing circuitry. The output of the measurement result is a digital signal which can directly be read by a computer.

The surface of the gold electrodes is bio-modified (functionalized) by covalent binding of single-stranded DNA probes. During in-field operation, the hybridization events of complementary DNA strands, probe and target molecules, is detected by a variation of the capacitance between the sensor site's electrode pair, which is measured by a circuit below the sensor electrode pair using a capacitance to frequency conversion.

For measurement and characterization purposes, the chip has been bonded on a circuit board which is then directly connected to a computer. For verification of the biochemical sensor operation, the electrodes have been functionalized and their capacitance variation has been measured both in case of complementary and non-matching target molecules in order to test specificity. The results clearly demonstrate that the DNA sensor array based on label free, capacitive detection technique can successfully detect specific DNA hybridization.

7.2 Related Work

DNA microarrays, allowing highly parallel and low-cost analysis, exploit the capability to fabricate a large number of miniaturized detection sites

on a substrate and to extract information from each of them after exposure to the solution containing the target DNA. Each site is specifically bio-functionalized, i.e. the sensor surface is equipped with single stranded DNA oligonucleotides with a known sequence, which covalently bind to the sensor's surface. Target molecules in the sample liquid selectively bind to probes with complementary sequence, resulting in hybridization of the two oligonucleotide strands. Their presence at specific sites reveals the composition of the sample solution.

Most of today's detection techniques used within microarrays require molecular signaling labels attached to the target DNA. The associated sensing system detects the presence of light emitting labels on sensor sites where hybridization has taken place by means of an optical scanner. Some innovative microarrays employ electrochemical labels resulting in an electrical current through sensor electrodes during readout in case of hybridization events ([65, 66, 19]).

Label-free techniques offer significant advantages in terms of costs, since they avoid the expensive reagents and pretreatment steps required to attach labels. Recently, a number of approaches have been proposed based on mass changes [24, 67, 68, 69]) or electrical properties of electrode/solution interfaces induced by DNA hybridization ([22, 16, 23, 70]).

Our approach is based on interface capacitance measurements. The sensing principle can be summarized as follows: DNA hybridization leads to a capacitance decrease at the electrode-to-solution interface due to the replacement of electrolytic solution with high dielectric constant by organic DNA oligonucleotides with low dielectric constant. This phenomenon has been studied extensively in the past, using a conventional electrochemical three electrodes system, by applying a 50 *mV* potentiostatic voltage step and measuring the electrode current [47]. In [29], bio-functionalized gold electrodes were characterized with impedance spectroscopy.

Since the capacitive measurement principle is not based on reduction or oxidation processes, two-electrodes configurations, as that used in this work, are sufficient. This simplifies the measurement set-up and on chip implementation. As far as integrable capacitance methods are concerned, it has already been proven that DNA hybridization can be detected by measuring interface capacitance with a system making use of two electrodes only, i.e. without the use of a reference terminal [40, 39]. Furthermore, more recently it has been shown that reliable measurements can be done exploiting microfabricated electrodes [71]. In this case, however, capacitance parameters were measured by means of external instruments and off-chip circuits, since electrodes were deposited on a passive silicon

chip.

In comparison to passive solutions, where each transducer element has to be connected to the readout device individually, the use of active CMOS sensor chips is required in applications where a large number of analysis has to be performed in parallel. Then, not only the sensitivity of the single sensor sites is increased, but also the electrical interconnect to the outside world is reduced, e.g. to a five pin serial interface [76].

In general, detection principles based on electrical or electrochemical signals are very sensitive to variations of the electrolyte or interface properties and compared to optical methods as DNA detection. These measurements required differential measurements and this also has implications on the circuit design of CMOS sensor arrays, such that different kinds of reference sensors and related signal processing should be used for improving the signal to background ratio of the active sensors.

Along this line of development, this work represents a further advance in the state of the art in that it presents a silicon chip featuring an array of sensor electrode pairs for capacitive measurement and integrated measurement circuits monolithically integrated in a standard CMOS chip.

7.3 Capacitance-based DNA Detection Principle

Under proper electrochemical conditions, bio-modified metal interfaces in a saline solution exhibit an almost ideal capacitive behavior. This is the case if gold electrodes are used modified with short DNA strands immobilized with alkanethiol ([39, 29]), in which the capacitance value of the electrode-solution interface has been estimated between 1 and $20\mu F/cm^2$, even if this value strongly depends on electrode surface treatment and roughness. The electrode-solution interface can be modeled by the equivalent circuit depicted in Fig. 7.1 (left) ([42, 73]), where R_S depends on the interface and on the solution characteristics and R_P is related to the insulating properties of the interface. For dense layers R_P is very high and can be considered negligible; C_P is mainly affected by the physical and chemical characteristics of the insulating bio-layer immobilized on the surface.

In our set-up, the dipole formed by two bio-modified electrodes in solution exhibits an equivalent capacitance whose value is given by the series of the two interface-capacitances, one for each electrode, in parallel with the geometrical capacitance formed by the two electrodes. The lat-

ter is several orders of magnitude smaller than the interface-capacitance, hence its contribution is negligible. As mentioned above, it has been observed that when a complementary DNA strands bind with the surface probes, C_P decreases [47, 39, 40]. When the DNA duplex is formed, the solution counterions attracted to the polarized metal surface are displaced [53]. This increases the distance between the charge inside the electrode and the ions in the electrolyte, thus decreasing the interface capacitance (Fig. 7.1, right).

Among the many techniques available to measure capacitances, we have opted for a technique based on the conversion of the capacitance value to a frequency value.

The measurement technique used in the mixed-signal circuit is based on a very simple principle, as shown in Fig. 7.2. A periodic current excitation, I_{REF} , is provided to the electrodes. The electrodes respond to the current pulses by changing their voltage difference in a transient waveform whose time constant is dominated by the capacitive component of the electrode-solution impedance. The inter-electrode potential is monitored for crossings of two fixed reference values, $+V_{REF}$ and $-V_{REF}$. The crossings of $+V_{REF}$ and $-V_{REF}$ produces a square waveform at the output of the comparator whose frequency is proportional to the rate of change of the voltage. Considering R_S negligible, since saline solution is 0,3 M NaCl, the crossing frequency follows the following relation

$$\frac{1}{f} = 2RC \ln \frac{1}{1 - \frac{V_{REF}}{I_{REF}R}} \quad (7.1)$$

where R and C represent the contribution of the capacitance, C_P , and parallel resistance, R_P , of both electrode/solution interface. Moreover, if the frequency is not too low (i.e. I_{REF} is not too small) the first order Taylor approximation of the logarithm returns the following equation:

$$\frac{1}{f} = \frac{2V_{REF}C}{I_{REF}}. \quad (7.2)$$

The frequency is measured by means of a counter which is enabled to count the edges of the square waveform for a fixed time. The data stored in the counter can be read and the interface capacitance value of each electrode can be computed.

One major advantage of this technique is that the digital read-out of the frequency is almost trivial. In fact, an accurate estimate of the frequency value is obtained by counting the number of reference crossings in a given time interval. If the interval is long enough, very good frequency

resolution can be obtained, assuming that the frequency is constant over the measurement interval. The circuit does not directly measure capacitance, but converts transient time into frequency of reference crossings.

7.4 Label-free DNA chip

In this section, we describe the architecture and the detailed operation of the chip, based upon the capacitance measurement technique described in the previous section.

7.4.1 Chip architecture

The chip architecture and signal flow are summarized in Fig. 7.3. The chip interface requires both analog and digital I/O signals. Voltage references are analog DC signals, and they determine the voltage ranges (V_{REF} eq. 7.1 and eq. 7.2) used for measurements. Electrodes are selected using digital addressing lines $A0 - A6$. Control logic includes reset and clock signal. The output is fully digital, as the chip performs internally capacitance measurement and analog-to-digital conversion. Each sensing site features an analog part which converts the impedance value into frequency and outputs the data digitally. Thus, 128 capacitance measurements and analog-to-digital conversions can be performed in parallel, and the results are then multiplexed on the shared output using the address signals which are generated on-chip by means of two decoders (Fig. 7.3). At the output pad, the data are processed by a PC to calculate the capacitance value of the interface for each pixel.

7.4.2 Sensing site circuitry

The mixed-signal circuit implemented for each sensing site is illustrated in Fig. 7.4. It includes an analog part (current source, comparator and switches) and digital part (22 bit counter). The current pulses required for the circuit operation are provided by a current source based on a cascode stage followed by a pair of switches that alternatively connect the mirror to the electrodes in a current push or pull mode. The p-MOS source is part of an in-sensor site p-MOS current mirror biased by an n-MOS current source. The n-MOS current sources bias voltages are generated by an external circuit realized on a PCB (see section 7.5.1). By adjusting the signal V_{MIRROR} it is possible to change the reference current used for the measurements, thereby increasing the range of capacitance

values that can be measured. In our case V_{CASC} is set to $2 V$ to guarantee that n-MOS transistors work in the saturation region. If we neglect transistor mismatches and parasitic, I_{IN} is equal to I_{OUT} and to I_{REF} . The switches are implemented with parallel n- and p-channel transistors in order to have full voltage range.

Comparison of the electrode difference voltage with the reference difference voltage level is performed by a high-gain differential CMOS stage. The output of the gain stage is then buffered by a simple CMOS inverter, thereby becoming a digital signal. Then number of oscillations within a given time is then counted by a digital 22-bit counter clocked. After a user-settable time period, the counter is stopped, and the final count value can be transferred to the output via a shift-register. The shift register is clocked from an external source resulting in a serial output of the counter's data bits at the chip's output. The counter/shift register circuit is similar to that described in [19]. As illustrated in Fig. 7.5, a "reset" signal is activated before each measurement to set all the counters to zero. Then, a "count" signal is set at high value for a fixed time, called integration time, enabling the counter. Finally, a clock signal is used to read the data stored in the shift register of the counter.

The described circuit guarantees that each pixel oscillates continuously at a frequency determined by the interface capacitance. It is important to note, that with this free-running oscillator concept, the data from all sites are sampled simultaneously.

7.4.3 Physical layout

The chip is fabricated in 6" n-well $0.5 \mu m$ CMOS process with three metal layers, the oxide thickness is $15 nm$ and supply voltage is $5 V$. The gold electrodes are deposited after standard CMOS processing. After the gold deposition, an annealing step is introduced applying N_2/H_2 at $350^\circ C$ for 30 minutes in order to guarantee sufficiently low values of the interface state density at the silicon/silicon dioxide interface [64]. Figure 7.6 shows a tilted SEM image of the interdigitated gold electrodes demonstrating the good quality of the deposition process. The sensor sites consist of interdigitated electrodes with $1.2 \mu m$ line width and spacing, the diameter of the circular arrangement is $200 \mu m$. The chip provides an 8×16 array of these sensors and the pitch is $250 \mu m$. Total chip is $6.4 mm \times 4.5 mm$ (7.8, bottom-left). The electrical interface includes analog as well as digital signals. Two different power supply and ground pads are also implemented on chip. A shield connected to ground is introduced to reduce noise between analog and digital circuits (Fig. 7.7).

7.5 Experimental results

7.5.1 Measurement set-up

The chip has been tested in a laboratory setup as shown in Fig 7.8 and Fig. 7.9. The chip is attached onto a PCB, and electrically contacted using gold bonding wires. Before performing a DNA experiment, the gold electrodes are accurately cleaned with oxygen plasma in order to facilitate uniform covalent binding of the thiolated DNA probes to the gold surface. A two-chambers fluidic cell protects both bonded wires and the chip's I/O pads from contact with saline solutions used during the experiments (Fig. 7.8). The different agents used, for instance, to rinse the electrodes after hybridization or to feed the biological sample to the sensor surface, are injected in the two chambers by means of single use syringes.

In our electrical measurements, the DC voltages necessary to perform measurements are generated by an external circuit implemented on the PCB. The output and digital input data from the counters are handled by means of a National Instruments DAQ board (PCI-6534E [61]). A Lab-View software records the frequency data of the sensor sites, calculates the capacitance values and writes the data to a file (Fig 7.9).

7.5.2 Electrical Characterization

The electrical behavior of our chip is tested using discrete precision capacitors (error less than 1%) within a range from 330 pF to 10 nF . In Fig. 7.10, measured results are shown for three different reference currents. As expected a linear behavior is obtained, the slope is 0.9837 and the error bars are negligible.

The influence of parallel resistive components is shown in Fig. 7.11. There, measured frequencies of four test circuits are plotted as a function of I_{REF} . Solid lines correspond to purely capacitive load, 1 nF and 4.7 nF , respectively, dotted lines to capacitances in parallel with resistances, 1 nF with 200 $k\Omega$ and 4.7 nF with 200 $k\Omega$, respectively. The plot clearly shows that a parasitic parallel resistor R_P does not affect the function of the integrated sensors. Moreover, the parasitic capacitance can be determined precisely, by evaluating the oscillation frequencies for different reference currents. If the application allows the use of large reference currents and hence high oscillation frequencies, the effect of the parasitic resistor can be neglected. The curve converges asymptotically to the ideal capacitive line for large reference currents (7.11).

Moreover, we have performed measurements for a fixed capacitance, 1 nF and three different R_P : $100\text{ k}\Omega$, $200\text{ k}\Omega$ and $680\text{ k}\Omega$ in order to characterize the circuit under realistic non ideal conditions. Fig. 7.12 shows measurement results in a frequency vs reference current plot. We can observe that only at low frequencies and low parallel resistance values, lower than $680\text{ k}\Omega$, the parallel resistance influences the measurement leaving ideal linear behavior.

The resistance per unit surface value of R_P using gold electrode modified with self assembled monolayer (SAM) in solution is approximated with $15\text{ k}\Omega\text{ cm}^2$ [29]. Since the area of our electrodes is approximately $0,03\text{ mm}^2$, we expect a parallel resistance of around $50\text{ M}\Omega$. This verifies the condition of approximately ideal capacitive behavior for our sensors. All the DNA hybridization measurements have been performed with I_{REF} is $1\text{ }\mu\text{A}$ and V_{REF} is 200 mV .

7.5.3 DNA detection

DNA detection is demonstrated by comparing measurements on electrodes in the two isolated chambers exposed to the same solution. In one chamber only bare electrodes are present (reference pixels) while in the second one DNA probes are immobilized on the gold surface (functionalized electrodes) (*step 1*). The use of reference pixels is important for correct measurements. The gold surface of the reference pixels is not functionalized with probe molecules, hence, DNA strands on the sample cannot bind to the surface. These electrodes provide the background signal, which includes all phenomena occurring at the electrodes/solution interface, with the exception of DNA hybridization. Then, solutions containing DNA molecules, non complementary (*step 2*) and complementary (*step 3*) to the immobilized probe molecules, are injected in the two chambers and measurements are performed after each step.

Frequency measurements, which takes typically around 1 s , have been performed for 8 minutes for each step in order to obtain a stable value. The capacitance value is calculated by means of equation 7.2 from the average value of the last 2 minutes of measurements. Since capacitance and frequency are inversely proportional, standard deviation, σ , can be calculated as follows:

$$\frac{\sigma_f}{f_{AVG}} = \frac{\sigma_C}{C_{AVG}} \quad (7.3)$$

Each step is analyzed by taking the difference signal between the gold electrodes (reference pixels) and the functionalized ones which, after

the first step, are subjected to the same treatment. Typical trend of measurement is shown in Fig. 7.13 where the transients and the final stable values are clearly shown. Drifts in interface impedance have been studied in depth in the literature. Cyclic voltammetry has shown that the transient behavior is due to complex ions double-layer structures occurring also in bare electrodes at the electrode/solution interfaces and evidenced by the polarization [29]. Moreover, a decreasing trend in time is also present along the different steps measurements. Decreasing trends like that shown in Fig. 7.13 are typical in DNA detection, and they are clearly observed also with other detection technologies [77].

In Fig. 7.14 typical results for different pixels are shown. The three columns indicate the difference between bare gold and the functionalized electrodes for each step. Important is to note that the behavior of the single electrodes are coherent. In particular, the measured differential capacitance in the case of non-specific binding is only slightly reduced as compared to the value observed at functionalized electrodes before exposure to the sample liquid. This means that the small amount of non-specific binding of target molecules to the DNA probes or non-specific adhesion of organic molecules to the sensor's surface is negligible. In fact, the direct comparison of the average differential capacitances and their standard deviations of the step 1 and the step 2 shows that the detection provide the same value, in terms of statistical significance. On the other hand, a direct comparison of step 1 and step 3 shows that the complementary DNA binding is detected with statistical significance. Moreover, little discrepancies of the single detection by different pixels but referred of the same step are, again, indistinguishable within a statistical range.

The average behavior of the pixels is shown in Fig. 7.15. It confirms the ability of the chip to reliably detect the hybridization process on the pixel's sensor electrode. The standard deviation of these values reflects statistical variations in the electrical behavior of the different pixels on one chip but also statistical variations of the electrode's functionalization SAM quality. However, the measurement results clearly show, that specific detection of label free DNA target molecules can be performed with statistical significance. Moreover, similar average values and error bars overlapping of the non-specific binding (step 2) compared to only probe state (step 1) demonstrates that the system is capable of rejecting false positives due to non-specific deposition of sample DNA on the electrode surfaces.

7.6 Figures

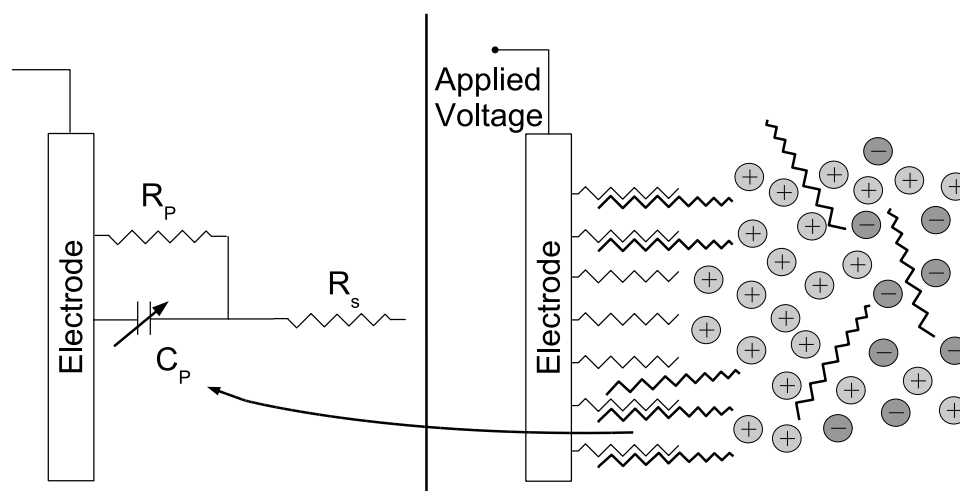


Figure 7.1: Left: Electrical metal/solution interface model. Right: DNA hybridization process and displacement of counterions.

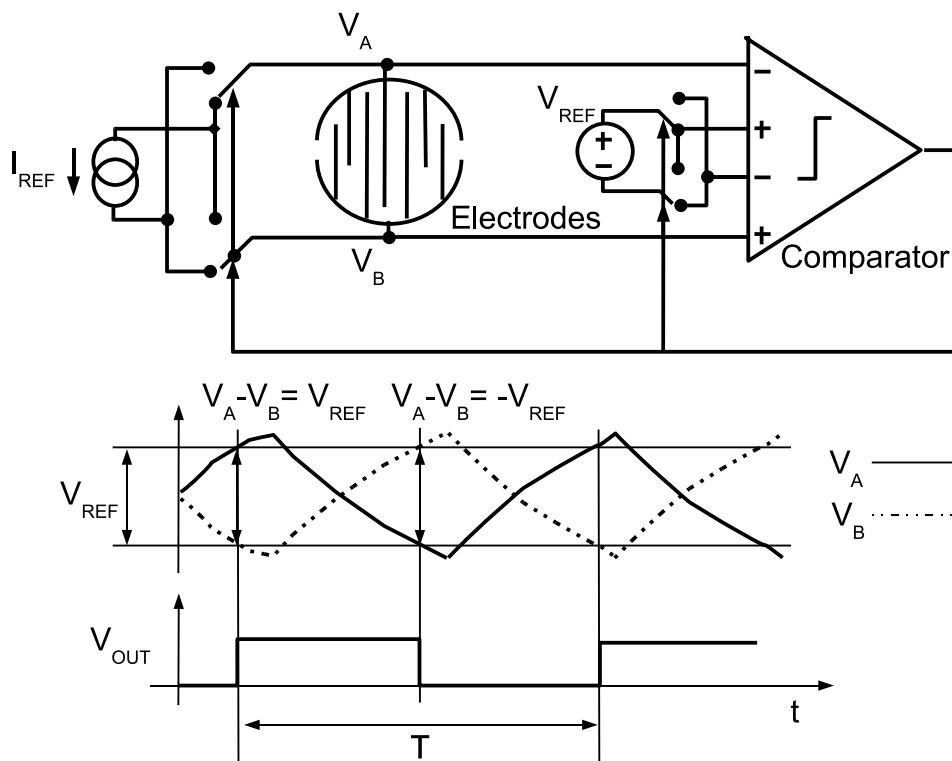


Figure 7.2: Measurement principle: interface capacitance determines the frequency of the electrodes charging and discharging transients. A comparator compares the inter-electrode potential with a reference voltage V_{REF} producing a digital signal at its output whose frequency is inversely proportional to capacitance.

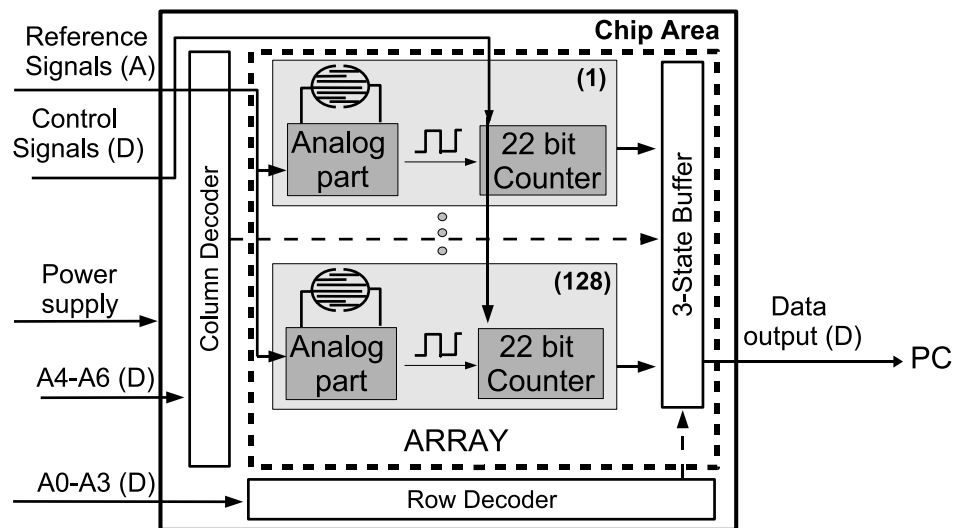


Figure 7.3: Schematic representation of the system and signal flow. *A* and *D* indicate analog and digital signals, respectively.

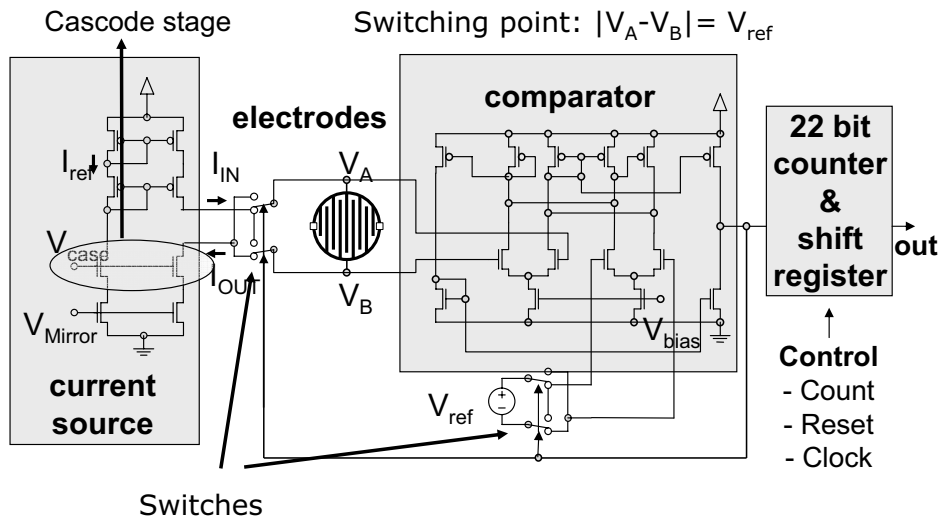


Figure 7.4: Schematic of the circuit associated to each sensing element. The current source is implemented by a current mirror circuit. The comparator features two differential input stages and an high-gain output stage. Finally a 22-bit counter and shift register samples and stores measurement data.

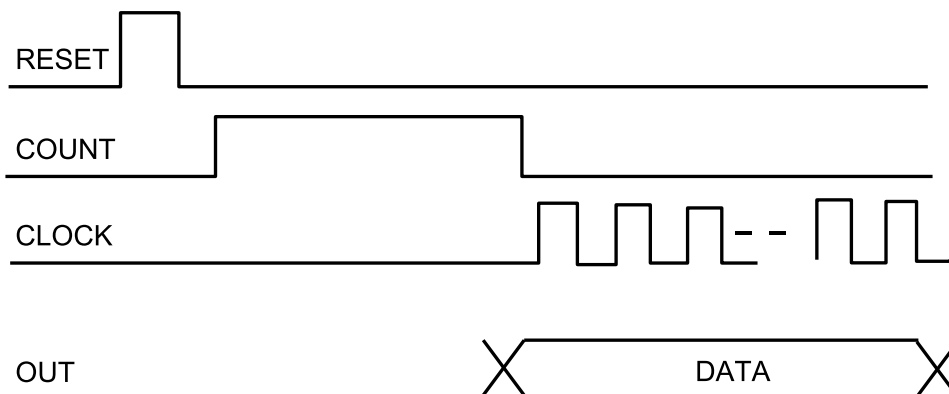


Figure 7.5: Signal flow of counter input/output.

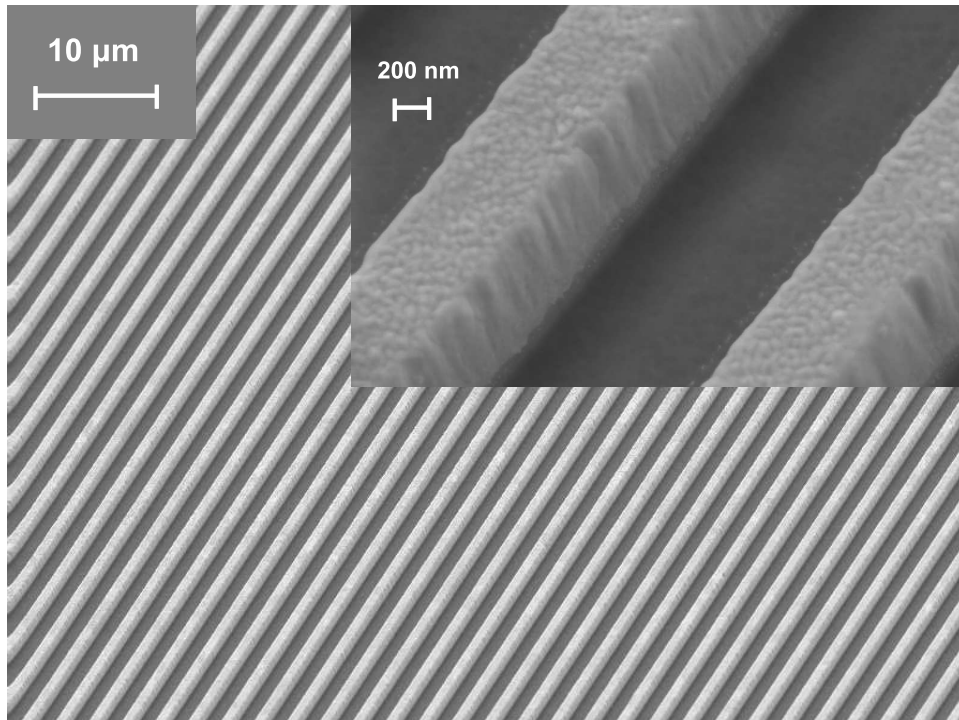


Figure 7.6: SEM image of interdigitated gold electrodes. Inset: zoom of single finger electrode.

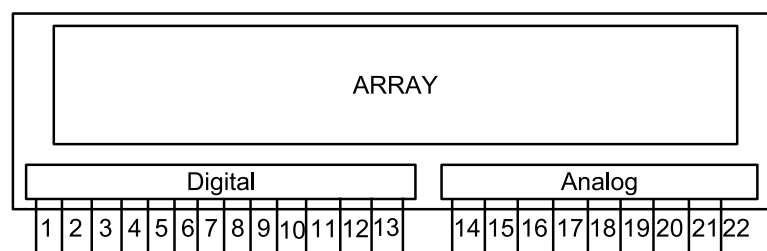


Figure 7.7: Pinout of the chip.

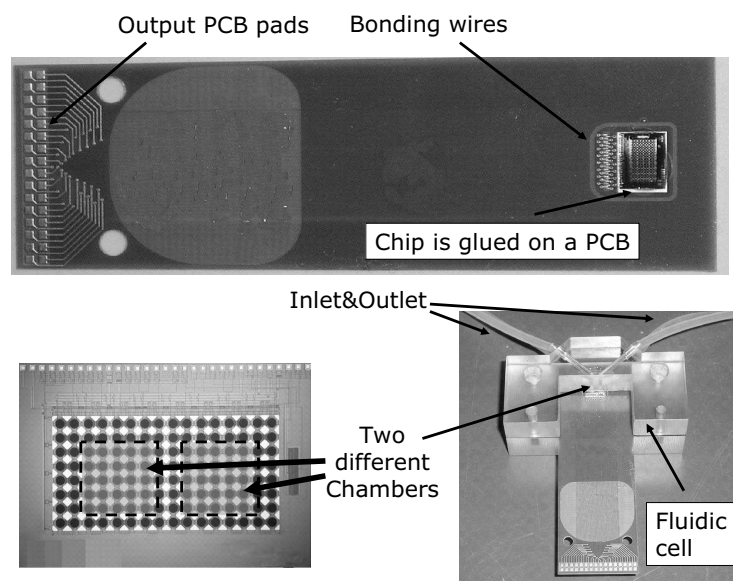


Figure 7.8: Photo of the PCB used to contact pads with the glued chip, bonding wires (top) and the applied fluidic cell (bottom-right). The cell determines two separated areas on the chip (bottom-left) which can be functionalized with different probes.

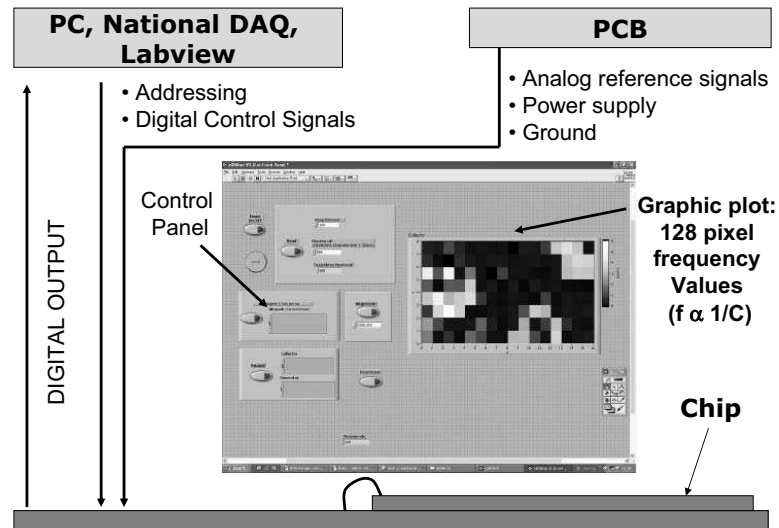


Figure 7.9: Schematic representation of the measurement set-up. Voltage reference signals and power supply are generated by circuitry on the PCB. Digital control signals are provided by a PC. The LabView interface manages all the parameters involved in the measurements and shows directly on the screen the measurement results of the whole array.

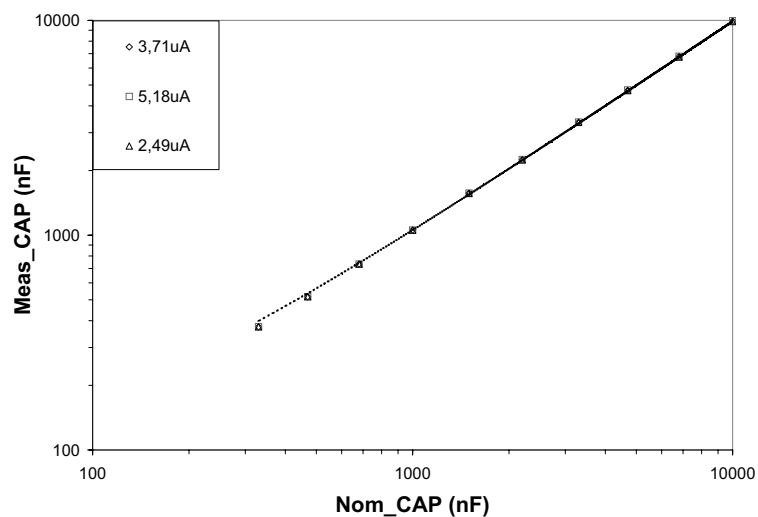


Figure 7.10: Measured capacitance vs nominal capacitance.

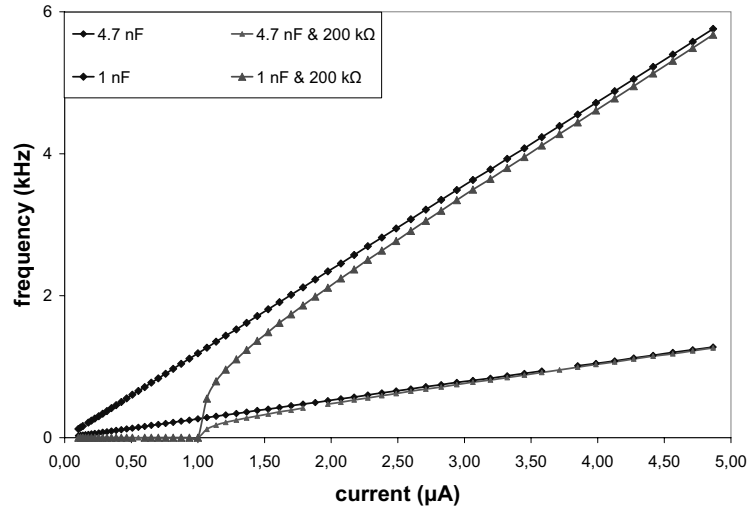


Figure 7.11: Frequency vs reference current showing the influence of the parallel resistor for two different capacitance values. A non linear behavior is evidenced in low frequencies regime.

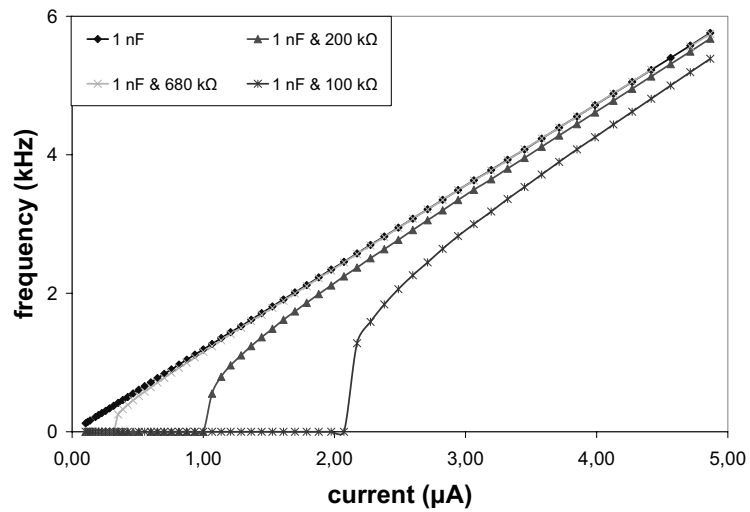


Figure 7.12: Frequency vs reference current showing that a significant influence of the parallel resistance on the measurement result occurs only at low current values and at R_P values lower than 680 k Ω .

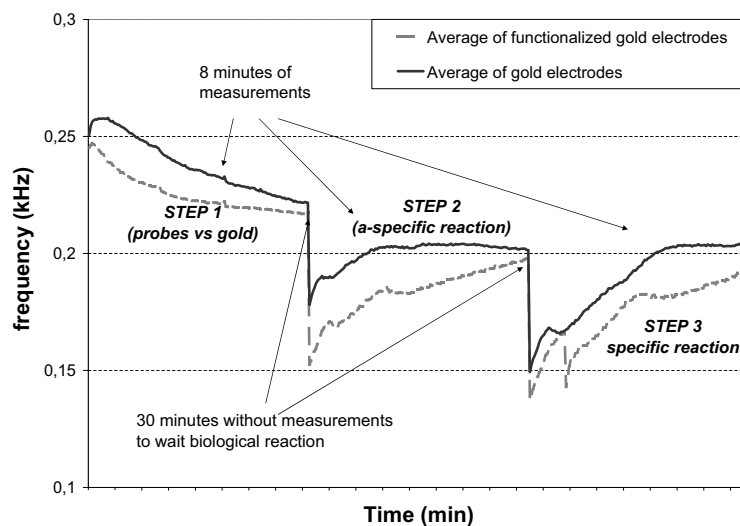


Figure 7.13: Frequency changes of the average of reference electrodes (continuous line), and the average of functionalized electrodes (dashed line) show a larger gap after DNA hybridization step considering the stable value reached at the end of the transient.

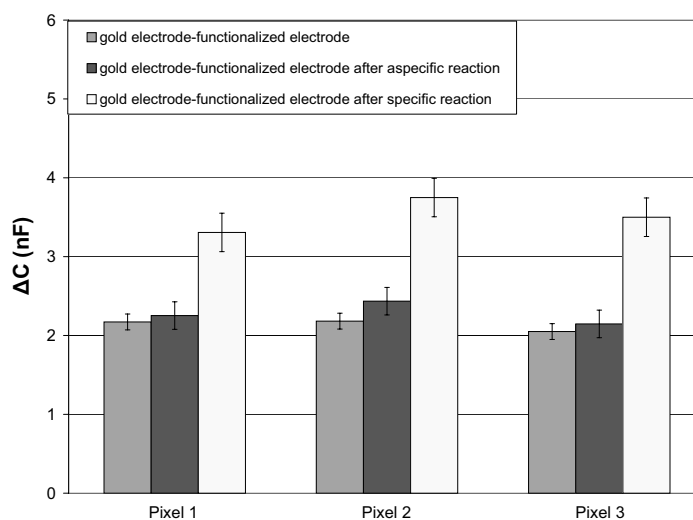


Figure 7.14: Typical variations for several pixels among functionalized electrodes and the average value of reference gold electrodes. Capability to distinguish between specific and a-specific binding is shown for each pixel.

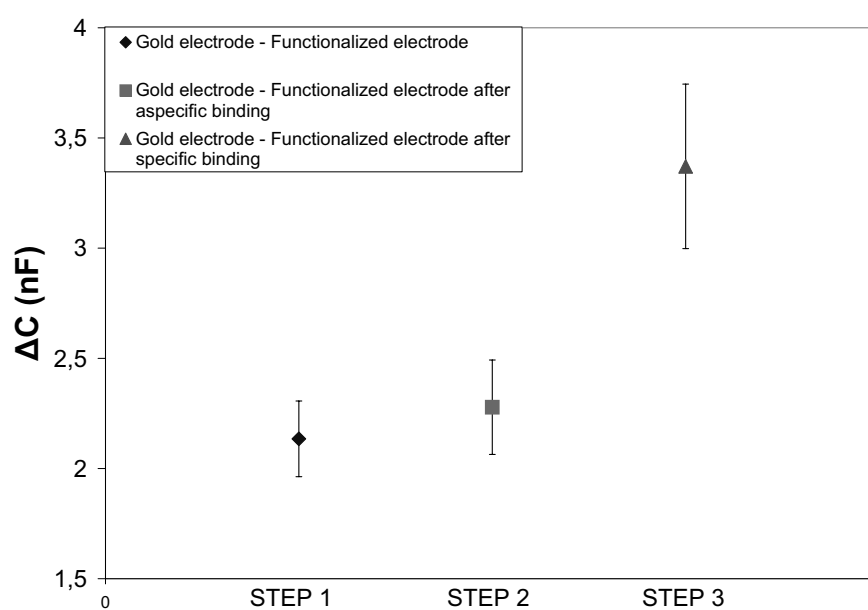


Figure 7.15: The average behavior of all the pixels confirms that a-specific and specific binding are distinguishable.

Chapter 8

Application on tumor marker and future steps on DNA

8.1 Tumor marker analysis

Early diagnosis of cancer is crucial for the successful treatment of the disease. Highly sensitive methods are urgently needed for measuring cancer diagnosis markers present at ultra-low levels during early stages of the disease. Such methods should facilitate early detection and an adequate selection of the treatment of diseases and should lead to increased patient survival rates. Existing diagnostic tests (e.g., ELISA) are not sensitive enough and detect proteins at levels corresponding to advanced stages of the disease. Smaller, faster, and cheaper (one-step) devices are highly desired for replacing time-consuming laboratory-analysis. Making analytical results available at patient bedside within few minutes will greatly improve the monitoring of cancer progress and patient therapy. Advances in molecular biology have led to a much understanding of potential biomarkers that can be used for cancer diagnosis. The realization of point-of-care cancer diagnostics thus requires proper attention to the major challenge of multi-target detection. Arrays of biosensors, detecting protein signature patterns or multiple DNA mutations, can be used to help screening and guide treatment. Innovative biosensor strategies would allow cancer testing to be performed more rapidly, inexpensively, and reliably in a decentralized setting. In this review article I will discuss the use of electrochemical biosensors for decentralized clinical testing and the prospects and challenges of using such devices for point-of-care cancer diagnostics.

8.2 Immunosensors

Abnormal concentrations of certain proteins can indicate the presence of various cancers. For the past two decades Heineman's group has developed highly sensitive enzyme electrochemical immunoassays [78]. Such protocols rely on labeling of the antibody (or antigen) with an enzyme which acts on a substrate and generate an electroactive product that can be detected amperometrically. Enzyme immunosensors can employ competitive or sandwich modes of operation. In addition to enzyme labels, it is possible to use metal markers and redox tags for electronic transduction of antigenantibody interactions.

The development of electrochemical immunosensors present the main aim of reduce costs and increase the preventive analysis in tumor diseases. Our approach is similar to what described in previous chapters of this thesis and is based on capacitance measurement. In particular, we started from CBCM technique based on commercial devices, as already described, and gold electrode.

8.3 Device and methods

The measurement system is exactly the same described in chapter 5 changing the I/V conversion resistance to $4.7\text{ k}\Omega$ since gold electrode are changed. In fact, the gold electrode used for the following experiment were made by Olivetti InkJet in Arnad (Italy). Fig. 8.1 shows the layout of the chip where it is ease to note 5 different sensing sites addressable by means of 4 pads. From chemical point of view binding of antibody on gold surface has been solved previously binding a layer of mercaptoundecanoic acid on gold. This layer expose a carboxylic group which allow after activation with EDC (1-ethyl-3-(3-dimethylaminopropyl) carbodiimide hydrochloride) and NHS (N-Hydroxysuccinimide)(Fig. 8.2), to bind the amino group of the antibody (Fig. 8.3). After that incubation for 4 hours with antigen (SCCA-specific for liver cancer) has been performed. Buffer solution used in all experiment is PBS (Phosphate Saline Buffer). A second way to functionalized the surface exploiting 3-glycol chain on the top of molecules before carboxylic group was tested in order to avoid aspecific binding on surface as demonstrated in [79]. Moreover this last surface modification has been used also to improve stability of capacitance measurement for DNA detection. In this case we have used the same DNA oligonucleotide already described in this thesis but probe molecules where modify with amino group instead that thiol group in

order to exploit the same protocol used for binding antibody.

8.4 Experimental results

Typical measurements in time after the first way of functionalization are shown in Fig. 8.4. A standard deviation of 9.2% is observed. This behavior reduce the possibility to increase the sensitivity of our system in particular for protein where the expected capacitance variation could be smaller because of a more distance respect to the gold electrode. Comparing this measurements with the ones shown in Fig. 8.5 that are obtained with the second way of gold modification described in the previous paragraph, it is easy to observe that stability of measurement in time increase of one order of magnitude. In fact, standard deviation in this second case is 1%. Therefore, all the following results are obtained using the more stable functionalization process. In order to test the capability of our system to detect Ab/Ag reaction without aspecific signal, we have tested the system on which were already bound Ab molecules with BSA (Bovine Serum Albumin) and afterward we add the specific molecules (SCCA). Results are shown in Fig. 8.6 where you can observe a small decrease after BSA incubation while a largest increase after incubation with SCCA. Small values of standard deviation allow to clearly and statistically distinguish capacitance variation. Moreover, also on DNA detection the previous treatment with 3-glycol molecules increase the capability to distinguish where hybridization reaction occurs compared to aspecific binding. Following the same protocol of Ab binding on 3-glycol molecules and the hybridization protocol described in the previous chapters, Fig. 8.7 shows measurements results on 4 different sensing sites of the chip. An increase in capacitance value is observed over all the chip after probe binding (probably due to reorganization of the SAM layer). Finally, where hybridization occurs a decrease is observed (site 1 and 2) while where aspecific binding (site 3) and only buffer solution (site 4), a small increase and a negligible variation respectively, is observed. This preliminary experiment encourage to proceed on this way of stabilization of capacitance measurement in order to increase reproducibility and sensitivity of our detection device also for genetic analysis. Observing the graphs differences among sites still have to be explained and improve working on surface chemistry but the trend and low standard deviation of measurement demonstrate the possibility of this technique to improve detection of biological reaction.

8.5 Figures

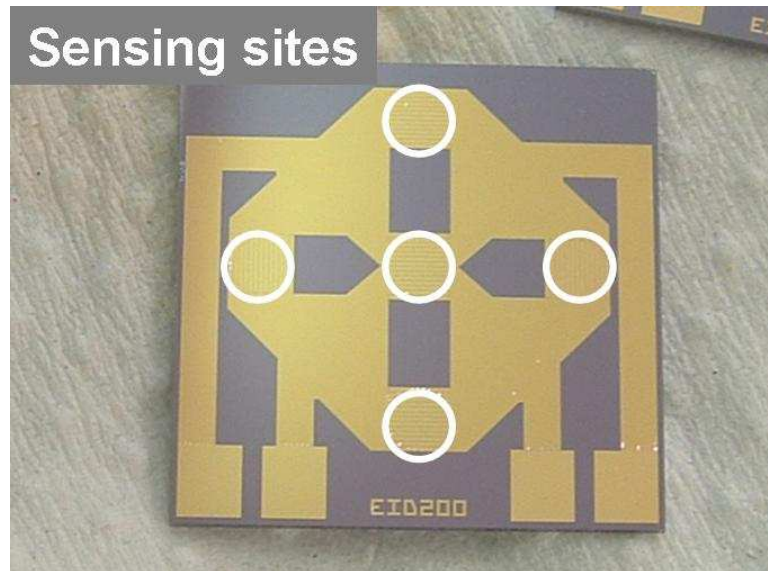


Figure 8.1: Photograph of the sensing chip.

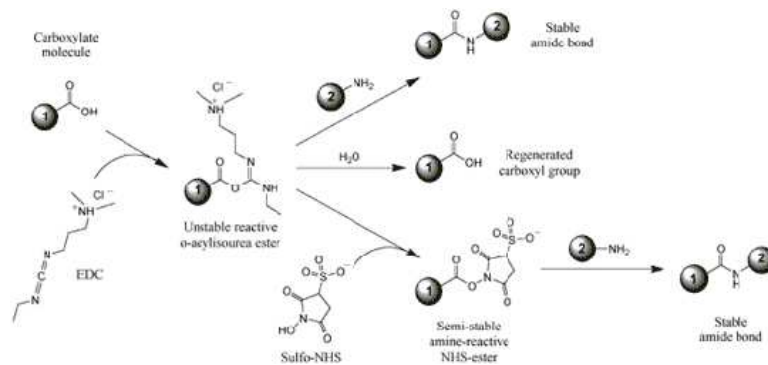


Figure 8.2: Activation of carboxylic group before antibody binding.

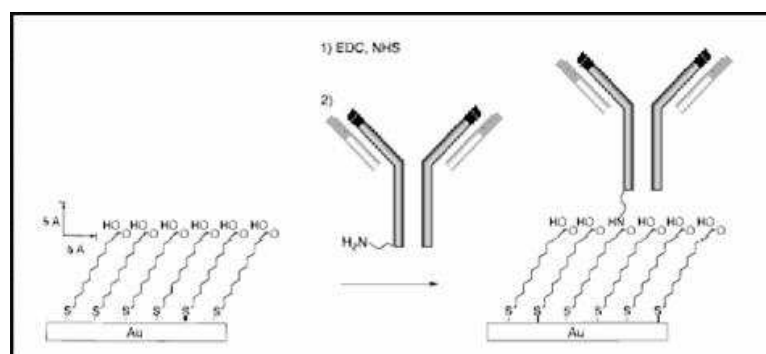


Figure 8.3: Antibody binding on gold surface modified with mercaptoundecanoic acid.

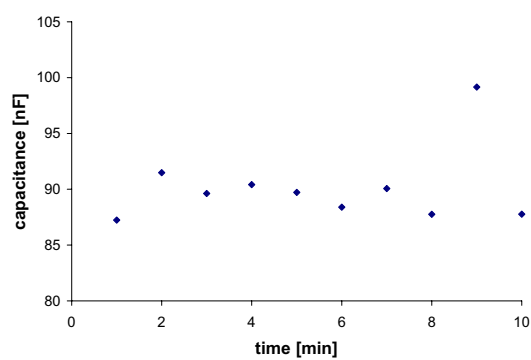


Figure 8.4: Typical measurement in time of mercaptoundecanoic acid.

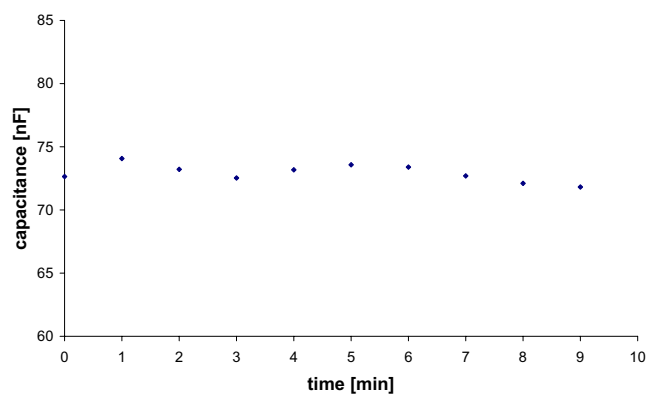


Figure 8.5: Typical measurements in time of 3-glycol modified gold surface.

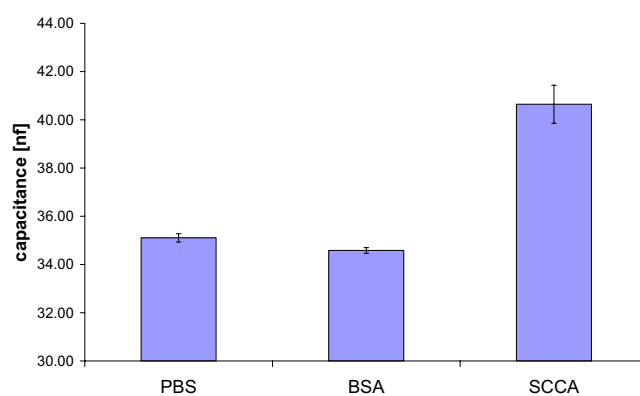


Figure 8.6: Aspecific binding signal compared with specific SCCA reaction.

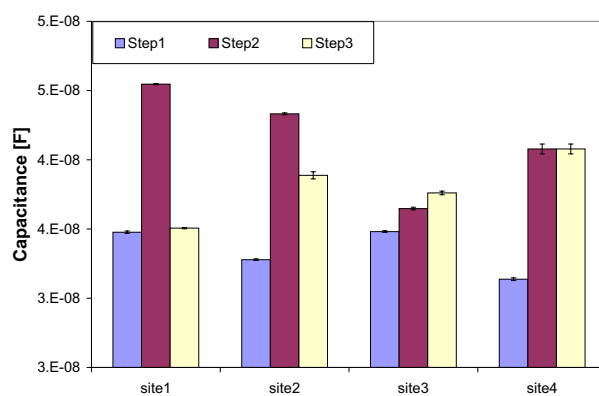


Figure 8.7: Results on DNA detection exploiting 3-glycol previous layer on 4 different sites: step1 is after 3G functionalization; step2 is after probe binding; step3 is after specific hybridization in sites 1 and 2 while is aspecific in site 3 and only buffer were added on site 4.

Chapter 9

EEPROM memory as DNA sensor

9.1 Introduction

In the last decade, genetic research has started to make large use of miniaturized devices (in general known as microarrays), consisting of glass or quartz slides featuring a two-dimensional array of small sites, each aimed at recognizing the presence of a specific base sequence within the unknown DNA "target" molecules to be analyzed/ recognized. To this purpose each site is "functionalized" with the immobilization of known single-stranded base sequences, called probes, able to selectively bind (hybridize) with the complementary ones possibly present within the DNA targets. In operation, all sites are simultaneously exposed to the material to be analyzed and the probes essentially work as "selective glue" for the target molecules. Thus, the recognition of the presence of specific sequences within the DNA targets is transformed in the identification of the sites where probe- target hybridization has taken place. Some of these devices, featuring densities up to hundreds of thousands sites [4], are able to perform tests on a whole genome scale. Moreover, low or medium density arrays (featuring from ten [80, 81, 82] to forty thousand sites [83]) are sufficient for analysis of a restricted number of genes. For the devices currently used to-day, the DNA strands to be identified (hereafter referred to as targets) are preliminary marked with fluorescent molecules and, when they hybridize with specific probes and are consequently immobilized in the corresponding sites of the array, their presence is revealed by means of an optical scanner or a fluorescence microscope. However, the high cost of the scanner, the unreliability due to the use of

markers (also called labels), and the complex data processing procedures needed to extract useful information from these arrays pose critical limits to the widespread use of these tools. In the attempt to overcome these drawbacks alternative detection techniques are intensely investigated. In this paper, we present a new approach based on measurements of UV absorbance without the use of any labels. This technique is particularly interesting because UV absorption by polynucleotide molecules is highly specific and commonly employed as a tool in standard spectrophotometers [84, 85]. However, until very recently [86], it has not been used as a basis of microfabricated DNA sensors/detectors. At system level, our approach envisages an array of "sensing" sites, each consisting of a bio-layer of specific probes, positioned between an external UV source and a UV detector. The bio-layer is conventional, in that it is obtained by means of DNA probes, aligned with the underlying sensor and working as "selective glue" with respect to the DNA target molecules. In operation, all sites are simultaneously exposed to the targets molecules, that will selectively hybridize only with complementary probes. Since DNA has a significant UV absorption, the sites where hybridization has taken place will present different UV absorption with respect to those where the same amount of DNA is in the non hybridized state. The radiation transmitted through such sites will be smaller in the first case, due to masking effect of the hybridized DNA. As already explained, the recognition of this difference implies that of complementary molecules. A previous work [86] presented an implementation of the concept described above consisting of bio-functionalized quartz slides, UV sensors fabricated in amorphous silicon and read-out electronics realized in the form of a PCB with standard components. The result is a low cost device, suitable for low-density arrays and aimed at point-of-care applications. In this work, instead, we present a complementary implementation of the same approach, aimed at high performance devices, exploiting all the advantages of silicon integration. In particular, both the UV sensors and the electronics needed to address and read the individual sites could be integrated on the same chip and the resulting devices would be extremely compact, fast and suitable for high-density arrays of sensing sites.

9.2 Devices and method

The key point of this work is the use of NV memory cells as UV sensors. As known, these cells can be erased by means of UV radiation, particularly if designed so that their Floating Gate (FG) can be directly exposed

to the incoming radiation. Since during erasing the cell threshold voltage shift ($\Delta V_{TH} = V_{TH0} - V_{TH}$, where V_{TH} and V_{TH0} denote the actual and initial value of the threshold voltage, respectively) increases with the UV dose, NV cells represent almost ideal UV dosimeters that can be exploited for the purpose of this work. Therefore, the DNA chip envisaged in this work features an array of suitable NV memory cells, all initially programmed at the same threshold voltage V_{TH0} (i.e. V_{THN} where V_{THN} is the cell threshold voltage with no charge on the FG). Each cell (or group of cells) is located below a specific bio-functionalized layer. After exposure to the target DNA the whole array is exposed to UV radiation for a fixed time. Consequently all cells are partially erased, but those covered by hybridized targets receive less radiation, hence exhibit a final higher value of V_{TH} . (i.e. a smaller ΔV_{TH}), compared with those where non DNA binding has occurred. Of course, all the electronics needed to individually select and read the cells in the array are essentially the same as in (multi-level) memories, hence can be integrated on the same chip as the cells. Moreover, since memory cells can be very small, a number of them can be used for each sensing sites, thus allowing the possible implementation of useful checking algorithms. In this context, the target of this work is the characterization of NV memory cells as DNA detectors, in order to show that they are suitable for the task. For this purpose, liquid DNA solutions in quartz containers will be "superimposed" to memory cells (fabricated ad hoc to be easily accessible and measurable). In this way, not only a possible implementation of DNA sensors (featuring microfabricated wells as liquid containers) is directly explored, but DNA concentrations can be controlled with great accuracy. The DNA "sensing site" used in this work is shown in Fig. 9.1. A quartz container with the DNA targets is placed between a UV lamp and the NV memory cell used as a dosimeter for the impinging UV radiation. A mechanical shutter allows to switch on and off the incident UV radiation. The memory cell is initially programmed at a fixed value (V_{TH0} i.e. V_{THN}) of threshold voltage. Then, the UV radiation is switched on and is transmitted through the DNA solution. Since the UV dose reaching the memory cell depends on the absorption of the DNA solution (namely on DNA concentration and whether or not DNA is in the double or single strand state), measuring ΔV_{TH} after a fixed time provides information about the fact that probe-target hybridization has or has not occurred. As for recognition of specific DNA sequences, the experiments of this work exploit the so called hypochromic effect, namely the fact that for the same number of DNA bases (nucleotides), the UV absorption of double-stranded molecules is smaller (by about 20%) than that of the single stranded form.

Of course, for the purpose of this work a major question concerns the sensitivity of NV cells used as UV detectors and, from this point of view, a suitable device has to be used. From this point of view, unfortunately, standard double poly Flash cells are not particularly suitable because, when exposed to UV, their FG is masked by the polysilicon Control Gate (CG), that absorbs most of the radiation. For this reason, "single-poly EEPROM devices" have been chosen. As known, in this technology, the CG is realized by means of a n+ diffusion under the FG, that extends outside the channel area (Fig. 9.1). This feature has some very important benefits, namely: a) the FG is completely exposed to U.V. radiation (i.e. no "masking" CG is present); 2) the FG area is larger than normal (thus more UV radiation can be collected); 3) the cell can be easily fabricated by CMOS technology. For the experiments of this work, test chips has been designed and fabricated with $0.25 \mu m$ CMOS technology at STMicroelectronics (Milan, Italy). The chips contains single memory cells that can be directly contacted by means of suitable pins. The area of the cells is approximately $20 \mu m^2$ but could easily be made larger to improve the UV sensitivity.

9.3 Measurement setup

The experimental set-up used in this work is schematically represented in Fig. 9.2. The source of UV radiation is a Xenon lamp characterized by a spectral distribution with high emission values in the range of interest (250 to 270 nm). The lamp filament is controlled by a special circuit which maintains the supplied power constant. However, since this does not guarantee radiation stability over long time periods, a specific circuit has been used to measure the instantaneous radiation and compute the total dose. This circuit is based on a photodiode (whose spectral sensitivity is particularly high in the range of interest) whose output current is amplified by an I/V converter and sampled by means of an acquisition board equipped with 16-bit converters. The photodiode is placed directly after the UV filter needed to select the radiation range of interest and before the quartz container: thus the UV dose is independent of the DNA solutions placed after. The sample data are processed by a LabVIEW program in order to evaluate the radiation dose of the experiments. The same program controls the shutter and switches off the radiation once the dose has reached a desired value. The EEPROM V_{TH} is measured, when the light source is disabled, by means of a HP4156 Semiconductor Parameter Analyzer (SPA) driven by the control PC. V_{TH} is conven-

tionally defined as the CG voltage needed to obtain a drain current of $2 \mu A$ when the drain is driven to $1 V$ and source and bulk are grounded. Resolution in V_{TH} measurements is $1 mV$. A LabVIEW program automatically controls the whole measurement. The operator sets the step dose and the number of steps. The controller then starts a measurement step consisting of: i) a first determination of V_{TH} , ii) the application of a step dose; iii) a subsequent re-determination of V_{TH} . This step is repeated a number of times selected by the user. After the last step the operator manually resets the cell to the initial state (by means of an over program operation followed by short UV erase steps to set the V_{TH} to $V_{TH0} = 5.5 V$ within $1 mV$ error). The whole measurement is repeated 5 times for each DNA solution to evaluate the standard deviation, hence the measurement reliability. Resulting data present very low standard deviation, thus no error bars have been plotted.

9.4 Experimental results

results described in this Section are shown as a function of UV dose (a parameter equivalent to, but more appropriate than exposure time). Fig. 9.3 shows the typical behavior of ΔV_{TH} as a function of the UV dose and, as can be seen, a difference is measured for different values of single-stranded DNA concentration. Fig. 9.4 shows the curves obtained for the same concentration of DNA but after an annealing step allowing the molecules to hybridize. The Fig. 9.3 and Fig. 9.4 show that the difference between different samples increase with UV exposure; however in the long run all cells would be completely erased, regardless of DNA concentration. Thus a question is in order about the optimum UV dose for maximum sensitivity. To investigate this problem, we introduce a new parameter denoted as Under Erasure (U.E.) defined as

$$U.E. = \Delta V_{TH-BUFFER} - \Delta V_{TH-DNA} \quad (9.1)$$

where $\Delta V_{TH-BUFFER}$ and ΔV_{TH-DNA} represent ΔV_{TH} measured in the case where only the buffer or the buffer containing DNA is interposed between the UV source and EEPROM cells, respectively (in this definition, of course, $\Delta V_{TH-BUFFER}$ merely represents a convenient common reference). The results indicate that an optimum dose is about 300 (in A.U.) and this value is found to be essentially independent of DNA concentration (while it may probably depend on the EEPROM cell technology and geometry). This value allows to obtain maximum measurement sensitivity. Taking this result into account, in our experiments UV dose of

225 is used to obtain a good trade-off between measurement signal and time exposure. As for DNA recognition, relevant results are illustrated in Fig. 9.6, where the experimental points are drawn in such a way that each value of concentration on the x axis corresponds to the same number of single-stranded DNA bases (i.e. the elements actually absorbing UV radiation), so that the difference among the various curves is due only to whether or not the DNA is in the bound (i.e. hybridized) state. In particular, the points indicated with squares and diamonds represents the case where the same number (N) of DNA single strands are presented in double and single-stranded form, respectively. As can be seen, the measurements allow to easily recognize the case of hybridization, that is the key for the DNA sensor envisaged in this work.

9.5 Discussion

The results presented before clearly indicate that a DNA microarray based on the approach suggested in this work and realized in a single chip with standard CMOS technology seems possible, since (at least) single-poly EEPROM cells represent a suitable UV detectors. Compared with the microarrays in use to-day, such a microarray would benefit of all advantages of integration. In particular: a) sophisticated electronics for site addressing and electrical read-out could be easily integrated on the same chip (in fact, these features are essentially the same as those of Multi-Level NV memories); b) a large number of small cells could be available, and this would allow to use a number of them for each sensing sites (to implement checking schemes for error detection and correction; c) sensors would be cost-effective (for mass production); d) devices would be highly reliable, and could be easily made user-friendly e) no markers are needed for the analysis In the case of fully integrated sensors, small containers (wells) for DNA could be fabricated directly on top of the IC passivating glass. Such containers would be much smaller than those used in this work. However, the relevant parameter is the number of DNA molecules along the optical path within the container, in practice the average number of molecules along a vertical path from the liquid upper level to the container bottom. This number decreases linearly with the vertical dimension of the container, however the amount of molecules along such a path can be easily brought back to an adequate level increasing the DNA concentration. At this regard, the results of Fig. 9.6 indicates that double and single-stranded molecules in 1 cm path length can be distinguished starting from a minimum concentration

of $1.5 \mu M$ bases Finally, it is worth mentioning that the ratio of the slopes of the lower to upper curve of Fig. 9.6 is 0.63, thus indicating that hybridization leads to a 37% decrease in UV absorption, in fair agreement with published data [87] on the hypochromic effect exploited in the experiments.

9.6 Figures

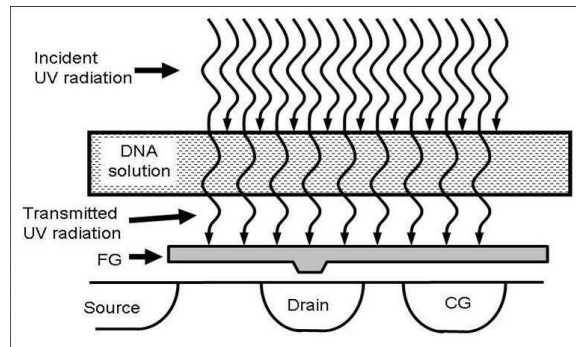


Figure 9.1: DNA detection principle.

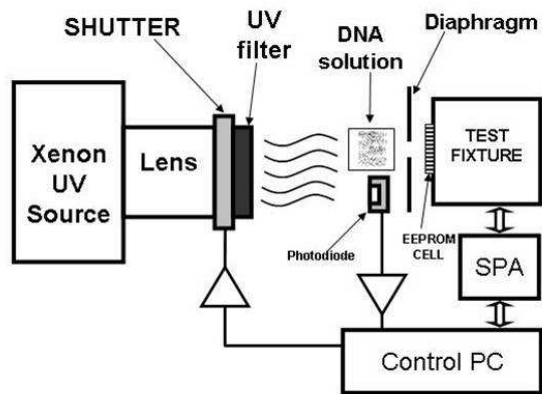


Figure 9.2: Schematic representation of the experimental set-up.

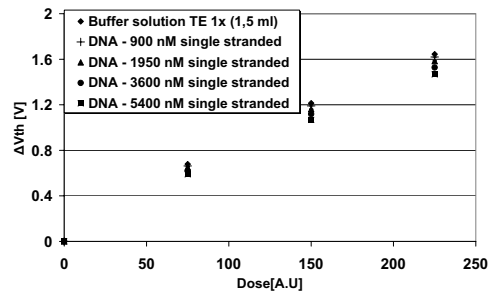


Figure 9.3: Variation of EEPROM cell threshold voltage shift as a function of the UV dose for the case of single-stranded (i.e. non hybridized) molecules.

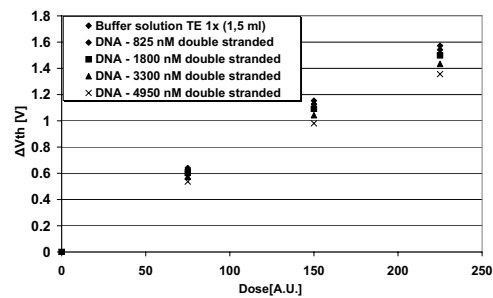


Figure 9.4: Variation of EEPROM cell threshold voltage shift as a function of the UV dose for the case of double-stranded (i.e. hybridized) molecules.

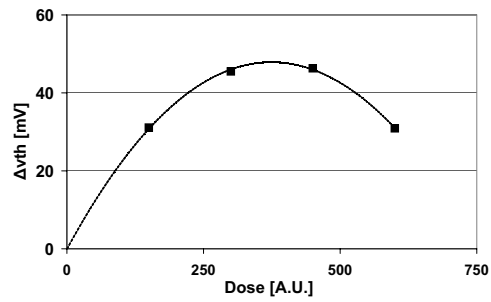


Figure 9.5: Typical behavior of the Under Erasure (U.E.) as a function of the UV dose (the DNA concentration here is 100 nM).

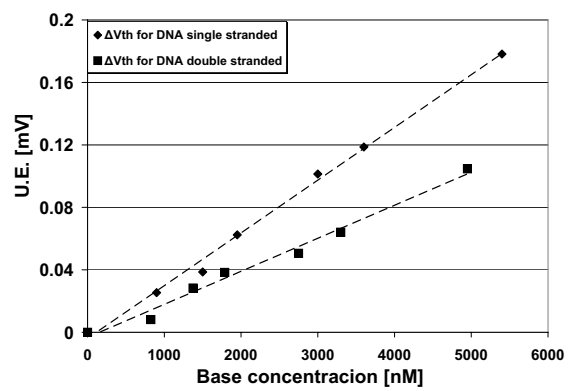


Figure 9.6: U.E. for the case of hybridized and non- hybridized DNA, lower and upper curves, respectively.

Chapter 10

Conclusions and perspectives

During PhD I have studied the possibility to detect by mean of fully electrical capacitance measurement DNA hybridization reaction on metal surface. I started from literauture where evidence of this detection were reported [40] but results were obtained with a laboratory setup. Therefore, I follow two ways in order to do a step in advance: i) low-cost board based on commercial electronics component (e.g. μ -controller, ADC, DAC,...); ii) integration of metal electrodes and electronic circuits for measurement on the same chip. Results show that both ways are able to detect DNA hybridization by means of capacitance measurements, therefore, different application can be satisfy by mean of different electronics. For example, the first approach is more useful for a low parallell sites detection and specific gene analysis (e.g. one or few viruses which determine a particular group of pathologies), while the second one can be addressed to thousands parallell analysis exploiting microfabrication process. Problems related to stable and reproducible measurements are still open since detection reported in this thesis are obtained by mean of a differential approach, but as shown in chapter 8 new molecules can be used to modified metal surface and stabilization of capacitance measurement has been observed showing higher reproducibility of capacitance measurement. Elegant research on new sensing concepts has opened the door to a widespread clinical applications of electrochemical devices. Such devices are extremely useful for delivering the diagnostic information in a fast, simple, and low cost fashion, and are thus uniquely qualified for meeting the demands of point-of-care cancer screening. The high sensitivity of modern electrochemical bioaffinity assays should facilitate early detection and treatment of diseases and should lead to increased patient survival rates. The attractive properties of electrochemical devices are thus extremely promising for improving the efficiency of diagnostic

testing and therapy monitoring, and for point-of-care cancer testing, in general. The main challenge is to bring electrochemical techniques to the patient's side for use by non-laboratory personnel without compromising accuracy and reliability. The realization of decentralized electronic testing of cancer would thus require additional extensive developmental work. Special attention should be given to non-specific adsorption issues that commonly control the detection limits of electrochemical bioaffinity assays. It is expected that the creativity of electrochemists and material scientists, coupled with proper resources, will revolutionize cancer diagnostics in a manner analogous to their current leading role in diabetes monitoring. Disposable cartridges, containing electrode strips (coated with numerous receptors) along with related sample processing, could thus offer early screening of cancer in a point-of-care setting, by measuring abnormalities in protein profiles within few minutes. Accordingly, there is no doubt that electrochemical biosensors will become a powerful tool for cancer diagnostics in the near future.

Chapter 11

Publications

11.1 Conferences

- C.Stagni, C.Guiducci, C.Paulus, M.Schienze, M.Augustyniak, G.Zuccheri, B.Samorí, L.Benini, B.Riccó, and R.Thewes, "*Fully Electronic CMOS DNA Detection Array Based on Capacitance Measurement with On-Chip Analog-to-Digital Conversion*", Proceedings of ISSCC06 pp. 69-78, 2006.
- C.Stagni, C.Guiducci, M.Lanzoni, L.Benini and B.Riccó, "*Hardware-Software Design of a Smart Sensor for Fully-Electronic DNA Hybridization Detection*", Proceedings of the Design, Automation and Test Conference, DATE05, vol. 3, pp. 198-203, 2005.
- C.Guiducci, C.Stagni, L.Benini, B.Riccó, U.Mastromatteo, "*DNA Detection on Microfabricated Gold Electrodes on Silicon*" Proceedings of the X conference of the Associazione Italiana Sensori e Microsistemi, AISEM05, 2005.
- C.Guiducci, C.Stagni, L.Benini, G.Zuccheri, B.Samorí, B.Riccó, "*Microfabricated Sensors for Label-free Electronic DNA Detection*", Proceedings of the Matter and Material Devices Meeting, 2005.
- C.Stagni, C.Guiducci, L.Benini, B.Riccó, G.Zuccheri, B.Samorí, U.Mastromatteo, "*Fully electronic DNA detection technique*", Proceedings of the IX conference of the Associazione Italiana Sensori e Microsistemi, AISEM 2004, vol. 1, p. 184, 2004.
- C.Guiducci, C.Stagni, L.Benini, G.Zuccheri, B.Samorí, B.Riccó, "*A fully-electronic DNA detection technique for point-of-care genetic analysis*", Proceedings of the INFMeeting, 2004.

11.2 Journals

- S.Carrara, F.K.Grakaynak, C.Guiducci, C.Stagni, L.Benini, Yu.Leblebici, B.Samorí, G.De Micheli "Interface Layering Phenomena in Capacitance Detection of DNA with Biochips" Sensors&Transducers Journal, Vol. 76, no 2,, pp. 969-977, 2007.
- C.Stagni, C.Guiducci, L.Benini, B.Riccó, S.Carrara, C.Paulus, M.Schienze and R.Thewes "CMOS DNA Sensor Array with integrated A/D Conversion Based on Label-free Capacitance Measurement" Journal of Solid-State Circuit, vol.41, no. 12, pp. 2956-2964 2006.
- C.Stagni, C.Guiducci, L.Benini, B.Riccó, S.Carrara, B.Samor, C.Paulus, M.Schienze and R.Thewes "A Fully-Electronic Label-Free DNA Sensor Chip", IEEE sensors Journal in press.
- C.Guiducci, C.Stagni, A.Fischetti, U.Mastromatteo, L.Benini and B.Riccó, "Microelectrodes on a Silicon Chip for Label-Free Capacitive DNA Sensing" IEEE Sensors Journal, vol. 6, no. 5, pp. 1084-1093, 2006.
- C.Guiducci, C.Stagni, G.Zuccheri, A.Bogliolo, L.Benini, B.Samorí, B.Riccó "DNA Detection by Integrable Electronics", Biosensors and Bioelectronics, vol. 19, no. 8, pp. 781-787, 2004.

11.3 Patents

- German Patent Office:
"Sensor-Anordnung und Verfahren zum Ermitteln eines Sensorereignisses",10 2004 045 210.5, 17.09.2004, C.Paulus, M.Schienze, C.Stagni Degli Esposti, R.Thewes.
- Italian Patent Office:
"Chip per effettuare misure Elettrochimiche in contemporanea a misure di Risonanza Plasmonica Superficiale in strumenti non predisposti per misure combinate" DEPOSITO N. BO2007A000091, 16.02.2007, Sandro Carrara, Claudio Stagni, Giampaolo Zuccheri, Bruno Samorí.

Bibliography

- [1] L. Cavalli-Sforza, P. Menozzi, and A. Piazza, *The history and geography of human genes*. Princeton: Princeton University Press, 1994.
- [2] A. Chakravarti, “Population genetics—making sense out of sequence,” *Nature genetics*, vol. 21, no. 1(suppl.), pp. 56–60, 1999.
- [3] P.-Y. Kwok, “Methods for genotyping single nucleotide polymorphisms,” *Annu. Rev. Genomics Hum. Genet.*, no. 2, pp. 235–258, 2001.
- [4] G. C. Kennedy, H. Matsuzaki, S. Dong, W.-M. Liu, J. Huang, G. Liu, X. Su, M. Cao, W. Chen, J. Zhang, W. Liu, G. Yang, X. Di, T. Ryder, Z. He, U. Surti, M. S. Phillips, M. T. Boyce-Jacino, S. PA Fodor, and K. W. Jones, “Large-scale genotyping of complex DNA,” *Nature Biotechnology*, vol. 21, no. 10, pp. 1233–1237, 2003.
- [5] M. Cargill, D. Altshuler, J. Ireland, P. Sklar, K. Ardlie, N. Patil, N. Shaw, C. Lane, E. Lim, N. Kalyanaraman, J. Nemesh, L. Ziaugra, L. Friedland, A. Rolfe, J. Warrington, R. Lipshutz, G. Daley, and E. Lander, “Characterization of single-nucleotide polymorphisms in coding regions of human genes,” *Nature genetics*, vol. 22, no. 3, pp. 231–238, 1999.
- [6] M. C. Pirrung, “How to make a DNA chip,” *Angewandte Chemie International Edition*, vol. 41, no. 8, pp. 1276–1289, 2002.
- [7] J. Wang, “From DNA biosensors to gene chips,” *Nucleic Acids Res.*, vol. 28, no. 16, pp. 3011–3016, 2000.
- [8] S. Abramowitz, “DNA analysis in microfabricated formats,” *Journal of Biomedical Microdevices*, vol. 1, no. 2, pp. 107–112, 1999.

- [9] N. Zammattéo, L. Jeanmart, S. Hamels, S. Courtois, P. Louette, L. Hevesi, and J. Remacle, "Comparison between different strategies of covalent attachment of DNA to glass surfaces to build dna microarrays," *Anal. Biochem.*, vol. 280, pp. 143–150, 2000.
- [10] P. N. Gilles, D. J. Wu, C. B. Foster, P. J. Dillon, and S. J. Chanock, "Single nucleotide polymorphic discrimination by an electronic dot blot assay on semiconductor microchips," *Nat. Biotechnol.*, vol. 17, pp. 365–370, 1999.
- [11] P. Caillat, D. David, M. Belleville, F. Clerc, C. Massit, F. Revol-Cavalier, P. Peltie, T. Livache, G. Bidan, A. Roget, and E. Crapez, "Biochips on CMOS: an active matrix address array for DNA analysis," *Sensors and Actuators B*, vol. 61, p. 154162, 1999.
- [12] S. Fodor, J. Read, M. Pirrung, L. Stryer, A. Lu, and D. Solas, "Light-directed, spatially addressable parallel chemical synthesis," *Science*, vol. 251, no. 4995, pp. 767–773, 1991.
- [13] A. Woolley, G. Sensabaugh, and R. Mathies, "High-speed DNA genotyping using microfabricated capillary array electrophoresis chips," *Anal. Chem.*, vol. 69, no. 11, pp. 2181–2186, 1997.
- [14] R. Liu, J. Yang, R. Lenigk, J. Bonanno, and P. Grodzinski, "Self-contained, fully integrated biochip for sample preparation, polymerase chain reaction amplification, and DNA microarray detection," *Anal. Chem.*, vol. 76, no. 7, pp. 1824–1831, 2004.
- [15] "Integrated portable genetic analysis microsystem for pathogen/infectious disease detection," *Anal. Chem.*, vol. 76, no. 11, pp. 3162–3170, 2004.
- [16] J. Fritz, E. B. Cooper, S. Gaudet, P. K. Sorger, and S. R. Manalis, "Electronic detection of DNA by its intrinsic molecular charge," *Proceedings of the National Academy of Science*, vol. 99, no. 8, p. 14142–14146, 2000.
- [17] T. Prasad, V. Colvin, and D. Mittleman, "Superprism phenomenon in three-dimensional macroporous polymer photonic crystals," *Physical Review B*, vol. 67, p. 165103, 2003.
- [18] M. J. Heller, A. H. Forster, and E. Tu, "Active microelectronic chip devices which utilize controlled electrophoretic fields for multiplex

-
- DNA hybridization and other genomic applications,” *Electrophoresis*, vol. 21, pp. 157–164, 2000.
- [19] M. Schienle, C. Paulus, A. Frey, F. Hoffmann, B. Holzapfl, P. Schindler-Bauer, and R. Thewes, “A fully electronic DNA sensor with 128 positions and in-pixel A/D conversion,” *IEEE journal of Solid-State Circuits*, vol. 39, no. 12, pp. 2438–2444, 2004.
- [20] R. Terbrueggen, Y.-P. Chen, H. Duong, K. Millan, R. Mucic, G. Olsen, P. Singhal, N. Swami, H. Wang, T. Welch, H. Yowanto, C. Yu, G. Blackburn, and J. Kayyem, “Electronic detection of DNA: robust platform for integrated devices,” *Device Research Conference*, pp. 119–121, 2001.
- [21] H. Berney, J. West, E. Haefele, J. Alderman, W. Lane, and J. Collins, “A DNA diagnostic biosensor: development, characterization and performance,” *Sensors and Actuators B*, vol. 68, pp. 100–108, 2000.
- [22] F. Uslu, S. Ingebrandt, S. Bcker-Meffert, D. Mayer, M. Krause, M. Odenthal, and A. Offenhusser, “Label-free fully electronic nucleic acid detection system based on a field-effect transistor device,” *Biosensors and Bioelectronics*, vol. 19, no. 12, pp. 1723–1731, 2004.
- [23] E. Souteyrand, J. Cloarec, J. Martin, C. Wilson, S. Lawrence, I. and Mikkelsen, and M. Lawrence, “Direct detection of the hybridization of synthetic homo-oligomer DNA sequences by field effect,” *J. Phys. Chem. B*, vol. 101, pp. 2980–2985, 1997.
- [24] R. Gabl, E. Green, M. Schreiter, H. D. Feucht, H. Zeininger, R. Primig, and D. Pitzer, “Novel integrated FBAR sensors: a universal platform for bio- and gas detection,” *Proc. IEEE Sensors*, vol. 2, pp. 1184 – 1188, 2003.
- [25] A. Almadidy, J. Watterson, P. E. Piunno, S. Raha, I. V. Foulds, P. A. Horgen, A. Castle, and U. Krull, “Direct selective detection of genomic DNA from coliform using a fiber optic biosensor,” *Analytica Chimica Acta*, vol. 461, pp. 37–47, 2002.
- [26] Z. Li, Y. Chen, X. Li, T. I. Kamins, K. Nauka, and R. S. Williams, “Sequence-specific label-free DNA sensors based on silicon nanowires,” *Nano Letters*, vol. 4, no. 4, pp. 245–247, 2004.

- [27] C. Gabrielli, "Electrochemical impedance spectroscopy: Principles, instrumentation, and applications." *In: Physical Electrochemistry. Principles, Methods and Applications*, ed. Rubinstein, I., Dekker, New York, pp. 243–292, 1995.
- [28] A. J. Bard, H. D. Abruna, C. E. Chidsey, L. R. Faulkner, S. W. Feldberg, K. Itaya, M. Majda, O. Melroy, R. W. Murray, M. D. Porter, M. P. Soriaga, and H. White, "The electrode/electrolyte interface - a status report," *J. Phys. Chem.*, vol. 97, pp. 7147–7173, 1993.
- [29] R. P. Janek, W. R. Fawcett, and A. Ulman, "Impedance spectroscopy of self-assembled monolayers on Au(111): Evidence for complex double-layer structure in aqueous $NaClO_4$ at the potential of zero charge," *J. Phys. Chem. B*, vol. 101, pp. 8550–8558, 1997.
- [30] J. Sagiv, "Organized monolayers by adsorption. formation and structure of oleophobic mixed monolayers on solid surfaces," *J. Am. Chem. Soc.*, vol. 102, pp. 92–98, 1980.
- [31] E. B. Troughton, C. D. Bain, G. M. Whitesides, R. G. Nuzzo, D. L. Allara, and M. D. Porter, "Monolayer films prepared by the spontaneous self-assembly of symmetrical and unsymmetrical dialkyl sulfides from solution onto gold substrates: Structure, properties, and reactivity of constituent functional groups," *Langmuir*, vol. 4, pp. 365–385, 1988.
- [32] K. R. Rogers and A. Mulchandani, *Affinity Biosensors: Techniques and Protocols*. New jersey: Humana Press, 1998.
- [33] R. Nuzzo and D. Allara, "Adsorption of bifunctional organic disulfides on gold surfaces," *J. Am. Chem. Soc.*, vol. 105, pp. 4481–4483, 1983.
- [34] H. Finklea, "Electrochemistry of organized monolayers of related molecules on electrodes," *In: Electroanalytical Chemistry*. ed. Bard, Dekker, New York, pp. 107–335, 1996.
- [35] A. Ulman, "Formation and structure of self-assembly monolayers," *Chem. Rev.*, vol. 96, pp. 1533–1554, 1996.

-
- [36] R. G. Nuzzo, L. H. Dubios, and D. L. Allara, "Fundamental studies of microscopic wetting on organic surfaces," *J. Am. Chem. Soc.*, vol. 112, pp. 558–569, 1990.
- [37] L. Strong and G. M. Whitesides, "Structures of self-assembled monolayer films of organosulfur compounds adsorbed on gold single crystals: Electron diffraction studies," *Langmuir*, vol. 4, pp. 546–558, 1988.
- [38] A. Ulman, *An introduction to ultrathin organic films*. New York: Academic Press, 1991.
- [39] M. Riepl, V. M. Mirsky, I. Novotny, V. Tvarozek, V. Rehacek, and O. S. Wolfbeis, "Optimization of capacitive affinity sensors: drift suppression and signal amplification," *Analytica Chimica Acta*, vol. 392, no. 1, pp. 77–84, 1999.
- [40] C. Guiducci, C. Stagni, G. Zuccheri, A. Bogliolo, L. Benini, B. Samorí, and B. Riccò, "DNA detection by integrable electronics," *Biosensors and Bioelectronics*, vol. 19, no. 8, pp. 781–787, 2004.
- [41] F. Pouthas, C. Gentil, D. Côte, and U. Bockelmann, "DNA detection on transistor arrays following mutation-specific enzymatic amplification," *Applied Physics Letters*, vol. 84, pp. 1594–1596, 2004.
- [42] J. R. Macdonald, *Impedance Spectroscopy*. New-York: John Wiley and Sons, 1987.
- [43] G. C. Kennedy, "Large-scale genotyping of complex DNA," *Nature Biotechnology*, vol. 21, no. 10, pp. 1233–1237, 2003.
- [44] F. Hofmann, A. Frey, B. Holzapfl, M. Schienle, C. Paulus, P. Schindler-Bauer, D. Kuhlmeier, J. Krause, R. Hintsche, E. Nebling, J. Albers, W. Gumbrecht, K. Plehnert, G. Eckstein, and R. Thewes, "Fully electronic DNA detection on a CMOS chip: device and process issues," in *Proceedings of IEEE International Electron Devices Meeting*, San Francisco (USA), 2002.
- [45] R. M. Umek, S. W. Lin, J. Vielmetter, R. H. Terbrueggen, B. Irvine, C. J. Yu, J. F. Kayyem, H. Yowanto, G. F. Blackburn, D. H. Farkas, and Y.-P. Chen, "Electronic detection of nucleic acids. a versatile platform for molecular diagnostics," *Journal of Molecular Diagnostics*, vol. 3, pp. 100–108, 2001.

- [46] K. Peterlinz and R. Georgiadis, "In situ kinetics of self-assembly by surface plasmon resonance spectroscopy," *Langmuir*, vol. 12, pp. 4731–4740, 1996.
- [47] C. Berggren, P. Stalhandske, J. Brundell, and G. Johansson, "A feasibility study of a capacitive biosensor for direct detection of DNA hybridization," *Electroanalysis*, pp. 74–84, 1999.
- [48] A. Bogliolo, L. Vendrame, L. Bortesi, and E. Barachetti, "Charge-based on-chip measurement technique for the selective extraction of cross-coupling capacitances," in *Proceedings of IEEE Signal Propagation on Interconnects*, Castelvechio Pascoli, Pisa (Italy), 2002, pp. 75–77.
- [49] D. Gregory, M. G. Hill, and J. K. Barton, "Electrochemical DNA sensors," *Nature Biotechnology*.
- [50] J. D. Watson, *Molecular biology of the gene, Fifth Edition*. Benjamin-Cummings Publishing Company, 2003.
- [51] M. Su, "Microcantilever resonance-based DNA detection with nanoparticle probes," *Applied Physics Letters*, vol. 82, no. 20, pp. 3562–3564, 2003.
- [52] I. Willner, "Amplified detection of single-base mismatches in DNA using microgravimetric quartz-crystal-microbalance transduction," *Talanta*, vol. 56, no. 5, pp. 847–856, 2002.
- [53] C. Berggren, "A feasibility study of a capacitive biosensor for direct detection of DNA hybridization," *Electroanalysis*, vol. 3, no. 11, pp. 156–160, 1999.
- [54] S. Ding, B. Chanq, C. Wu, M. Lai, and H. Chanq, "Impedance spectral studies of self-assembly of alkanethiols with different chain lengths using different immobilization strategies on au electrodes," *Analytica Chimica Acta*, vol. 554, no. 1-2, pp. 43–51, december 2005.
- [55] J. Chen, "An on-chip, attofarad interconnect charge-based capacitance measurement (CBCM) technique," *International Electron Devices Meeting*, 1996.
- [56] Atmel, www.atmel.com.
- [57] MAXIM, www.maxim-ic.com.

-
- [58] TexasInstruments, www.ti.com.
- [59] AnalogDevices, www.analog.com.
- [60] LinearTechnology, www.linear.com.
- [61] NationalInstruments, www.ni.com.
- [62] S. Mouterau, R. Narwa, C. Matheron, N. Vongmany, E. Simon, and M. Goossens, "An mproved electronic microarray-based diagnostic assay for identification of MEFV mutations," *Human Mutation*, vol. 23, no. 6, pp. 621–628, 2004.
- [63] P. K.Riggs, J. M.Angel, E. L.Abel, and J. Digiovanni, "Differential gene expression in epidermis of mice sensitive and resistant to phorbol ester skin promotion," *Molecular Carcinogenesis*, vol. Articles online in advance of print, 2003.
- [64] F. Hoffmann, A. Frey, B. Holzapfl, M. Schienle, C. Paulus, P. Schindler-Bauer, D. Kuhlmeier, J. Krause, E. Hintsche, Nebling, J. Albers, W. Gumbrecht, K. Plehnert, G. Eckstein, and R. Thewes, "Fully electronic DNA detection on a cmos chip: device and process issues," in *IEDM Tech. Dig.*, pp. 488–491, 2002.
- [65] Motorola Life Sciences Inc - www.motorola.com.
- [66] C. Yu, Y. Wan, H. Yowanto, J. Li, C. Tao, M. D. James, C. L. Tan, G. F. Blackburn, and T. J. Meade, "Electronic detection of single-base mismatches with ferrocene-modified probes," *J. Am. Chem. Soc.*, vol. 123, no. 45, pp. 11 155–11 161, 2001.
- [67] R. Brederlow, S. Zauner, A. L. Scholtz, K. Aufinger, W. Simburger, C. Paulus, A. Martin, M. Fritz, H.-J. Timme, H. Heiss, S. Marksteiner, L. Elbrecht, R. Aigner, and R. Thewes, "Biochemical sensors based on bulk acoustic wave resonators," *IEDM Tech.Digest*, pp. 992–994, 2003.
- [68] Y. Li, C. Vancura, C. Hagleitner, J. Lichtenberg, O. Brand, and H. Baltes, "Very high q-factor in water achieved by monolithic, resonant cantilever sensor with fully integrated feedback," *Proc. IEEE Sensors*, vol. 2, pp. 809–813, 2003.
- [69] K.-U. Kirstein, Y. Li, M. Zimmermann, C. Vancura, T. Volden, W. H. Song, and J. Lichtenberg, "Cantilever-based biosensors in CMOS technology," *Proc. DATE05*, vol. 2, pp. 210–214, 2005.

- [70] F. Perkins, S. J. Fertig, K. A. Brownt, D. McCarthy, L. Tender, and M. Peckerar, "An active microelectronic transducer for enabling label-free miniaturized chemical sensors," in *Technical Digest. International Electron Devices Meeting (IEDM'00)*, San Francisco, USA, 2000, pp. 407–410.
- [71] C. Guiducci, C. Stagni, A. Fischetti, U. Mastromatteo, L. Benini, and B. Riccò, "Micro-fabricated two-terminal capacitors for label-free DNA sensing/recognition," *IEEE Sensors*, vol. 6, no. 5, pp. 1084–1093, 2006.
- [72] A. Bogliolo, L. Vendrame, L. Bortesi, and E. Barachetti, "Charge-based on-chip measurement technique for the selective extraction of cross-coupling capacitances," in *Proceedings of IEEE Signal Propagation on Interconnects*, Castelvechio Pascoli, Pisa (Italy), 2002.
- [73] J. Israelachvili, *Intermolecular and Surface Forces*. London: Academic Press, 1992.
- [74] J. Hicks, F. Zamborini, and R. Murray, "Dynamics of electron transfers between electrodes and monolayers of nanoparticles," *Journal of Physical Chemistry B*, vol. 106, pp. 7751–7757, 2002.
- [75] L. M. Demers, C. A. Mirkin, R. C. Mucic, R. A. R. III, R. L. Letsinger, R. Elghanian, and G. Viswanadham, "A fluorescence-based method for determining the surface coverage and hybridization efficiency of thiol-capped oligonucleotides bound to gold thin films and nanoparticles," *Analytical Chemistry*, vol. 72, no. 22, pp. 5535–5541, 2000.
- [76] A. Frey, M. Schienle, C. Paulus, Z. Jun, F. Hofmann, P. Schindler-Bauer, B. Holzapfl, M. Atzesberger, G. Beer, M. Fritz, T. H. H.-C. Hanke, and R. Thewes, "A digital cmos dna chip," *ISCASS05*, vol. 3, pp. 2915–18, 2005.
- [77] J. Fritz, E. Cooper, S. Gaudet, P. K. Sorger, and S. R. Manalis, "Electronic detection of DNA by its intrinsic molecular charge," *Proceedings of the National Academy of Science*, vol. 99, pp. 14 142–46, 2002.
- [78] N. Ronkainen-Matsuno, J. Thomas, A. Halsall, and W. Heineman, "Electrochemical immunoassays moving into the fastlane," *Trends Anal. Chem.*

-
- [79] J. Lahiria, L. Isaacs, J. Tien, and G. Whitesides, "A strategy for the generation of surfaces presenting ligands for studies of binding based on an active ester as a common reactive intermediate: A surface plasmon resonance study," *Anal. Chem.*
- [80] D. Wang, A. Urisman, Y. Liu, M. Springer, T. Ksiazek, D. Erdman, E. Mardis, M. Hickenbotham, V. Magrini, J. Eldred, J. Latreille, R. Wilson, D. Ganem, and J. DeRisi, "Viral discovery and sequence recovery using dna microarrays," *Plos Biology*, vol. 1, no. 2, pp. 257–260, 2003.
- [81] L. Abruzzo, K. Lee, A. Fuller, A. Silverman, M. Keating, L. Medeiros, and K. Coombes, "Validation of oligonucleotide microarray data using microfluidic low-density arrays: a new statistical method to normalize real-time RT-PCR data," *Biotechniques*, vol. 38, no. 5, pp. 785–792, 2005.
- [82] M. Lacroix, N. Zammateo, J. Remacle, and G. Leclercq, "A low-density DNA microarray for analysis of markers in breast cancer," *Int. Journal of Biological Markers*, vol. 17, no. 1, pp. 5–23, 2002.
- [83] S. D. Conzone and C. G. Pantano, "Glass slides to microarray," *Materials Today*, vol. 7, no. 3, pp. 20–26, 2004.
- [84] M. Liu and L. Jie, "Layer-by-layer assembly of dna films and their interactions with dyes," *J. Phys. Chem. B*, vol. 103, no. 51, pp. 11 393– 11 397, 1999.
- [85] R. Pei, X. Cui, X. Yang, and E. Wang, "Assembly of alternating polycation and DNA multilayer films by electrostatic layer-by-layer adsorption," *Biomacromolecules*, vol. 2, no. 2, pp. 463–468, 2001.
- [86] G. de Cesare, D. Caputo, A. Nascetti, C. Guiducci, and B. Ricco, "Hydrogenated amorphous silicon ultraviolet sensor for deoxyribonucleic acid analysis," *Appl. Phys. Lett.*, vol. 88, pp. 083 904–0 839 044, 2006.
- [87] I. Tinoco, K. Sauer, J. Wang, and J. Pugliesi, *Physical Chemistry: Principles and Applications in Biological Sciences*. Prentice Hall College Div, 2001.